NAVAL POSTGRADUATE SCHOOL
Monterey, California

THESIS

A 3D PARABOLIC EQUATION (PE) BASED TECHNIQUE FOR PREDICTING PROPAGATION PATH LOSS IN AN URBAN AREA

by

Keem Boon Thiem

September 2001

Thesis Supervisor:	Ramakrishna Janaswamy
Thesis Committee Members:	David Jenn
	Tri Ha

Approved for public release; distribution is unlimited

Report Documentation Page

Report Date	Report Type	Dates Covered (from... to)
30 Sep 2001	N/A	-

Title and Subtitle	Contract Number
A 3D Parabolic Equation (PE) Based Technique for Predicting Propagation Path Loss in an Urban Area	Grant Number
	Program Element Number

Author(s)	Project Number
Keem Boon Thiem	Task Number
	Work Unit Number

Performing Organization Name(s) and Address(es)	Performing Organization Report Number
Research Office Naval Postgraduate School Monterey, Ca 93943-5138	

Sponsoring/Monitoring Agency Name(s) and Address(es)	Sponsor/Monitor's Acronym(s)
	Sponsor/Monitor's Report Number(s)

Distribution/Availability Statement
Approved for public release, distribution unlimited

Supplementary Notes

Abstract

Subject Terms

Report Classification	Classification of this page
unclassified	unclassified

Classification of Abstract	Limitation of Abstract
unclassified	UU

Number of Pages
108

THIS PAGE INTENTIONALLY LEFT BLANK

REPORT DOCUMENTATION PAGE		*Form Approved OMB No. 0704-0188*
Public reporting burden for this collection of information is estimated to average 1 hour per response, including the time for reviewing instruction, searching existing data sources, gathering and maintaining the data needed, and completing and reviewing the collection of information. Send comments regarding this burden estimate or any other aspect of this collection of information, including suggestions for reducing this burden, to Washington headquarters Services, Directorate for Information Operations and Reports, 1215 Jefferson Davis Highway, Suite 1204, Arlington, VA 22202-4302, and to the Office of Management and Budget, Paperwork Reduction Project (0704-0188) Washington DC 20503.

1. AGENCY USE ONLY (*Leave blank*)	2. REPORT DATE September 2001	3. REPORT TYPE AND DATES COVERED Engineer's Thesis
4. TITLE AND SUBTITLE: A 3D Parabolic Equation (PE) Based Technique for Predicting Propagation Path Loss in an Urban Area		5. FUNDING NUMBERS
6. AUTHOR(S) Keem Boon Thiem		
7. PERFORMING ORGANIZATION NAME(S) AND ADDRESS(ES) Naval Postgraduate School Monterey, CA 93943-5000		8. PERFORMING ORGANIZATION REPORT NUMBER
9. SPONSORING / MONITORING AGENCY NAME(S) AND ADDRESS(ES) N/A		10. SPONSORING / MONITORING AGENCY REPORT NUMBER

| 11. SUPPLEMENTARY NOTES The views expressed in this thesis are those of the author and do not reflect the official policy or position of the Department of Defense or the U.S. Government. |

12a. DISTRIBUTION / AVAILABILITY STATEMENT Approved for public release; distribution is unlimited	12b. DISTRIBUTION CODE

13. ABSTRACT *(maximum 200 words)* A mobile radio environment places fundamental limitations on the performance of wireless communication systems. Most models developed to predict propagation path loss have been historically performed in a statistical approach. These models are expensive to develop and do not offer the accuracy, computational advantages, and sufficiency as the parabolic equation (PE). The goal of this thesis is to develop a 3D model based on PE for predicting propagation path loss in urban areas on flat and hilly terrains. The PE method offers the computational advantages, where one can approximate the elliptic operator governing the true wave behavior by a much simpler parabolic operator that permits marching in range. Moreover those all-important aspects of propagation such as reflection and diffraction are included automatically in the formulation. Four test problems on flat terrain and two test problems on hilly terrain will be simulated. For the flat terrain, the 3D PE model results will be compared with the two-ray, the four-ray, the UTD, and the numerical integration technique results. For the hilly terrain, the results of the 3D PE model will be compared with the UTD and the numerical integration technique results.

14. SUBJECT TERMS Radiowave Propagation, Parabolic Equation Techniques, Wireless Communications, Large-Scale Propagation Path Loss			15. NUMBER OF PAGES 106
			16. PRICE CODE
17. SECURITY CLASSIFICATION OF REPORT Unclassified	18. SECURITY CLASSIFICATION OF THIS PAGE Unclassified	19. SECURITY CLASSIFICATION OF ABSTRACT Unclassified	20. LIMITATION OF ABSTRACT UL

NSN 7540-01-280-5500

Standard Form 298 (Rev. 2-89)
Prescribed by ANSI Std. 239-18

i

THIS PAGE INTENTIONALLY LEFT BLANK

A 3D PARABOLIC EQUATION BASED TECHNIQUE FOR PREDICTING PROPAGATION PATH LOSS IN AN URBAN AREA

By

Keem B. Thiem
Electronics Engineer, GS-13, United States Air Force Civil Service
B.S.E.E., **California State Polytechnic University**, Pomona, 1990
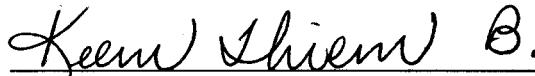M.S.E.E, **Naval Postgraduate School**, Monterey, 1993

Submitted in partial fulfillment of the
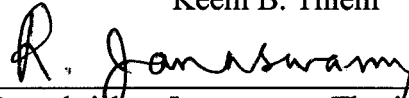requirements for the degree of

ELECTRICAL ENGINEER

from the
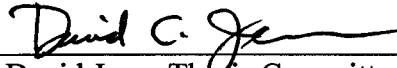
NAVAL POSTGRADUATE SCHOOL
September 2001

Author: _____

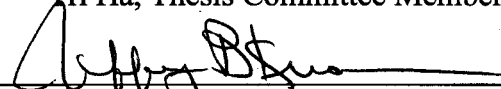Keem B. Thiem

Approved by: _____

Ramakrishna Janaswamy, Thesis Supervisor

_____

David Jenn, Thesis Committee Member

_____

Tri Ha, Thesis Committee Member

_____

Jeff Knorr, Chairman
Department of Electrical and Computer Engineering

iii

THIS PAGE INTENTIONALLY LEFT BLANK

ABSTRACT

A mobile radio environment places fundamental limitations on the performance of wireless communication systems. Most models developed to predict propagation path loss have been historically performed in a statistical approach. These models are expensive to develop and do not offer the accuracy, computational advantages, and sufficiency as the parabolic equation (PE). The goal of this thesis is to develop a 3D model based on PE for predicting propagation path loss in urban areas on flat and hilly terrains. The PE method offers the computational advantages, where one can approximate the elliptic operator governing the true wave behavior by a much simpler parabolic operator that permits marching in range. Moreover those all-important aspects of propagation such as reflection and diffraction are included automatically in the formulation. Four test problems on flat terrain and two test problems on hilly terrain will be simulated. For the flat terrain, the 3D PE model results will be compared with the two-ray, the four-ray, the UTD, and the numerical integration technique results. For the hilly terrain, the results of the 3D PE model will be compared with the UTD and the numerical integration technique results.

THIS PAGE INTENTIONALLY LEFT BLANK

TABLE OF CONTENTS

THIS PAGE INTENTIONALLY LEFT BLANK

LIST OF FIGURES

THIS PAGE INTENTIONALLY LEFT BLANK

LIST OF TABLES

THIS PAGE INTENTIONALLY LEFT BLANK

To the memories of my grandmother, uncles, aunts, cousins and millions of fellow Cambodians who died during the Killing Fields and the victims of Phnom Dangrek.

THIS PAGE INTENTIONALLY LEFT BLANK

ACKNOWLEDGMENTS

THIS PAGE INTENTIONALLY LEFT BLANK

EXECUTIVE SUMMARY

A mobile radio environment places fundamental limitations on the performance of wireless communication systems. Most models developed to predict the propagation path loss have been historically performed by statistical approach. These models are often complicated and expensive to develop and do not offer the accuracy, computational advantages, and sufficiency such as the *parabolic equation* (PE) technique or a ray based technique.

The aim of this thesis is to develop a *3D model* based on PE for predicting the propagation path loss in urban areas on flat and hilly terrains. The PE method offers the computational advantages, where one can approximate the elliptic operator governing the true wave behavior by a much simpler parabolic operator that permits marching in range. This method has the advantage that all-important aspects of propagation such as reflection and diffraction are included automatically in the formulation. Two types of terrains are considered, the flat earth and the hilly terrain. For the flat earth case, four test problems are examined. We compare the results from these cases with the results available in open literature from the *two-ray model*, *the four-ray model*, the *UTD*, the theoretical model proposed by Lee, and the numerical integration technique presented by Bertoni. For the hilly terrain case, two test problems are considered. The results of these cases are compared with the results presented by Piazzi and Bertoni.

For the flat earth, the first test problem is to simulate and determine the propagation factor F at the final range over flat earth without obstacles being placed between the transmitter and the receiver. F is defined as the normalized field $\left| H_y(x, y, z) / H_y(f.s.) \right|$, where $H_y(f.s.)$ is the free-space magnetic field. A transmitting antenna height of $H_t = 30$ m, and the operating frequency of 1 GHz is used. The results of the 3D PE model are compared with the two-ray model. This is the simplest validation case we consider.

The second test problem is to simulate and determine F with a single absorbing screen placed between the transmitter and the receiver that has a height $H_k = 50$ m and a

width, $W_k = 49.5$ m. The screen represents a building. The transmitting antenna height is $H_t = 60$ m, and the operating frequency is 1 GHz. We compare the results of the 3D PE model with the results of the four-ray model which considers reflection and diffraction in the vertical plane joining the transmitter and receiver.

In the third test problem, nine absorbing screens of uniform heights, equal spacing, variable screen widths are placed between the transmitter and the receiver. A transmitting antenna height of $H_t = 10$ m, and operating frequency of 1 GHz is used. This test case is equivalent to the radiowave propagating over a row of houses in an urban area. The three different screen widths of 50 m, 25 m, and 12.5 m are considered. Each screen has a height of 10 m and is spaced 50 m from the previous one. Their effects on the propagation factor F are studied. The propagation factors are determined at the rooftops. The results of the 3D PE model are compared with the UTD results presented by Andersen and the theoretical results proposed by Lee.

The last test problem for the flat earth case involves 120 absorbing screens of uniform heights and equal spacing between the transmitter and the receiver. These screens represent row of buildings or houses. The transmitting antenna has a height of $H_t = 125$ m, and the operating frequency is 900 MHz. The screens have the height, $H_k = 20$ m, and the width, $W_k = 50$ m. They are spaced 50 m apart. The propagation factor is determined at the final range. We compare the results of the 3D PE model with the results of the UTD method and the numerical integration technique presented by Bertoni.

For the hilly terrain case, the first test problem involves a single rounded hill with multiple absorbing screens of uniform heights, equal spacing and variable screen widths. The three variable screen widths are 25 m, 50 m and 100 m. The screen height $H_k = 7$ m, and the spacing of 50 m are maintained constant. Their effects on the propagation factor F are studied. The transmitting antenna height is $H_t = 57$ m, and the operating frequency is 900 MHz. The field strengths are determined on the rooftops. We compare the results of the 3D PE model with the results of the numerical integration technique proposed by Piazzi and Bertoni.

For the second test problem in this class, the propagation took place over two hills of sinusoidal shape with multiple absorbing screens of uniform heights, equal spacing, and variable screen widths. The three variable screen widths are 25 m, 50 m and 100 m. A screen height $H_k = 7$ m, and spacing of 50 m is used. Their effects on the propagation factor F are studied. The transmitting antenna has a height of $H_t = 57$ m, and the operating frequency is 900 MHz. Again, we compare the results of the 3D PE model with the results presented by Piazzi and Bertoni.

Finally, the 3D model results based on PE for predicting propagation path loss in urban areas over flat and hilly terrains are simulated. Six different test problems are considered. We compare the results of the 3D PE model with the available results from the literature, and they show excellent agreement. We also demonstrate that the 3D PE model can support both flat and hilly terrains with multiple absorbing screens of uniform heights, equal spacing, and variable screen widths.

THIS PAGE INTENTIONALLY LEFT BLANK

I. INTRODUCTION

A. BACKGROUND

A typical mobile radio environment in an urban area for wireless communication systems has no direct line-of-sight path between the transmitter and the receiver. The environment is so dynamic and the path between the transmitter and the receiver can vary drastically from simple line-of-sight to one that is severely obstructed by buildings, mountains, and trees. Hence, the mobile radio environment places fundamental limitations on the performance of wireless communication systems. Since the environment is extremely random, most analysis done on it has been historically performed in a statistical approach, often based on measurements made specifically for an intended communication system or spectrum allocation [Ref. 1].

Currently, there are large-scale propagation path loss models being utilized in commercial cellular communication systems in America, Europe, Asia, and around the world. Some of these popular models include the Okumura model, the Hata model, and the COST-231-Walfish-Ikegami model [Ref. 2]. As previously mentioned, these models were developed by measurements and statistical analysis made specifically for frequency coverage between 150 MHz and 2 GHz, and are typically based on a certain city environment like Tokyo or New York. These models provide reasonable approximation for current cellular communication applications. However, they are complicated and expensive to develop and do not offer the accuracy, computational advantages, and efficiency of models such as the parabolic equation (PE), ray methods, etc.

Previously developed 2D parabolic equation based on the vertical plane method does not account for the lateral propagation of waves. Consequently, the mean path loss is overestimated and the standard deviation of error tends to be rather high [Ref. 3]. Therefore, a 3D PE formulation based on the split-step algorithm was developed and demonstrated for forward propagation around perfectly reflecting obstacles located on ground that includes the laterally propagating waves [Ref 4]. The 3D formulation is expected to substantially improve the accuracy relative to the 2D vertical plane method for the test problems. The goal of this thesis is to develop a 3D model based on a scalar

1

parabolic equation for predicting propagation path loss in urban areas on flat earth and hilly terrains.

B. RESEARCH DEFINITION

Given an operating frequency f, the transmitting antenna height H_t and the 3-dB beam width, and the terrain profile, we want to calculate the field at a certain range from the transmitting antenna. We use the parabolic equation (PE) method to determine the field at the desired location. Although there are several computational techniques for predicting the field at a desired range from the transmitting antenna including the ray tracing approach, and the integral equation method etc., few offer the computational advantages of the parabolic equation (PE) method, where one can approximate the elliptic operator governing the true wave behavior by a much simpler parabolic operator that permits marching in range. The PE method has the advantage that all-important aspects of propagation such as reflection and diffraction are included automatically in the formulation. However, the penalty for employing the PE method is that it neglects back scattering [Ref. 5]. This assumption will not contribute any significant errors for the class of applications considered in this thesis since radiowaves predominantly propagate in the forward direction.

We consider a vertically polarized current source $f(z)$ that produces only vertically polarized electric field component E_z or equivalently a circumferential magnetic field component. We look at the y component of the magnetic field H_y because the depolarization is ignored. Thus initial magnetic field $H(0, y, z)$ at the location $x = 0$ is set up by the current source on a flat plane, and it is directly related to the current source density $\vec{J}$. It is easier to relate the magnetic field to the current source [Ref. 3, 4]. For this reason, we use the magnetic field in the 3D PE algorithm instead of electric field; however, the electric field and magnetic field in the far-zone are related via the medium impedance. The field is then split into even and odd parts to ensure that there are no discontinuities at zero crossing which leads to erroneous results during numerical evaluation.

In the presence of vertical screens that are perpendicular to the preferred axis (*x*-axis), we still ignore the depolarization. These screens represent a row of buildings or houses in an urban area. In this thesis, we assume that they are perfectly absorbing which means that all incident fields on them are zeroed out. Figure 1 illustrates how the 3D PE model algorithm handles the incident fields on the screens. First, we determine the fields $H(x, y, z)$ in the absence of the screens and then make local adjustments to them. After making the adjustments, the field $H(x^+, y, z)$ continues to march in range where the superscript $^+$ indicates the fields immediately after the screen. This is then repeated till the desired receiver location is reached.
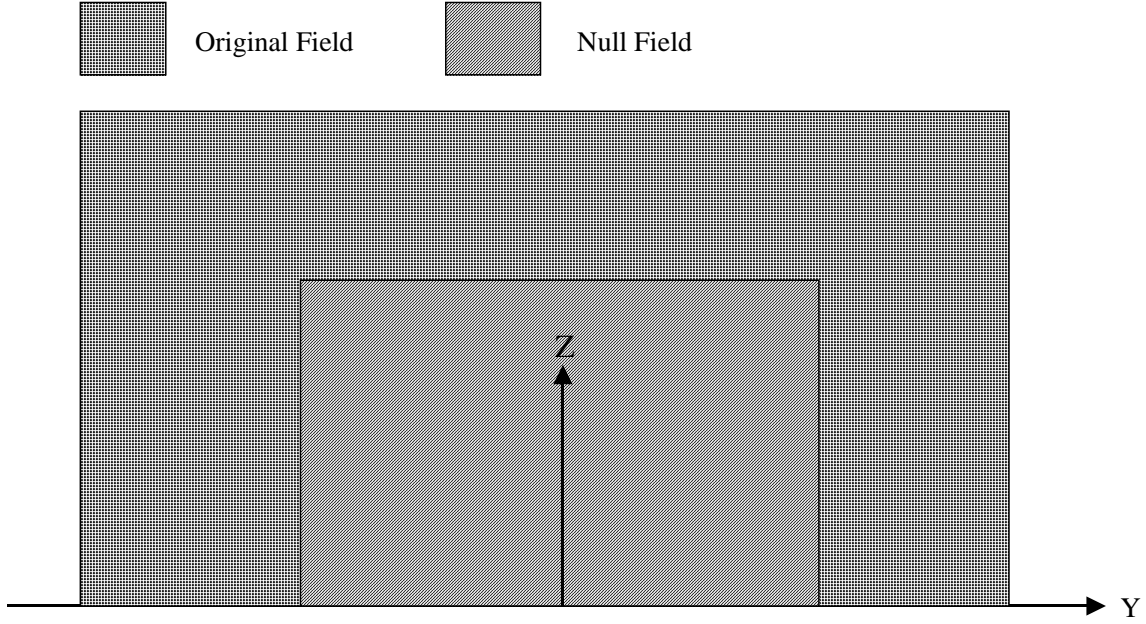
Figure 1.   Fields Incident on a Perfectly Absorbing Screen.

Therefore, this work will attempt to design a more accurate large-scale propagation path loss model based on the scalar 3D parabolic equation (PE) over the frequency band of 300 MHz to 10 GHz. The algorithm will predict the lateral and vertical wave propagation in an urban area that is comprised of vertical buildings with arbitrary cross section and perfectly absorbing surfaces on flat and hilly terrains. The 3D PE algorithm also includes the log-normal shadowing effects. We will compare the 3D

PE results to the two-ray model [Ref. 2], four-ray model [Ref. 2], the results given by Andersen [Ref. 6] obtained from the uniform theory of diffraction (UTD) method, the theoretical results given by Lee [Ref. 7], and the numerical results obtained by Piazzi and Bertoni [Refs. 8-10]. The 3D PE algorithm is implemented in MatLab.

In Chapter II we provide detailed discussions on the numerical evaluation of the 3D parabolic equation and the MatLab implementation. The current source has vertical extent along the z-axis and has a Gaussian distribution. The source standard deviation, σ_z, is chosen to produce the required transmitting antenna 3 dB elevation beam width, Θ_{el}. A detailed discussion on the current source and its relationship to the magnetic field is also given in this chapter.

In Chapter III and IV, we discuss our results and comparison efforts in detail. We compare the 3D parabolic equation (PE) results with the results reported in the literature. In Chapter III, first, we examine a flat earth and perfectly reflecting ground. The results of the 3D PE model of this case are compared with the results of the two-ray model. Then we introduce single and multiple perfectly absorbing screens of uniform heights and equal spacing between the transmitter and the receiver over a flat earth and non-perfectly reflecting ground. These absorbing screens represent row of buildings of arbitrary widths. The effects of finite screen widths on simulation are also examined.

In Chapter IV, we introduce a rounded hill and two hills of sinusoidal shape with multiple absorbing screens the uniform heights and equal spacing between the transmitter and the receiver. These scenarios are representative of well built-up urban areas. In both cases, we also examine the effects of finite screen widths versus the infinitely long screen widths on the simulation results. Results from these cases are compared with the results presented by Piazzi and Bertoni. Chapter V provides the conclusions and recommendations. All MatLab codes are listed in the Appendices.

4

II. NUMERICAL EVALUATION OF 3D PARABOLIC EQUATION

A detailed method for evaluating the 3D parabolic equation (PE) numerically is presented in this chapter. First the 3D PE model algorithm flow diagram is presented in Section A. Then the initial current source and its characteristics are discussed in Section B. This is followed in Section C by a detailed discussion on how the magnetic field is related to the current source. A Hanning window is used throughout the algorithm to contain the fields both in spatial and wavenumber domains before taking *2D (Ny* x *Nz)* Fourier transforms *(2FFT's)* or *2D* inverse Fourier transforms *(IFFT's)*. The Hanning window is discussed in detail in Section D. Brief descriptions of the auxiliary parameters are provided in Section E.

In the parabolic equation the fields are coupled causally from one range to the next. There is no path for waves to return information from obstacles located ahead of the receiver. The initial fields are set up by the current source on an impedance plane. Presence of a vertical screen perpendicular to the preferred axis (*x*-axis) is handled by first determining the fields in the absence of the screen and then making local adjustments to them. This process is then repeated till the desired receiver location is reached.

Figure 2 illustrates the geometry of the scalar 3D PE model approach. To find the field over an impedance plane at a particular range, $x + \Delta x$, given the field at a previous range, x, the latter is first decomposed into a spectrum of plane waves traveling in the positive *x*-direction. Each plane wave is then propagated to the new range using the appropriate propagator. The plane waves at the new range are then added to compose the field at $x + \Delta x$. The various spectral decompositions are carried out using 2D Fourier transforms (2*FFTs)* in the *y-z* plane. Furthermore, the magnetic field can be defined in terms of odd and even parts to ensure that there are no discontinuities at zero crossing which leads to erroneous results during the 2D Fourier transform (*FFT*) computation. In this thesis, the current source is assumed to be along the positive *z*-direction, and the antenna is vertically polarized. Over flat plane, the only non-zero field components are

E_z, E_ρ, and H_ϕ. Where ρ, z, ϕ are the standard cylindrical coordinates, and ϕ is measured from the *x*-axis. We ignore depolarization and continue this assumption to hold in the presence of the screens. Thus the vertically polarized current source $f(z)$ produces only vertically polarized electric field component E_z or equivalently a circumferential magnetic field component. In this thesis, we choose to use the *y* component of the magnetic field H_y because the antenna depolarization is ignored.
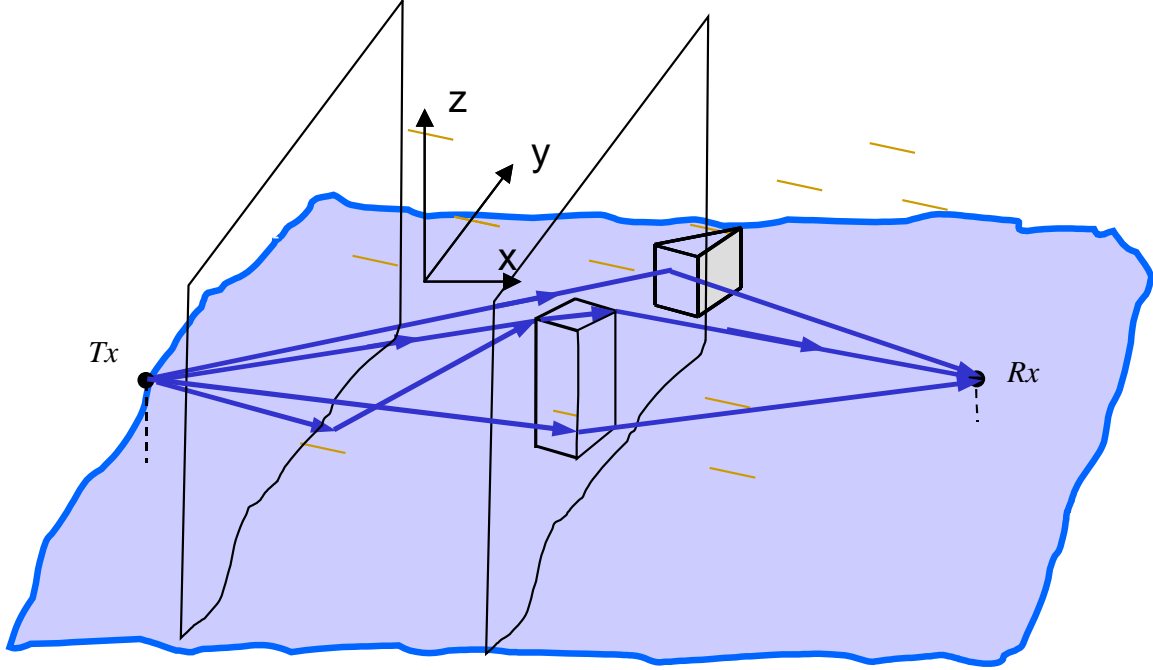
Figure 2.   Geometry of the Scalar 3D PE Model [From: Ref. 11].

A.   3D PARABOLIC EQUATION ALGORITHM

This section provides an overall view of the 3D PE model algorithm flow diagram as illustrated by Figure 3. The method of implementing the algorithm in MatLab is also presented. Obstacles' placements and terrains are also discussed in the context of simulation. Additional details are provided in the subsequent sections.

$$\tilde{H}_y(0^+, k_y, k_z) = \frac{1}{2}\left[1 + \Gamma_{\parallel}(k_z)\right]\tilde{H}_{ye}(0^+, k_y, k_z) + \frac{1}{2}\left[1 - \Gamma_{\parallel}(k_z)\right]\tilde{H}_{yo}(0^+, k_y, k_z)$$

Apply Hanning window
in frequency domain

$x \rightarrow x + \Delta x$

$e^{ik_x\Delta x}$ (free space propagator)

2D IFFT w.r.t. k_y and k_z
Hanning window in spatial domain

$H_y(x, k_y, k_z)$

Insert Obstacles

$H_y(x^+, y, z)$ Field adjust for screens at x

Even part   Odd part

$H_{ye}(x, y, z)$ $H_{yo}(x, y, z)$

2D FFT w.r.t. y & z

$\tilde{H}_{ye}(x, k_y, k_z)$ $\tilde{H}_{yo}(x, k_y, k_z)$

Hanning Window
in frequency domain

$\frac{1}{2}\left[1 + \Gamma_{\parallel}(k_z)\right]$ $\tilde{H}_y(x, k_y, k_z)$ $\frac{1}{2}\left[1 - \Gamma_{\parallel}(k_z)\right]$
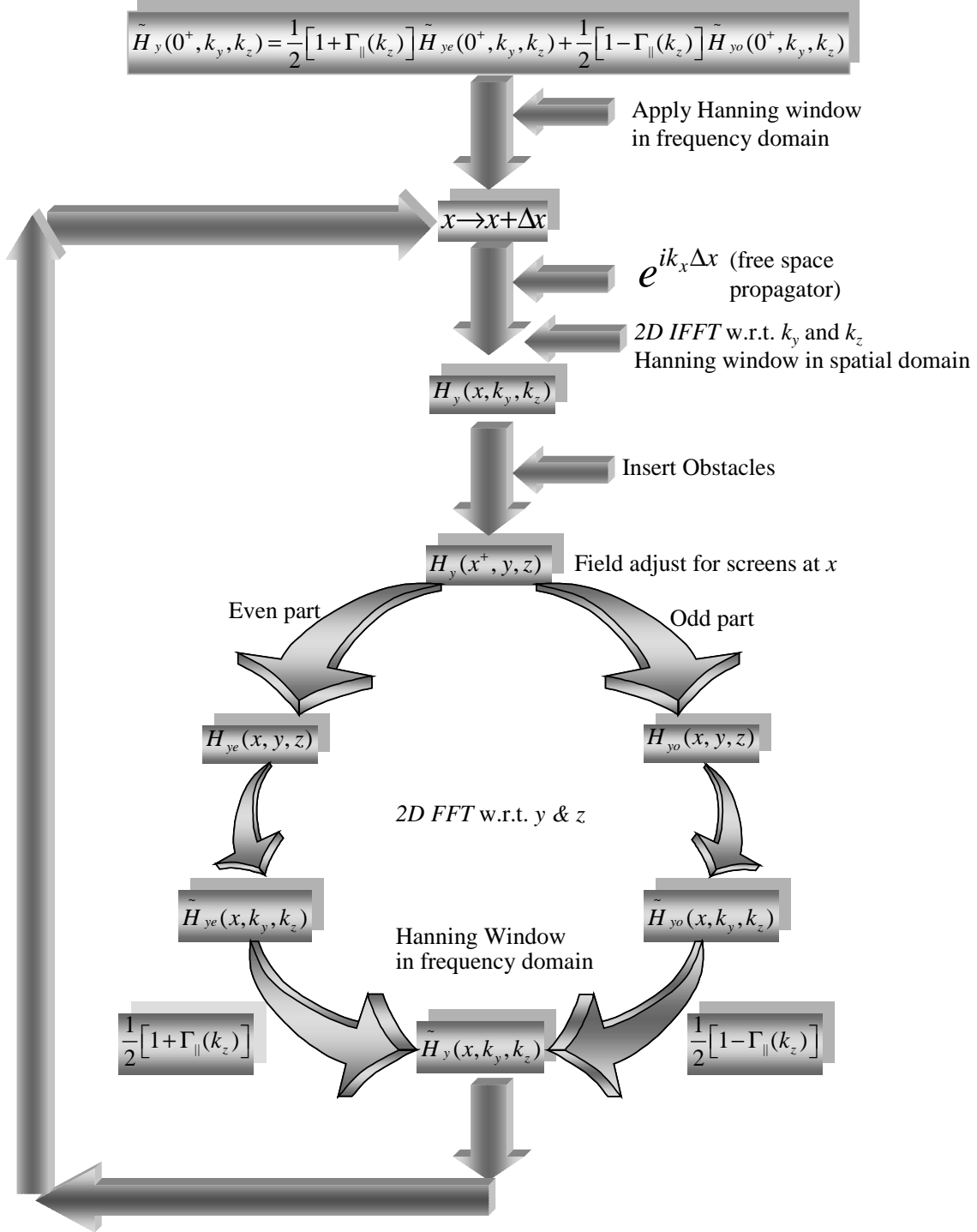
Figure 3.   3D PE Numerical Evaluation Flow Diagram.

The initial magnetic field $H(0, y, z)$ is assumed to be generated by the current source on a flat plane. The Gaussian current source along the *z*-axis gives rise to a

7

circumferential magnetic field with a lateral component, $H_y(x, y, z)$. It is described in

Section C. The transformed magnetic field $\tilde{H}_y(0^+, k_y, k_z)$ provides the initial field for

the beginning of the main loop of the algorithm as shown in Figure 3, where the tilde

indicates the transformed. When $\tilde{H}_y(0^+, k_y, k_z)$ is multiplied by the free-space

propagator $e^{ik_x\Delta x}$, the initial transformed field has marched from the previous location x

to a new location $x + \Delta x$ and is given by equation (2.1). The field is split into even and

odd parts for numerical convenience.

$$\tilde{H}_y(x+\Delta x, k_y, k_z) = \left\{ \begin{array}{l} \dfrac{1}{2}\left[1+\Gamma_{\parallel}(k_z)\right]\tilde{H}_{ye}(x^+, k_y, k_z) \\[2mm] +\dfrac{1}{2}\left[1-\Gamma_{\parallel}(k_z)\right]\tilde{H}_{y0}(x^+, k_y, k_z) \end{array} \right\} e^{ik_x\Delta x} \qquad (2.1)$$

The quantity $\Gamma_{\parallel}(k_z)$ is the reflection coefficient of a plane wave for parallel polarization.

Then the magnetic field $H_y(x, y, z)$ at a new location $x + \Delta x$ just right before the

screen is found by double integrating equation (2.1) and is expressed by equation (2.2).

$$H_y(x, y, z) = \frac{1}{4\pi^2} \int_{-\infty}^{\infty}\int_{-\infty}^{\infty} \tilde{H}_y(x+\Delta x, k_y, k_z) e^{i(k_y z + k_z z)} dk_y dk_z \qquad (2.2)$$

If we examine equation (2.2), it is basically a 2D inverse Fourier transform, *(IFFT)*, of

the left hand side of equation (2.1) with respect to k_y and k_z. Then instead of evaluating

equation (2.2) by complex double integrations, the *2D (N_y x N_z) IFFT* is used to evaluate

it. The equivalent MatLab expression to equation (2.2) is defined by equation (2.3).

$$H_y(x, y, z) = \frac{\Delta k_y \Delta k_z}{(2\pi)^2} IFFT2\left(\tilde{H}_y(x, k_y, k_z)\right)(N_y N_z). \qquad (2.3)$$

Also, MatLab divides the results by N_y x N_z when it performs a *2D IFFT* operation;

therefore, the results are de-normalized by multiplying them by N_y x N_z. The results are

multiplied by a Hanning window in spatial domain to prevent aliasing effects.

8

At this point, after the magnetic field $H_y(x, y, z)$ has been found just before the screen, the obstacles are introduced that represent buildings, houses, trees, etc. in the simulation. In all the test problems, screens are used as obstacles and assumed to be perfectly absorbing. These screens represent rows of buildings having height H_k and width W_k. The H_k and W_k parameters are used to study the effects on the propagation factor and field strengths. All incident fields on the screens are eliminated since they are perfectly absorbing. The fields that propagate forward consist of the diffracted and the reflected waves. The $H_y(x^+, y, z)$ indicates the field after adjusting for screens at location x. Then the fields begin their march immediately after the screen. Figure 4 illustrates an example of a hilly terrain with multiple screens of uniform heights and equal spacing between the transmitter and the receiver. The propagation factor F and the field strengths may be determined at each marching step as the fields propagate forward. The data are stored as an array.
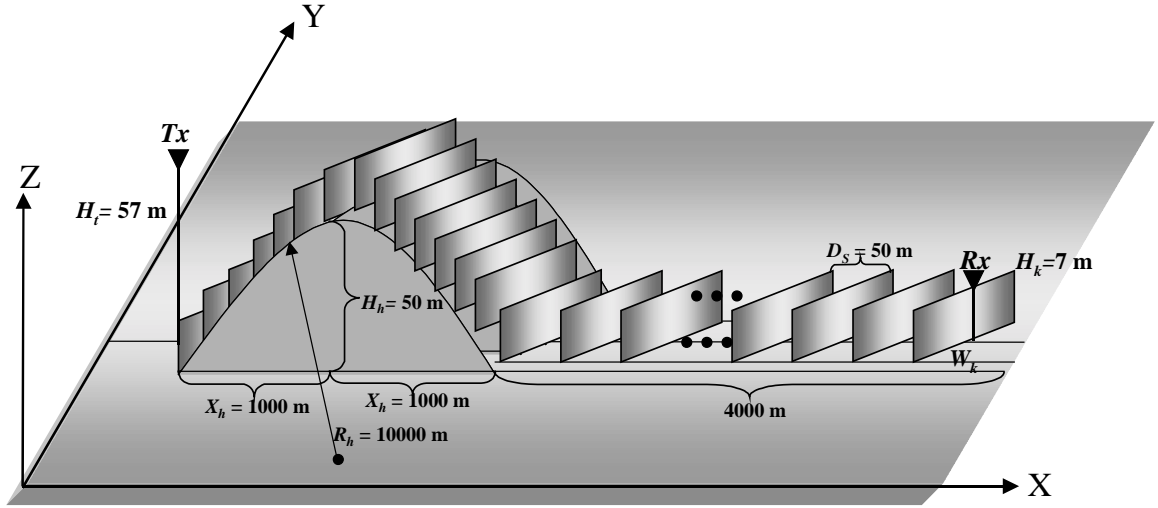
Figure 4.   Hilly Terrain and Multiple Equal Height and Equally Spaced Screens.

Once the magnetic field $H_y(x, y, z)$, at a new location x, has been found, it may be expressed in terms of odd and even parts to ensure there are no discontinuities at zero crossing that cause erroneous results during the 2D Fourier transform (*FFT*) operations. The odd $H_{y0}(x, y, z)$ and even $H_{ye}(x, y, z)$ fields are given as:

9

$$H_{yo}(x,y,z) = \begin{cases} H_y(x,y,z) & z > 0 \\ -H_y(x,y,-z) & z < 0 \end{cases} \tag{2.4}$$

$$H_{ye}(x,y,z) = \begin{cases} H_y(x,y,z) & z > 0 \\ H_y(x,y,-z) & z < 0 \end{cases} \tag{2.5}$$

The transformed quantities $\tilde{H}_{y0}(x,k_y,k_z)$ and $\tilde{H}_{ye}(x,k_y,k_z)$ are found by the following equations:

$$\tilde{H}_{y0}(x,k_y,k_z) = \int_{-\infty}^{\infty}\int_{-\infty}^{\infty} H_{y0}(x,y',z')e^{-i(k_y y' + k_z z')}dy'dz' \tag{2.6}$$

$$\tilde{H}_{ye}(x,k_y,k_z) = \int_{-\infty}^{\infty}\int_{-\infty}^{\infty} H_{ye}(x,y',z')e^{-i(k_y y' + k_z z')}dy'dz' \tag{2.7}$$

Equations (2.6) and (2.7) are essentially the 2D Fourier transforms, *2D FFT's*, of $H_{y0}(x,y,z)$ and $H_{ye}(x,y,z)$ with respect to y and z. The equivalent Matlab operations of equations (2.6) and (2.7) are defined as:

$$\tilde{H}_{y0}(x,k_y,k_z) = \Delta y \Delta z FFT2\big(H_{y0}(x,y,z)\big) \tag{2.8}$$

$$\tilde{H}_{ye}(x,k_y,k_z) = \Delta y \Delta z FFT2\big(H_{ye}(x,y,z)\big) \tag{2.9}$$

Next the odd and even transformed magnetic fields are multiplied by the Hanning window in frequency domain to prevent aliasing. Then the odd transformed $\tilde{H}_{y0}(x,k_y,k_z)$ is multiplied by a factor $\frac{1}{2}\big[1-\Gamma_{\parallel}(k_z)\big]$, and the even transformed $\tilde{H}_{ye}(x,k_y,k_z)$ is multiplied by $\frac{1}{2}\big[1+\Gamma_{\parallel}(k_z)\big]$. These fields are then combined to provide the newly transformed magnetic field immediately after the screen, i.e. $\tilde{H}_y(0^+,k_y,k_z)$. The steps in the main loop as illustrated in Figure 3 are repeated until the desired receiver location is reached. The propagation factor F at the final range is

10

defined as the normalized field $\left| H_y(x,y,z)/H_y(f.s.)\right|$, where $H_y(f.s.)$ is the free-space magnetic field and is defined as:

$$H_y(f.s.) = -ik_0 \sin(\theta)\cos(\phi)\frac{1}{4\pi}\tilde{g}\left(k_0 \cos(\theta)\right)\frac{e^{ik_0 R}}{R} \qquad (2.10)$$

where θ and ϕ are the angles in spherical coordinates, $i = \sqrt{-1}$, and $\tilde{g}(k_z)$ defined by equation (2.20) is the vertical plane response of the current source. R is a range between the transmitter and receiver, and k_0 is the free space wave number. R, ρ, θ, and ϕ are defined by the following equations:

$$R = \sqrt{(z - H_t)^2 + \rho^2} \qquad (2.11)$$

$$\rho = \sqrt{x^2 + y^2} \qquad (2.12)$$

$$\theta = \sin^{-1}\left(\frac{\rho}{R}\right) \qquad (2.13)$$

$$\phi = \sin^{-1}\left(\frac{y}{\rho}\right) \qquad (2.14)$$

The current density and its characteristics are discussed in the next section.

B. GAUSSIAN CURRENT SOURCE

The fields are excited by a vertically polarized current source with a prescribed aperture distribution $f(z)$. We choose a Gaussian distribution current source to allow us to match the source standard deviation, σ_z, to the transmitting antenna 3 dB elevation beam width, Θ_{el} [Ref. 3, 4]. It is also convenient to relate the magnetic field to the current source. We consider a transmitting antenna at height $z = H_t$ and the current source density $\vec{J}$ as defined by equation (2.15).

$$\vec{J} = \hat{z} I_o l \delta(y - 0) f(z) \qquad (2.15)$$

where

11

$$f(z) = \frac{1}{\sigma_z \sqrt{2\pi}} e^{-(z-H_t)^2/2\sigma_z^2} \qquad (2.16)$$

is a Gaussian current source with a standard deviation of σ_z, $I_o l$ is a current moment [Ref. 11], and $\delta(y-0)$ is a dirac function. Figure 5 shows the vertically polarized Gaussian current density function $\vec{J}$ placed over an impedance plane. The current is assumed to be independent of y and has a peak at $z = H_t$. σ_z is its standard deviation and may be chosen from Table 1 to fit the required transmitting antenna 3 dB elevation beam width, Θ_{el} [Ref. 3]. It may be observed that $R = \sqrt{(z-H_t)^2 + \rho^2}$ is the direct distance from the source, $\rho = \sqrt{x^2 + y^2}$ is the horizontal distance from the source, and θ and ϕ are angles in spherical coordinate defined by $\theta = \sin^{-1}\left(\frac{\rho}{R}\right)$ and $\phi = \sin^{-1}\left(\frac{y}{\rho}\right)$. For the geometry shown, the only non-zero field components are E_z, E_ρ, and H_ϕ.
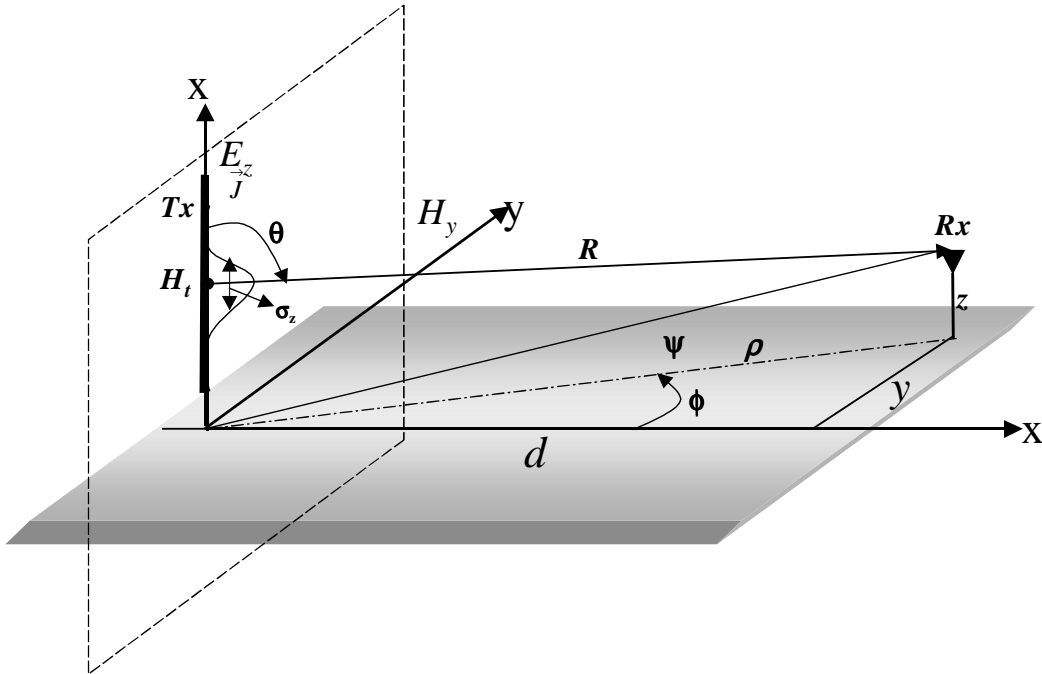
Figure 5.   Gaussian Density Current Source over an Impedance Plane.

12

Figure 6 illustrates the Gaussian current source function $f(z)$ with $H_t = 10$ m and $\sigma_z = \lambda$. We discuss the magnetic field in detail in the next section.

Θ_{el} , deg	σ_z / λ
60	0.20
45	0.30
30	0.45
15	1.00
10	1.52
5	3.03

Table 1. Transmitting Antenna Elevation Beam Width Versus σ_z [From: Ref. 3].
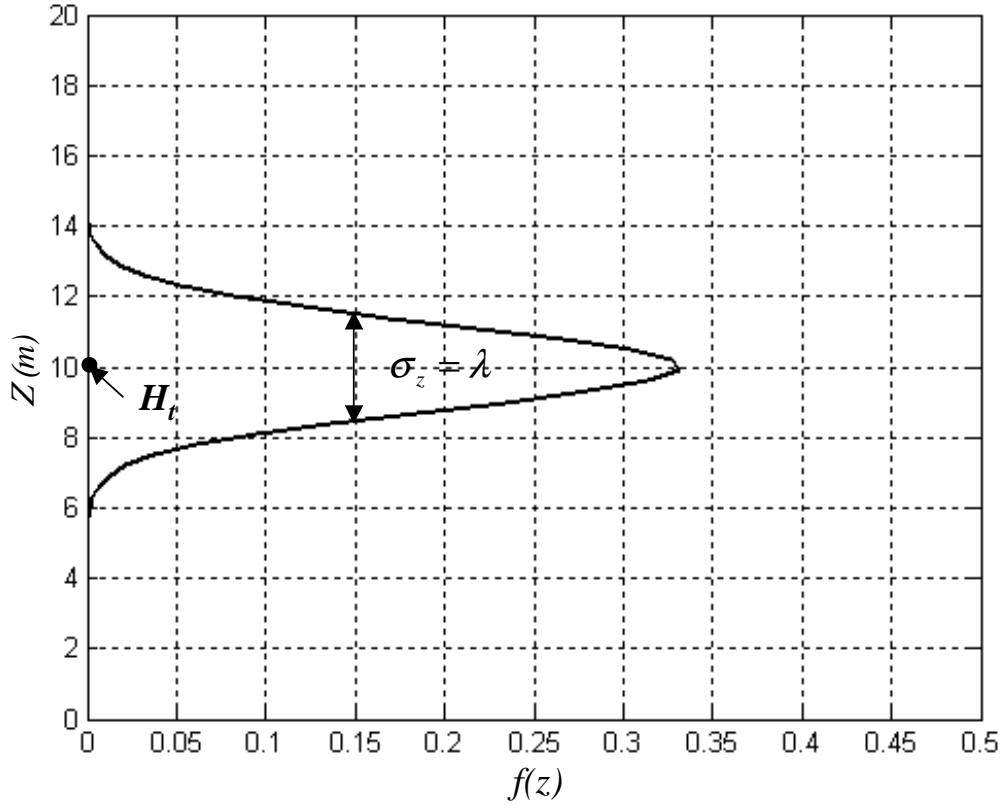
Figure 6. Gaussian Current Source Distribution Function.

13

The function $f(z)$ can be written in terms of its odd and even functions, $f_o(z)$ and $f_e(z)$, respectively, to permit a more accurate computation of the Fourier transform in the vertical direction. The odd and even extensions of $f(z)$ are given in equations (2.17) and (2.18).

$$f_o(z) = \begin{cases} f(z) & z > 0 \\ -f(-z) & z < 0 \end{cases} \qquad (2.17)$$

$$f_e(z) = \begin{cases} f(z) & z > 0 \\ f(-z) & z < 0 \end{cases} \qquad (2.18)$$

The functions $f_o(z)$ and $f_e(z)$ are shown in Figures 7 and 8. If we add the $f_o(z)$ and $f_e(z)$ together and divide by ½, we will get back the original function $f(z)$. Hence, the function decomposition into its odd and even parts to facilitate computation is a valid one.
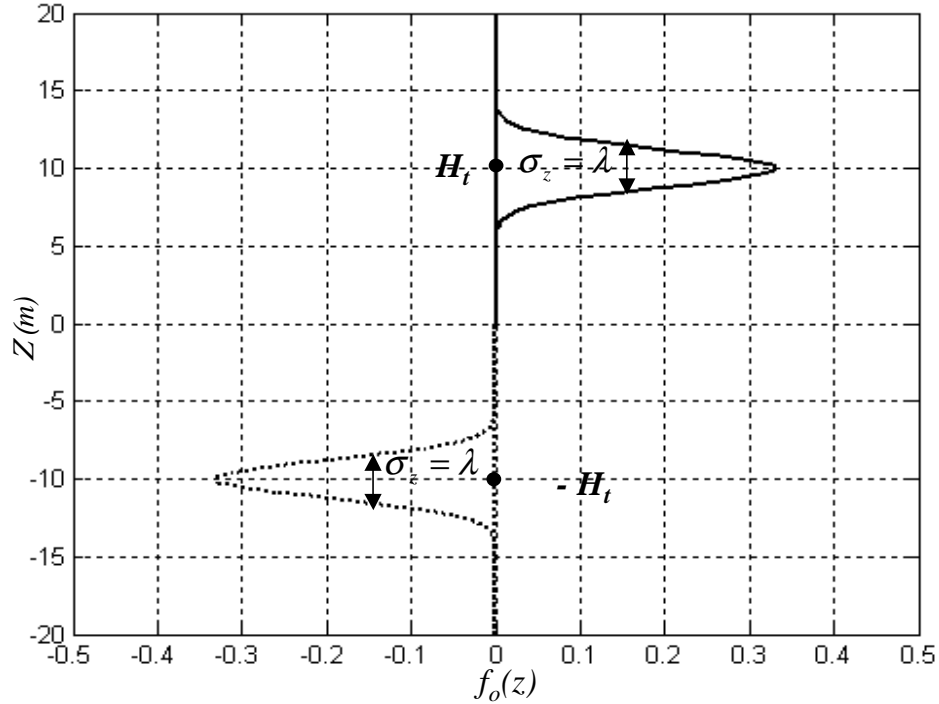
Figure 7.   Odd Part of $f(z)$.

14
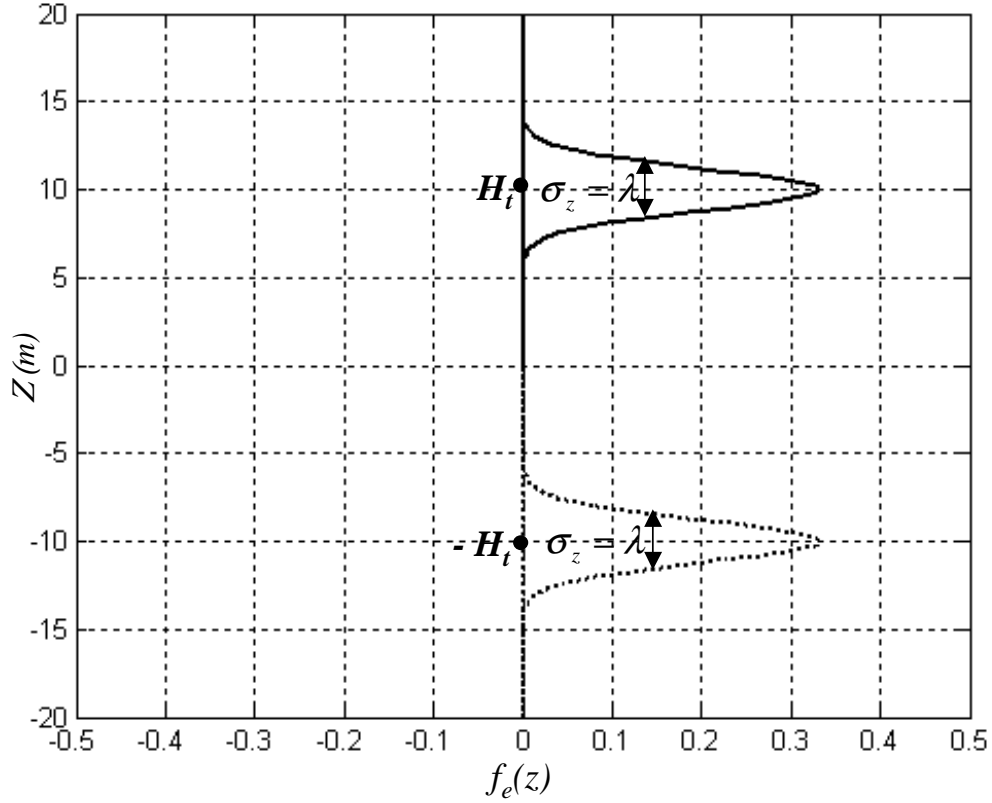
Figure 8.   Even Part of $f(z)$.

We need to examine the Fourier transform of the current source density $\vec{J}$. We shall use the transformed information to derive the initial transformed magnetic field in Section B. Since $\vec{J}$ is independent of *y*, if we take the Fourier transform of equation (2.15) with respect to *z*, which is tantamount to taking the Fourier transform *(FFT)* of $f(z)$. The *FFT* of $\delta(y-0)$ with respect to *y* is equal to 1. Therefore, the Fourier transform of $f(z)$ with respect to *z* is given below:

$$\tilde{f}(k_z) = e^{-ik_z H_t} e^{-k_z^2 \sigma_z^2 /2} = \tilde{g}(k_z) e^{-ik_z H_t} \tag{2.19}$$

where $\tilde{g}(k_z)$ is defined as

$$\tilde{g}(k_z) = e^{-k_z^2 \sigma_z^2 /2} \tag{2.20}$$

15

It is easy to see that

$$\tilde{f}_e(k_z) = 2\,\tilde{g}(k_z)\cos(k_z H_t) \tag{2.21}$$

$$\tilde{f}_o(k_z) = -2i\,\tilde{g}(k_z)\sin(k_z H_t) \tag{2.22}$$

C.   MAGNETIC FIELDS

In this section, we derive the initial transformed magnetic field $\tilde{H}_y(x, k_y, k_z)$ from the transformed current source $\tilde{f}(k_z)$. The fields march in the transformed space, and the propagation factor or the field strength is determined in the physical space. Then the basic 3D parabolic equation (PE) algorithm will start with the initial transformed magnetic field $\tilde{H}_y(0^+, k_y, k_z)$ as illustrated in Figure 3, where 0^+ indicates the field immediately after the screen. Since there is no screen for the initial field, 0^+ is equal to 0.

First we need to define the relationship between the initial magnetic field $H_y(0^+, y, z)$ and the current density function $\vec{J}$. The initial $H_y(0^+, y, z)$ relates to the current density $\vec{J}$ is described by equation (2.23) [Ref. 11]

$$
\begin{aligned}
H_y(0^+, y, z) &= \frac{1}{2} \int_{-\infty}^{\infty}\int_{0}^{\infty} \delta(y'-0) f(z')\, dy'\, dz' \\
&\quad + \frac{1}{4\pi} \int_{-\infty}^{\infty} e^{ik_z(z+z')}\Gamma_{\|}(k_z)\, dk_z \int_{-\infty}^{\infty} dy' \int_{0}^{\infty} f(z')\, dz' \\
&\quad - \frac{i}{2}\sum \text{Res}\left[\Gamma_{\|}(k_z)\right] e^{ik_{zn}z} \int_{-\infty}^{\infty} dy' \int_{0}^{\infty} dz'\, \delta(y'-0) f(z') e^{ik_{zn}z'} \\
&= \frac{1}{2} f(z) + \frac{1}{2} \int_{0}^{\infty} f(z')\, dz'. \\
&\quad \left[\frac{1}{2\pi} \int_{-\infty}^{\infty} e^{ik_z(z+z')}\Gamma_{\|}(k_z)\, dk_z - i\sum \text{Res}\left[\Gamma_{\|}(k_z)\right] e^{ik_{zn}(z+z')}\right] \\
&\approx \frac{1}{2} f(z)
\end{aligned}
\tag{2.23}
$$

16

where the second part of equation (2.23) describes the surface waves. In many long-range propagation problems, particularly in the VHF band and above, it is possible to completely ignore the surface wave terms as they decay rapidly with range [Ref. 5]. Then equation (2.23) is reduced to a simple relationship between the $H_y\left(0^+, y, z\right)$ and the Gaussian current source function $f(z)$.

Again, to ensure there is no discontinuity at zero crossing that gives erroneous results in the 3D PE numerical calculation, the magnetic field may be defined in terms of its odd and even parts, $H_{yo}\left(x, y, z\right)$ and $H_{ye}\left(x, y, z\right)$, respectively. The methods are the same as in equations (2.4) and (2.5).

From equations (2.4), (2.5), (2.23), and the transformed odd $\tilde{f}_o\left(k_z\right)$ and even $\tilde{f}_e\left(k_z\right)$ current sources as defined by equations (2.21) and (2.22), we can easily derive the initial transformed odd $\tilde{H}_{yo}\left(0^+, k_y, k_z\right)$ and even $\tilde{H}_{ye}\left(0^+, k_y, k_z\right)$ magnetic fields. The initial odd transformed magnetic field $\tilde{H}_{yo}\left(0^+, k_y, k_z\right)$ is defined by equation (2.24)

$$
\begin{aligned}
\tilde{H}_{y0}\left(0^+, k_y, k_z\right) &= \frac{1}{2}\tilde{f}_o(k_z) \\
&= -ie^{-k_z^2\sigma_z^2/2}\sin\left(k_z H_t\right)
\end{aligned}
\tag{2.24}
$$

The initial even transformed magnetic field $\tilde{H}_{ye}\left(0^+, k_y, k_z\right)$ is defined by equation (2.25)

$$
\begin{aligned}
\tilde{H}_{ye}\left(0^+, k_y, k_z\right) &= \frac{1}{2}\tilde{f}_e\left(k_z\right) \\
&= e^{-k_z^2\sigma_z^2/2}\cos\left(k_z H_t\right)
\end{aligned}
\tag{2.25}
$$

These fields are defined as column vectors having N_z elements. From Section A, we know that the current density function $\vec{J}$ is independent of y, and the

$FFT(\delta(y-0))=1$; then we can repeat the column of the initial transformed $\tilde{H}_{y0}(0^+,k_y,k_z)$ and $\tilde{H}_{ye}(0^+,k_y,k_z)$ N_y times. Now we have the *2D* initial transformed $\tilde{H}_{y0}(0^+,k_y,k_z)$ and $\tilde{H}_{ye}(0^+,k_y,k_z)$ with dimension of N_y x N_z. The number of elements along the y-axis and z-axis are N_y and N_z, respectively.

The transformed magnetic field $\tilde{H}_y(x,k_y,k_z)$ is defined by equation (2.26).

$$\tilde{H}_y(x,k_y,k_z)=\int_{-\infty}^{\infty}dy'\int_0^{\infty}dz'e^{-ik_yy'}\left[e^{-ik_zz}+\Gamma_{\parallel}(k_z)e^{ik_zz'}\right]H_y(x,y',z') \qquad (2.26)$$

Recall that e^{-ik_zz} and e^{ik_zz} are the free-space propagators for direct and reflected rays, respectively, and *y'* and *z'* are dummy variables of integration. $\Gamma_{\parallel}(k_z)$ is the reflection coefficient for the parallel polarization as a function of k_z in the complex k_z plane and in terms of normalized impedance Z_s. $\Gamma_{\parallel}(k_z)$ and Zs are expressed as :

$$\Gamma_{\parallel}(k_z)=\frac{k_z-k_0Z_s}{k_z+k_0Z_s} \qquad (2.27)$$

$$Z_s=\frac{1}{\sqrt{\varepsilon_{rc}}} \qquad (2.28)$$

$$\varepsilon_{rc}=\varepsilon_r+\frac{i18\sigma(mS/m)}{f(MHz)} \qquad (2.29)$$

where *f* is the operating frequency measured in MHz. We use equations (2.4) and (2.5) to decompose the magnetic field $H_y(x,y',z')$ into $H_{yo}(x,y',z')$ and $H_{ye}(x,y',z')$ and substitute them into equation (2.26). Now we add the $H_{yo}(x,y',z')$ and $H_{ye}(x,y',z')$ together for $z>0$ and perform variable substitutions to change the inner limit of integration from 0 to ∞ to -∞ to ∞ and divide it by ½, and similarly for $z<0$. The result is:

$$\tilde{H}_y\left(x, k_y, k_z\right) = \frac{1}{2}\left[1 + \Gamma_{\parallel}\left(k_z\right)\right] \int_{-\infty}^{\infty} \int_{-\infty}^{\infty} H_{ye}\left(x, y', z'\right) e^{-i\left(k_y y' + k_z z'\right)} dy' dz'$$

$$\frac{1}{2}\left[1 - \Gamma_{\parallel}\left(k_z\right)\right] \int_{-\infty}^{\infty} \int_{-\infty}^{\infty} H_{y0}\left(x, y', z'\right) e^{-i\left(k_y y' + k_z z'\right)} dy' dz' \qquad (2.30)$$

$$= \frac{1}{2}\left[1 + \Gamma_{\parallel}\left(k_z\right)\right] \tilde{H}_{ye}\left(x, k_y, k_z\right) + \frac{1}{2}\left[1 - \Gamma_{\parallel}\left(k_z\right)\right] \tilde{H}_{y0}\left(x, k_y, k_z\right)$$

If we examine equation (2.30), we see that the double integrations of $H_{ye}\left(x, y', z'\right)$ and $H_{yo}\left(x, y', z'\right)$ are the *2D* Fourier transforms (*FFT's*) of these fields. Thus equation (2.30) can be evaluated with the *2D (N_y x N_z) FFT's* instead of complex double integrations. Thus $\tilde{H}_y\left(x, k_y, k_z\right)$ can be defined in terms of $\tilde{H}_{yo}\left(x, y, z\right)$ and $\tilde{H}_{ye}\left(x, y, z\right)$. This is how we are going use the *2D FFT's* in the MatLab codes to implement equation (2.30).

After making the adjustment for the screens, the fields begin their march in range immediately after the screen expressed as

$$\tilde{H}_y\left(x^+, k_y, k_z\right) = \frac{1}{2}\left[1 + \Gamma_{\parallel}\left(k_z\right)\right] \tilde{H}_{ye}\left(x^+, k_y, k_z\right)$$

$$+ \frac{1}{2}\left[1 - \Gamma_{\parallel}\left(k_z\right)\right] \tilde{H}_{y0}\left(x^+, k_y, k_z\right). \qquad (2.31)$$

Equation (2.31) provides the initial transformed magnetic field for the beginning of the main loop of the 3D PE algorithm as shown in Figure 3. Once again, x^+ indicates the fields immediately after the screen. The initial fields $\tilde{H}_{y0}\left(x^+, k_y, k_z\right)$ and $\tilde{H}_{ye}\left(x^+, k_y, k_z\right)$ are defined as matrices having N_y x N_z elements. These fields will allow the algorithm to account for all the vertical and lateral propagation of waves, which is the fundamental goal of the 3D PE formulation. Previously developed 2D PE algorithms based on the vertical plane method did not account for the laterally propagating of waves. Consequently, the mean path loss was overestimated and the standard deviation of error tends to be higher [Ref. 11]. Therefore, the 3D PE formulation is expected to

substantially improve the accuracy relative to the *2D* vertical plane method for the test problems.

When we previously performed column-repeating the initial $\tilde{H}_{y0}\left(0^+, k_y, k_z\right)$ and $\tilde{H}_{ye}\left(0^+, k_y, k_z\right)$ by N_y times to create the *2D (N_y x N_z)* $\tilde{H}_{y0}\left(0^+, k_y, k_z\right)$ and *2D* $\tilde{H}_{ye}\left(0^+, k_y, k_z\right)$, it was to ensure that the matrices always have dimension of N_y x N_z since this is a general aperture case. When N_y is not equal to N_z, we have a rectangular aperture, and when they are equal to each other, we have a square aperture. The 3D PE algorithm is implemented to support any N_y x N_z aperture. Where N_y and N_z are elements along the vertical and horizontal ranges, respectively, with a suitable power of 2, i.e., N_y = 1024 or 2048.

Discussion thus far pertains to what happens outside of the main loop of the algorithm. Equation (2.31) provides the initial transformed field for the beginning of the main loop for the 3D PE algorithm; then we multiply $\tilde{H}\left(0^+, k_y, k_z\right)$ by the Hanning window in frequency domain before marching. We always multiply the fields by the Hanning window before taking *2D* Fourier transform *(FFT's)* or *2D* inverse Fourier transform *(IFFT's)* to contain them in space and wavenumber domains. The Hanning window is discussed in the next section.

D.   THE HANNING WINDOW

In order to contain the fields in space and wavenumber domains we multiply them with the Hanning window [Ref. 3] before taking *2D* Fourier transform *(FFT's)* or *2D* inverse Fourier transform *(IFFT's)*. The Hanning window provides a gradual rolloff to zero over the last quarter of the domain, and may be constructed from the two Hanning sequences below. Equations (2.32) and (2.33) are the Hanning sequences along the horizontal range *(y-direction)* and the vertical range *(z-direction)*, respectively. The mirror images of $h_y(t)$ and $h_z(t)$ below $t = 0$ are used for negative wave numbers.

$$h_y(t) = \begin{cases} 1 & \text{for } 0 \le t \le 3N_y/8 \\ \sin^2\left(\dfrac{4\pi t}{N_y}\right) & \text{for } 3N_y/8 \le t \le N_y/2 \end{cases} \qquad (2.32)$$

$$h_z(t) = \begin{cases} 1 & \text{for } 0 \le t \le 3N_z/8 \\ \sin^2\left(\dfrac{4\pi t}{N_z}\right) & \text{for } 3N_z/8 \le t \le N_z/2. \end{cases} \qquad (2.33)$$

The Hanning window, in general, has a rectangular shape since N_y and N_z are not necessarily equal. When N_y and N_z are equal, then the Hanning window has a square shape as discussed in the previous section. Figures 9 and 10 illustrate the examples of 512 elements of $h_y(t)$ and $h_z(t)$ Hanning sequences.
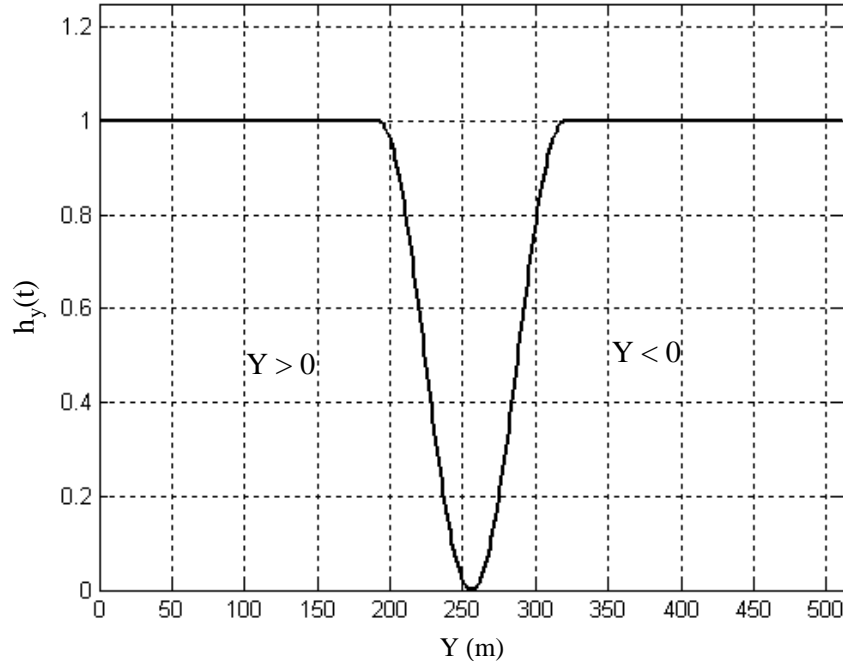
Figure 9. $h_y(t)$ Hanning Sequence.
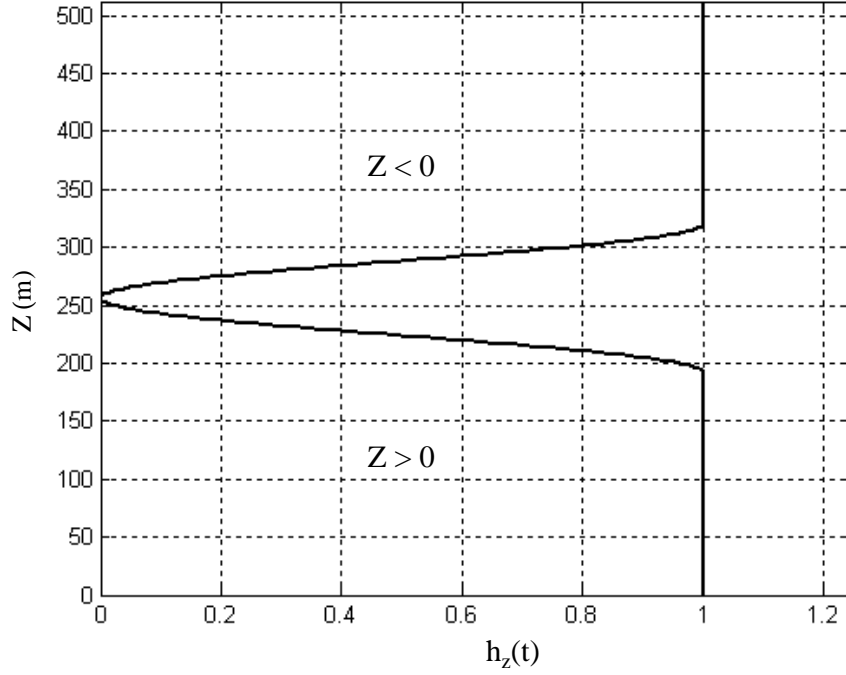
Figure 10. $h_z(t)$ Hanning Sequence.

As in the previous section, the Hanning window must have a dimension of N_y x N_z. Again, the procedure is similar to Section C; we first create a matrix from the Hanning sequence $h_z(t)$ by column repeating the sequence N_y times. This method creates a N_y x N_z matrix from the $h_z(t)$ sequence. Then we construct the second matrix from the Hanning sequence the $h_y(t)$ by row-repeating it N_z times (thereby constructing a N_y x N_z matrix from $h_y(t)$ sequence). We column-repeated $h_z(t)$ N_y times to also ensure that we do not create a matrix that has a column dimension greater than N_y. The same is true for the $h_y(t)$ case. We row-repeated N_z times to ensure that the row of the matrix does not have dimension greater than N_z. This implements the Hanning window in MatLab.

Figure 11 shows the two Hanning matrices created from $h_z(t)$ and $h_y(t)$. To construct the final Hanning window, the two matrices are multiplied together element by element. Figure 12 shows an example of a 512 x 512 Hanning window. A similar

22

Hanning window is used in the 3D PE algorithm depending on the dimensions of N_y and N_z.
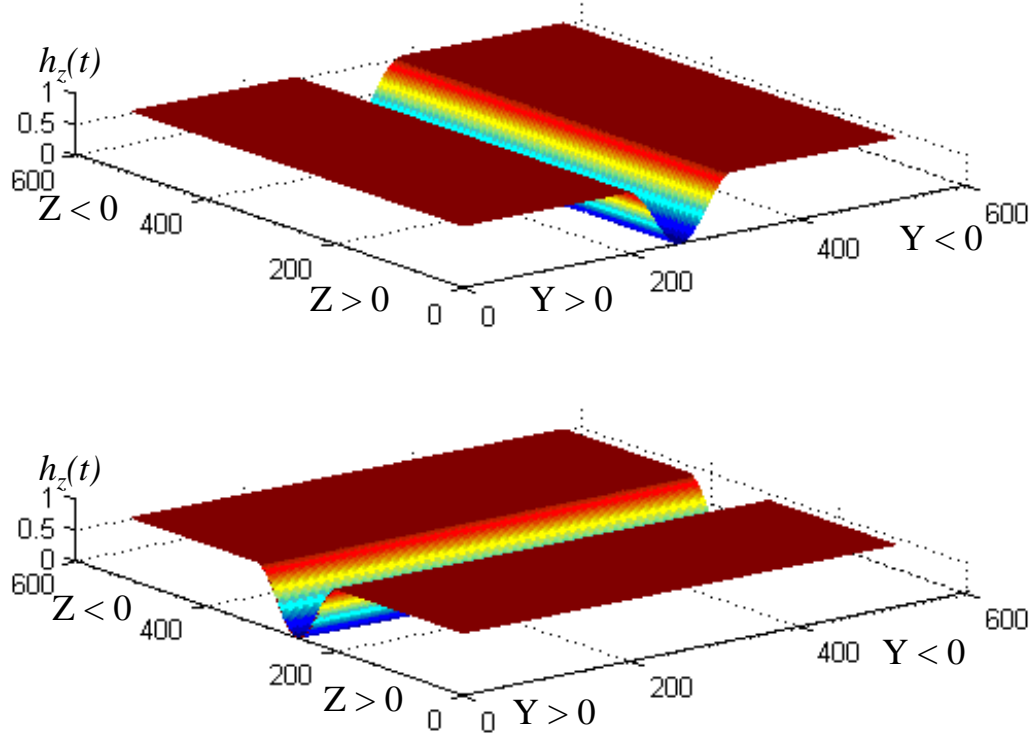
Figure 11. $h_y(t)$ and $h_z(t)$ Hanning Matrices.
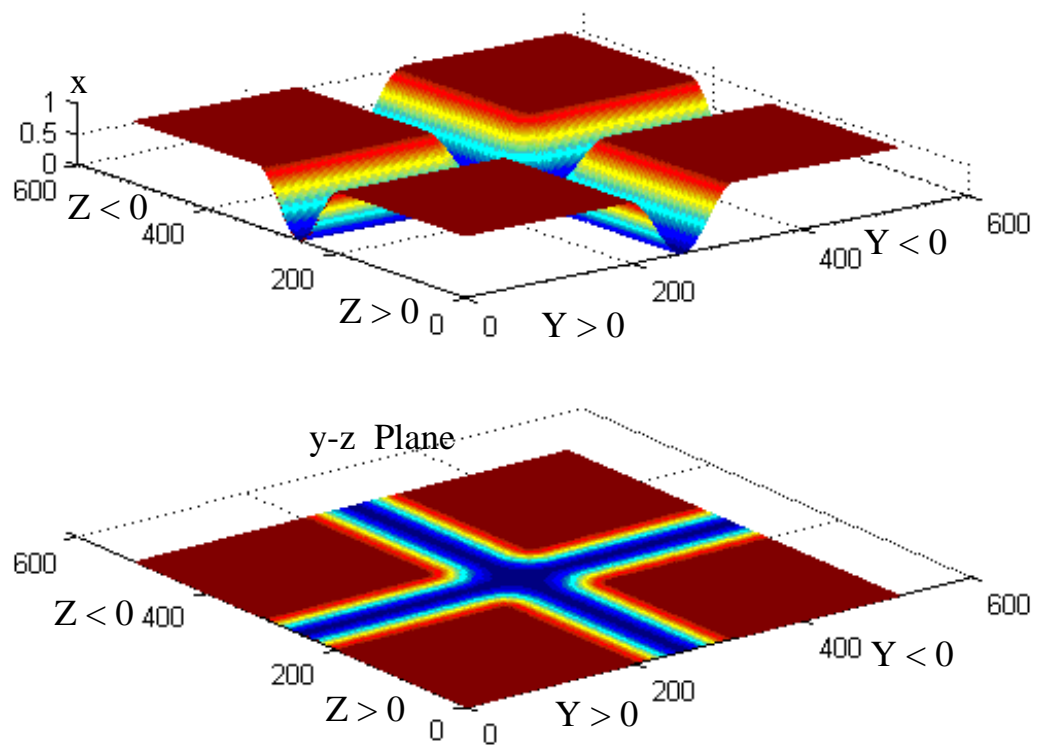
Figure 12.   3D Hanning Window.

24

E. SPATIAL AND FREQUENCY PARAMETERS

The values of Δx, Δy, Δz, Δk_y, and Δk_z, and the range of k_x, k_y, and k_z are dictated by the Nyquist sampling theorem. Δx is the range increment, Δy is the horizontal increment, and Δz is the vertical increment. k_x, k_y, and k_z are the range wavenumber, the horizontal wavenumber, and the vertical height wavenumber, respectively. Δk_y and Δk_z are the increments of the horizontal and the vertical wavenumbers, respectively. References 3, 11, and 12 provide details to obtain the values for these parameters.

For all the test problems in this thesis, we assume that $\Delta y = \Delta z = \lambda$ and $\sigma_z = \lambda$. We pick Δx between 25 m and 150 m. If we choose a smaller Δx, the computation takes longer. If we choose a larger Δx, the computation is accelerated, but we might miss the obstacles that are within in the marching step. Therefore, Δx has to be optimally chosen accordingly for each problem. However, Δx can be chosen to have variable values within a simulation. Furthermore, for $\sigma_z = \lambda$ corresponding to the transmitting antenna of a 3-dB bandwidth of 15° is shown in Table 2. The value of σ_z can be picked from Table 2 to match the transmitting antenna 3-dB bandwidth.

We compute the propagation factor F at the final range as well as at each marching step. We also consider the field strengths at each marching step and on the rooftops. In Chapter III, we shall present the results for the flat earth case. The hilly terrain test problems are presented in Chapter IV.

THIS PAGE INTENTIONALLY LEFT BLANK

III. FLAT EARTH RESULTS

In this chapter, we present results for the propagation factors for the flat earth and perfectly reflecting ground. The propagation factor at the final range without obstacles between the transmitter and the receiver is simulated in Section A. The result of the 3D PE model is compared with the result of the two-ray model [Ref 2]. Next, in Section B, we place a single absorbing screen between the transmitter and the receiver and present the result for the propagation factor at the final range. The screen represents a building. The simulation result is compared with the result of the four-ray model [Ref. 2]. Then, in Section C, we place nine absorbing screens of uniform heights, equal spacing, and variable widths between the transmitter and the receiver. These screens represent a row of buildings or houses in residential areas of a city. In this case, the relative propagation factors are measured at the rooftops for each marching step. The results of the 3D PE model are compared with the results presented by Andersen [Ref. 6] and Lee [Ref. 7]. Finally in Section D, we examine 120 absorbing screens of uniform heights and equal spacing and measure the relative propagation factor at the final range. Again, these screens represent a row of buildings or houses in residential areas of a city. The result of the 3D PE model is compared with the numerical integration technique result proposed by Bertoni [Refs. 10].

A.   3D PE AND THE TWO-RAY MODEL RESULTS COMPARISON

In this section we stimulate the two-ray model and the 3D PE model with the same parameters and compare their results. Figure 13 shows the two-ray model over flat earth. The two-ray model propagation factor, F_{2ray}, [Ref. 2] is defined as follow with

$$F_{2ray} = \left|1 + \Gamma e^{ik_0 \Delta R}\right|, \qquad (3.1)$$

where $\Delta R = \dfrac{2H_t H_r}{d}$, $\Gamma = \dfrac{\sin\psi - Z_s}{\sin\psi + Z_s}$, $\psi = \tan^{-1}\left(\dfrac{H_t H_r}{d}\right)$, $\varepsilon_{rc} = \varepsilon_r + \dfrac{18\sigma(mS/m)}{f(Mhz)}$,

and $Z_s = \sqrt{\varepsilon_{rc} - \cos^2(\psi)}\,/\,\varepsilon_{rc} \approx \dfrac{1}{\sqrt{\varepsilon_{rc}}}$ $\quad \left|\varepsilon_{rc}\right| \gg 0$.

The H_t and H_r are the heights of the transmitter and receiver's antennas, respectively, and d is the horizontal distance between the transmitter and receiver. ΔR is the path difference between direct and reflected rays, and Γ is the reflection coefficient for parallel polarization as a function of the grazing angle ψ and the complex impedance Z_s. ε_{rc} and S are the complex dielectric constant and conductivity of the medium, respectively. It has been assumed that $d \gg H_t$ and H_r.
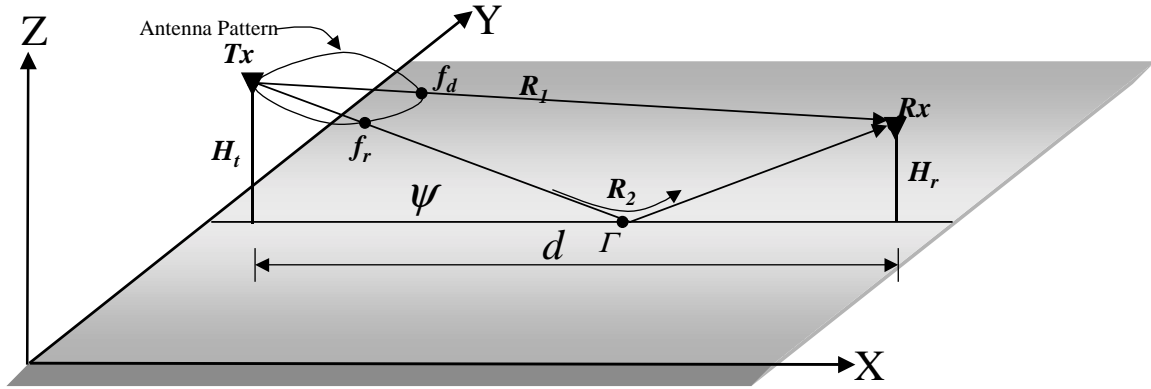
Figure 13.   Two-ray Model Over Flat Earth.

Figure 14 shows the vertical cut of the relative propagation factors, *F's*, of the two-ray model and 3D PE model. The two models are stimulated by the same parameters as listed on Figure 14. The results were taken at a range of 1000 m from the transmitter a over flat plane.   The circle with the solid line corresponds to the two-ray model and the plain solid line is the 3D PE result. The difference between the two results is within 1%. If we increase the height of the receiving antenna, the reflected ray will tend to decrease and the direct ray will dominate. Therefore, we expect the two *F's* to approach zero dB for large heights.
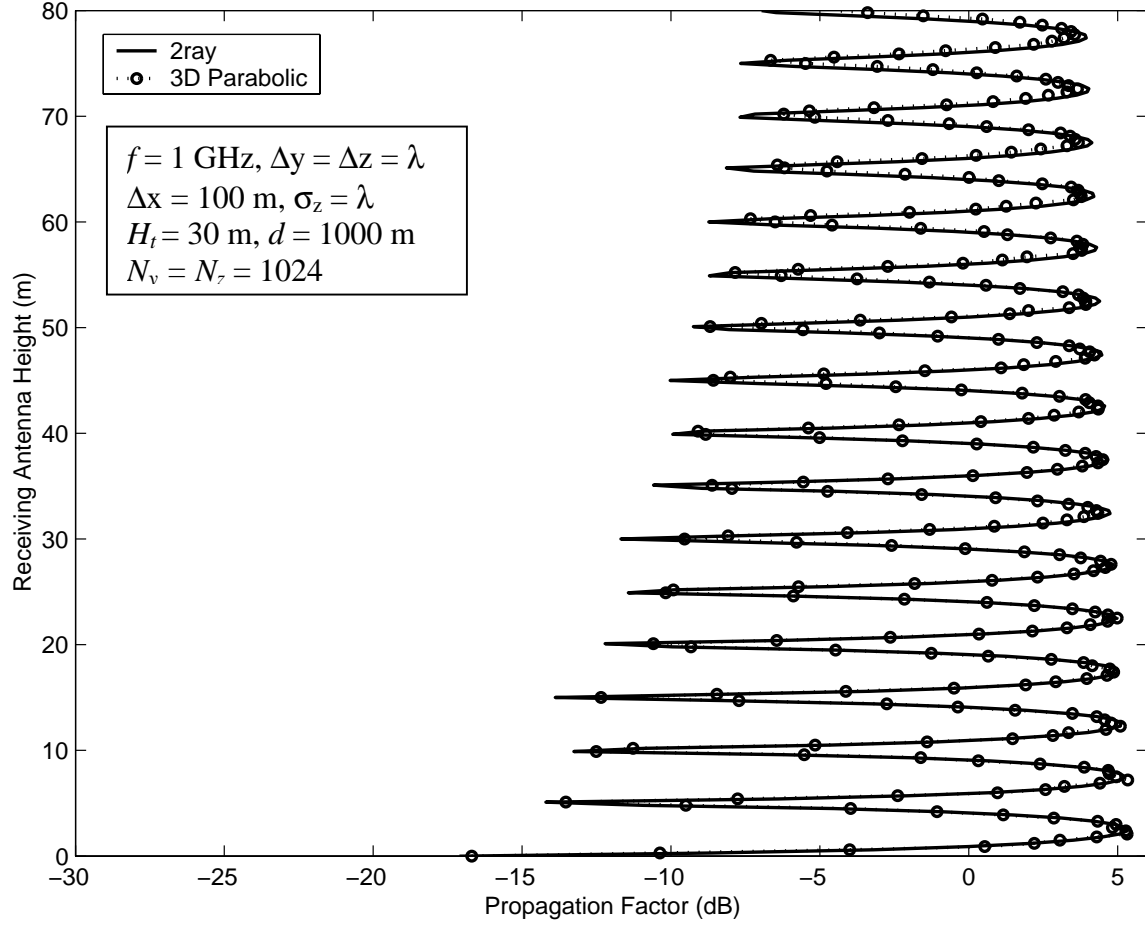
Figure 14.   3D PE and Two-ray Comparison (Vertical Cut).

B.   3D PE AND FOUR-RAY RESULTS COMPARISON

In Section A, we have shown that the result of the 3D PE agreed with the two-ray results. Now, we place a 50 m by 49.5 m absorbing screen (a single knife-edge) in the 3D PE model located 125 m from the transmitter and 375 m to the receiver with the frequency of operation of 1 GHz.   The loss in this case depends on the height of the knife-edge above ground, its relative location from the transmitter/receiver, the ground constants, and the frequency of operation. Figure 15 shows an absorbing knife-edge between the transmitter and the receiver. Table 2 provides the quantities required for the evaluation of the propagation factor $F_{k.e.}$ for the 2D-four-ray model [Ref. 2]. The 3D PE model and the four-ray model are simulated for the same assumed parameters. The four paths may be identified from the transmitter to receiver via the tip of the knife-edge. The

29

total received signal is the sum of the direct wave, if any, and the diffracted waves received via each one of the four paths. The total diffracted field in the presence of the knife-edge is defined by equation (3.2).

$$E_d = \sum_{n=1}^{4} E_{0n} F_n .$$ (3.2)
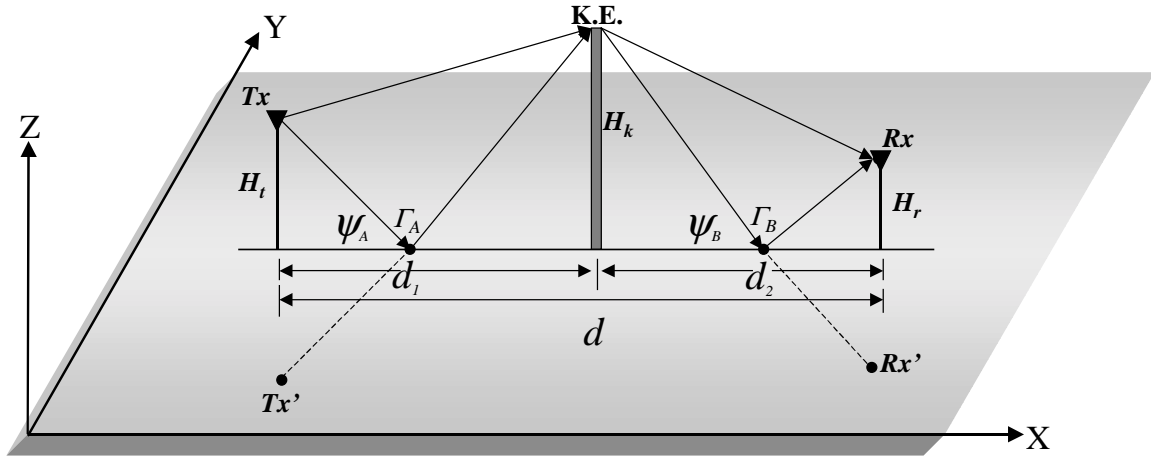
Figure 15.   An Absorbing Knife-Edge Between Transmitter and Receiver.

Case n	Transmitter Location	Receiver Location	Free-Space Path Length r_n	Clearance Height h_n	Reflection Coefficient, Γ_n
1	T_x	R_x	$T_x R_x = \sqrt{d^2 + (H_t - H_r)^2}$	$H_k - \dfrac{H_t d_2 + H_r d_1}{d}$	1
2	$T_x{}'$	R_x	$T_x' R_x = \sqrt{d^2 + (H_t + H_r)^2}$	$H_k + \dfrac{H_t d_2 - H_r d_1}{d}$	Γ_A
3	T_x	$R_x{}'$	$T_x R_x' = T_x' R_x$	$H_k - \dfrac{H_t d_2 - H_r d_1}{d}$	Γ_B
4	$T_x{}'$	$R_x{}'$	$T_x' R_x' = T_x R_x$	$H_k + \dfrac{H_t d_2 + H_r d_1}{d}$	$\Gamma_A \Gamma_B$

Table 2.   Quantities For The Evaluation of $F_{k.e,}$ [After: Ref. 2].

where E_{on} is the free-space field for the nth situation, F_n is the normalized field for that path, and H_k is the height of the knife-edge. Assuming omni-directional patterns for the transmitting and receiving antennas the free-space field is defined as follows

$$E_{on} = \frac{e^{-jk_o r_n}}{r_n}, \quad n=1,...,4, \tag{3.3}$$

where r_n is the free-space path length for the nth situation, and the individual knife-edge normalized fields are given by

$$F_n = \frac{1}{2}\left[1-(1+j)F\left(\sqrt{2}\frac{h_n}{H_1}\right)\right]\Gamma_n, \tag{3.4}$$

where F is the Fresnel integral, Γ_n is the total reflection factor, and h_n is the clearance height for the nth path. H_1 is the radius of the first ellipsoid in the plane perpendicular to the line-of-sight (LOS) path and can be obtained from equation (3.5):

$$H_1 = \sqrt{\frac{n\lambda d_1 d_2}{d_1 + d_2}}, \tag{3.5}$$

where d_1 is the distance between the transmitter to the knife-edge, d_2 is the distance between the knife-edge and the receiver, and λ is the operating wavelength. The propagation factor $F_{k.e.}$ of the four-ray model can then be obtained from equation (3.6).

$$F_{k.e.} = \left|\frac{E_d}{E_{o1}}\right|. \tag{3.6}$$

Additional details of the four-ray model are provided in reference 2.

Figure 16 shows the vertical cut of the relative propagation factors, $F's$, of the four-ray model and 3D PE model. The circle with the solid line corresponds to the four-ray model and the plain solid line is the 3D PE result. The results were taken at a range of 500 m from the transmitter over flat plane. The screen was placed 125 m from the transmitter and 375 m to the receiver. The two results are in excellent agreement. As previously mentioned, the relative propagation factors $F's$ approach zero dB as we

31

increase the receiving antenna height. In this case, it is already close to zero dB at a receiving antenna height of only 80 meters.
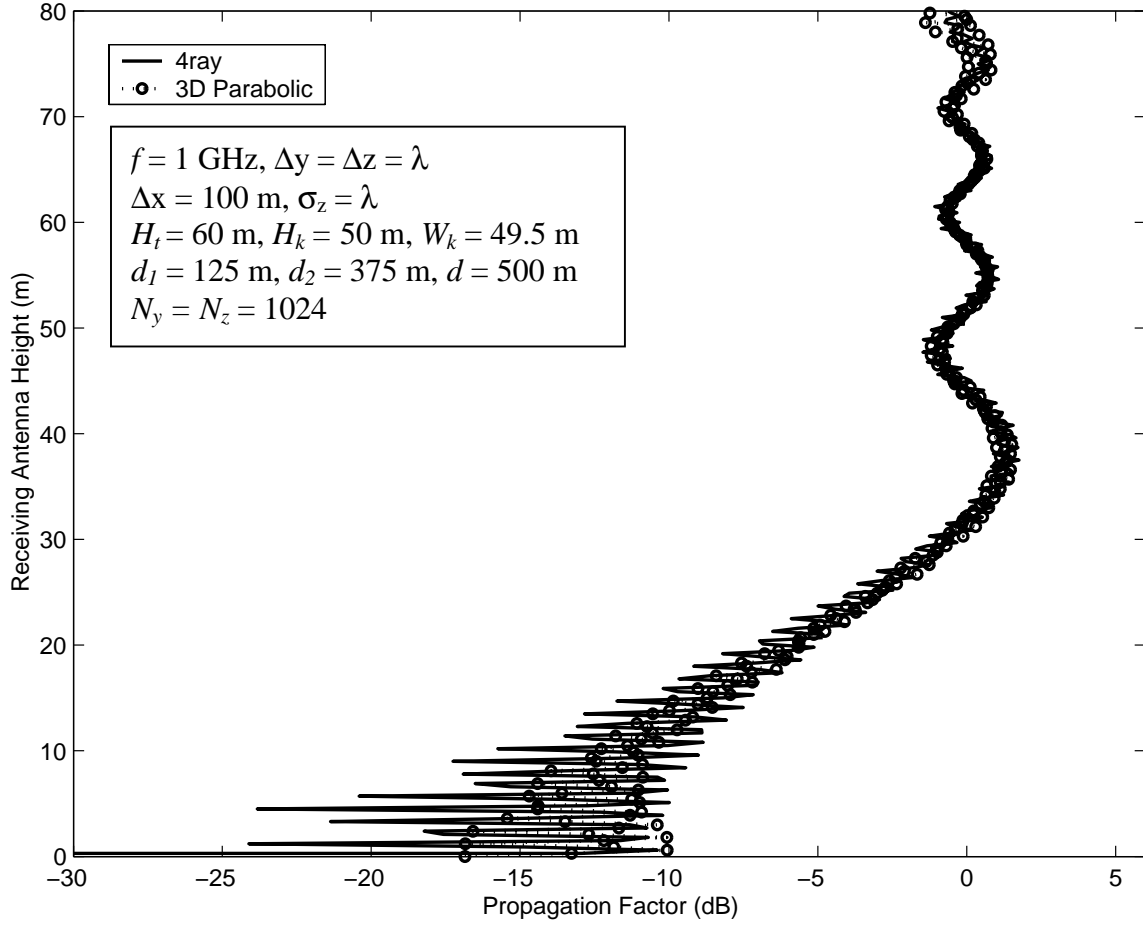
Figure 16.   3D PE and Four-ray Comparison (Vertical Cut).

C.   3D PE MODEL AND ANDERSEN'S AND LEE'S RESULTS COMPARISON

In the previous section, we have demonstrated that the results of 3D PE model corresponded well with the results of the four-ray model. In this section, we consider nine absorbing screens (multiple knife-edges) of uniform heights, equal spacing, and variable widths. The results of the 3D PE model are compared with the results presented by Andersen [Ref. 6] and Lee [Ref. 7]. Andersen's results were obtained from the uniform theory of diffraction (UTD) method. Lee presented the theoretical results in

reference 7. Both the UTD and theoretical results assumed that the screen widths are infinitely long, and the screen heights are finite. Full details on the UTD method are provided by references 6, 7, and 14.

We also examine the effects of three finite screen widths on the relative propagation factors, *F's*. The three finite screen widths are 50 m, 25 m, and 12.5 m. In each case, nine absorbing screens were placed between the transmitter and the receiver with each screen having a height of $H_k = 10$ m. The screens are placed 100 m apart from the each others. The first screen is 100 m from the transmitting antenna, and the last screen is 100 m to the receiving antenna. The distance between the transmitter and the receiver is 1000 m. The propagation factors are determined at the top of the screens.

The theoretical propagation factor, F_{th}, in dB is defined by equation (3.7). It is a function of edge numbers, where the edge number is $N + 1$, and N is a number of screens.

$$F_{th} = 20\log_{10}\left(\frac{1}{N+1}\right) \tag{3.7}$$

Again, these screens represent a row of buildings or houses in residential areas of a city. In these types of environments, the base station antennas of cellular communication systems are typically located above or near to the rooftops of the surrounding buildings. In these cases, the propagation takes place over the buildings, which can be modeled by multiple forward diffraction past rows of buildings. We model each row of buildings as an absorbing knife-edge, and via the 3D PE numerical technique we determine the loss associated with multiple forward diffraction over the knife-edges. Furthermore, depending on their construction, buildings may have a flat roof, a peaked roof, a flat roof with a parapet, or a myriad of other roof designs [Ref. 13]. Figure 17 illustrates building profiles that mobile communication systems designers can be expected to encounter for typical urban environments between the base stations and mobile units. Figure 17 (a) shows that two absorbing screens model a double parapets roof building. Figure 17 (b) illustrates that a single parapet roof building is modeled by one absorbing screen with the screen placement at the start of the building. And Figure 17 (c) shows that a peaked roof building is also modeled by one screen, but the screen

placement is at the center of the building corresponding to the peak of the building. Reference 13 provides more details on building profiles and screen placements.
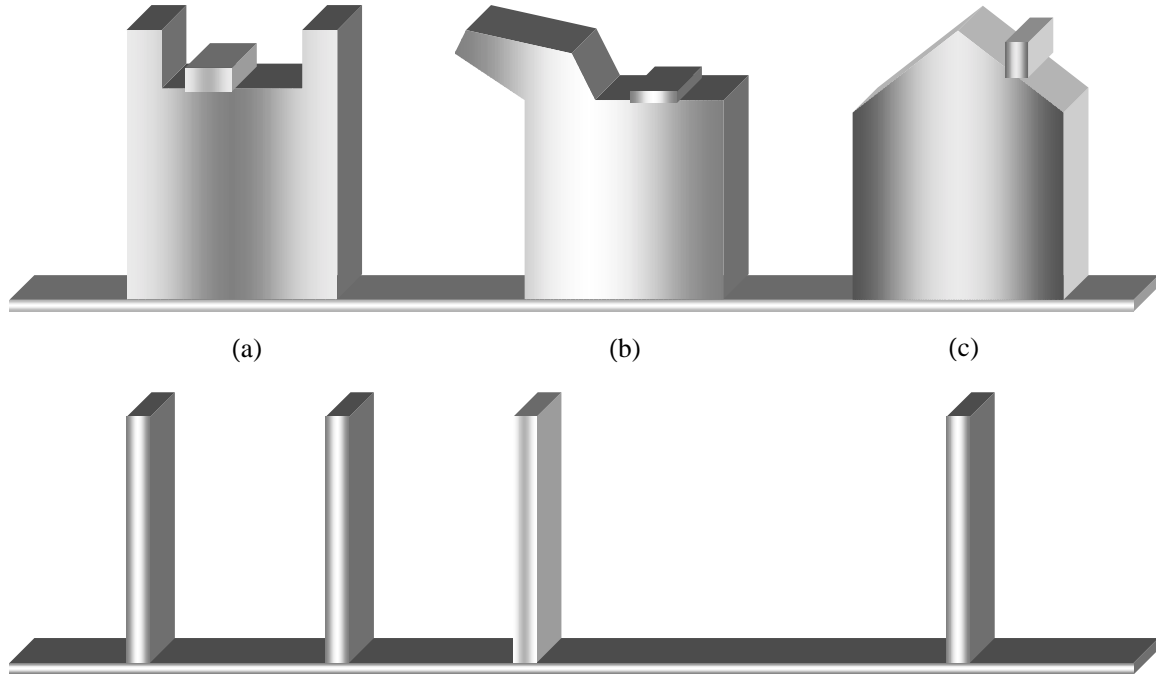
Figure 17.   Typical Building Profiles in Urban Areas, with Their Equivalent Screens Placements [After: Ref. 13].

Figure 18 illustrates the multiple absorbing knife-edges with equal heights and equal spacing for this test problem. The assumed parameters used in the 3D PE model are listed on Figure 19.
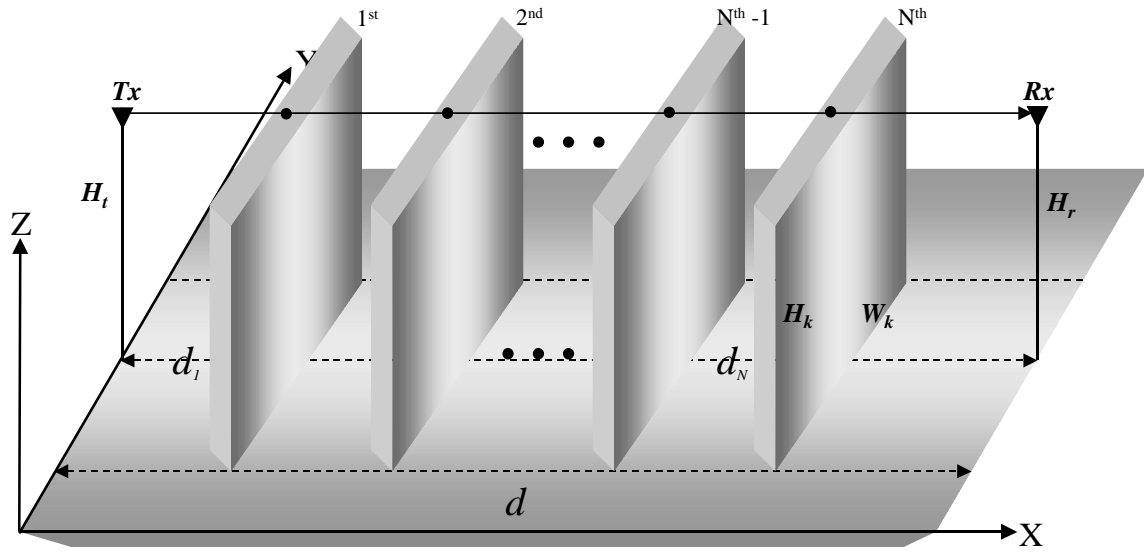
Figure 18.   Perfectly Absorbing Equal Heights and Equal Spacing Multiple Screens.
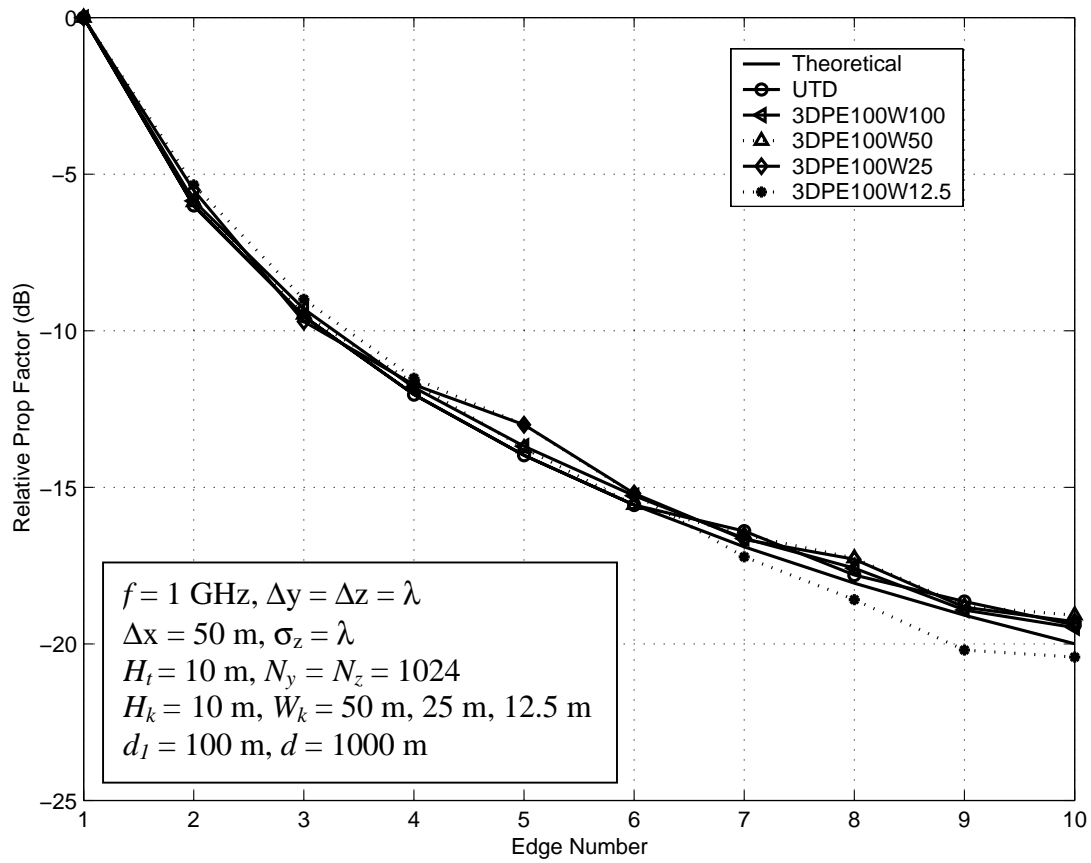
Figure 19.   3D PE, UTD, and Theoretical Results.

Figure 19 shows the results of the 3D PE model with the results presented by Andersen and Lee. The solid line is the theoretical result for 2D. The circle with solid line represents the results presented by Andersen. The triangle with dashed line are the results of 50 m screen width, the diamond with solid line are the results of the 25 m screen width, and the star with dashed line are the results of the12.5 m screen width. The UTD, the 50 m and 25 m screen width cases, the curve slope track the theoretical closely up to the seventh screen. After the seventh screen, they are only 0.5 dB different from the theoretical. For the case of 12.5 m screen width, the results do not quite agree with the theoretical, UTD, 50 m, and 25 m results, but the difference is still less than 1 dB. These differences are caused by the fact that the smaller screen width allows the lateral waves and diffracted waves to constructively add or destructively add. These lateral and diffracted waves might have added constructively when they arrive at the receiving antenna up to the seventh screen; then added destructively after the seventh screen, which resulted in a 1 dB different from the theoretical and approximately 1.5 dB different from the UTD and the two cases of the 3D PE model. However, we expect to see the results of the 3D PE model approach the theoretical results if we consider wider screen widths that allow less lateral waves to contribute to the overall results.

All presented data used absorbing screens of uniform heights and equal spacing, but the 3D PE algorithm is capable of supporting multiple screens of variable heights, widths, and spacing. Based on the comparison results in sections A, B, and this section, we may assume that the 3D PE model is capable of computing the propagation factors over flat earth with multiple absorbing screens of non-uniform heights, unequal spacing, and variable screen widths. Next we consider 120 screens of uniform heights and equal spacing over flat earth and perfectly reflecting ground.

D.   3D PE MODEL AND 120 UNIFORM HEIGTH AND EQUAL SPACING SCREENS

In this section we consider 120 screens of uniform heights and equal spacing. Again, the propagation takes place over the buildings. As previously mentioned, the 3D PE model is capable of supporting multiple absorbing screens of variable heights, widths, and spacing. But for the purpose of this study, we will only consider absorbing screens of uniform heights and equal spacing. We compare the 3D PE model results with the

results presented by Bertoni [Ref. 10]. Figure 20 shows setup geometry of this test case. We consider a plane wave incident at an angle $\alpha = 1^\circ$ at an operating frequency of 900 MHz. The distance between screens is 50 m, which means that the distance between the transmitter and the receiver is 6050 m apart. Based on the incident angle α of 1° and the separation distance between the transmitter and the last screen, we determine that the vertical clearance height, H_{ch}, from the top of the 120th screen to the tip of the transmitting antenna is 105 m. If the screen height of 20 m is chosen, then the transmitting antenna height should be 125 m. We assume the screens width to be 50 m.
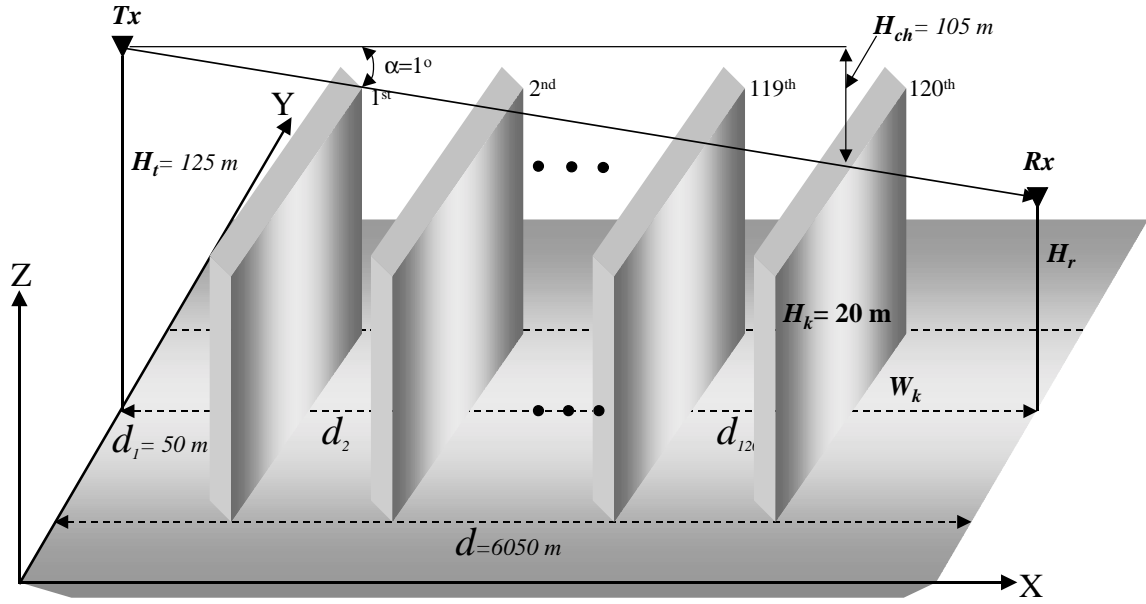
Figure 20.   120 Equal Height and Equal Spacing Screens.

Figure 21 shows the height variation of the relative field strength, F, computed by 3D PE model, incident on the row of 120 screens of 20 m heights and 50 m spacing for the parameters assumed the previous paragraph. The receiving antenna height is measured in wavelength (m) while the magnitude of the field strength is in linear scale. Figure 19 also shows the simple diffraction in the shadow region of the receiving antenna $H_r < 0$. We use the rooftop as the reference point for $H_r = 0$. Above the rooftops, the field variation is similar to that of a standing wave resulting from the summation of the direct waves and reflected waves from the plane of the rooftops. The reflected waves are in fact the sum of the waves diffracted from the rooftops, whose phase variations cause

them to add constructively in the specular direction and other grating lobe directions. Because the diffraction coefficients decrease with angle, the reflected field is greatest in the specular direction.
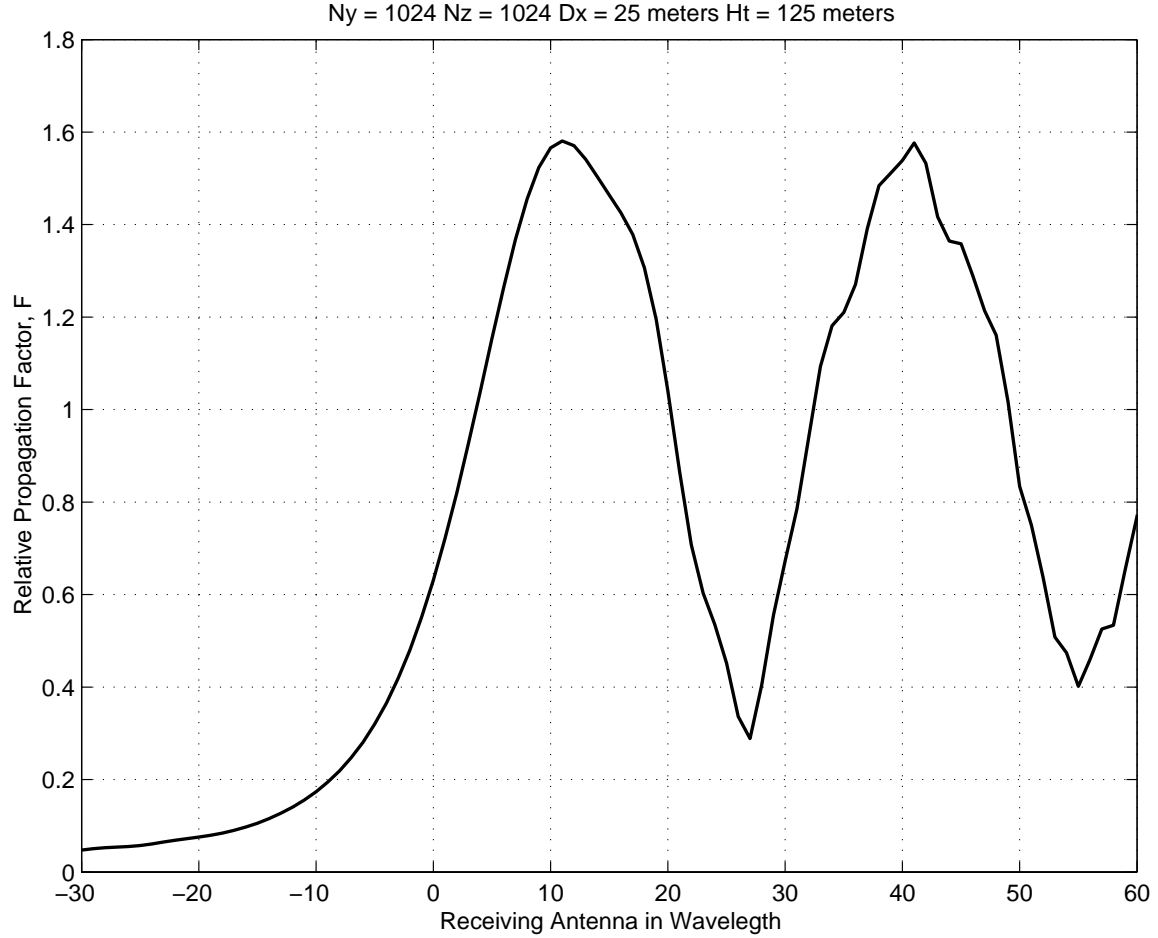
Figure 21.   120 3D PE Results For Equal Height and Equal Spacing.

Figure 22 shows the height dependence of the field strength, *F*, of the 3D PE model with the result from the numerical integration method presented by Bertoni and the result from the UTD [Ref. 10]. The circle with solid line is the sampling result of the 3D PE model shown in Figure 21. The asterisk with solid line is the result of the numerical integration method, and the triangle with solid line is the result of the UTD. In the shadow region, the results of the 3D PE model and the numerical integration method have good agreement, but the result of the UTD is slight higher, which implies that the UTD overestimates the field amplitude [Ref. 10].   Above the shadow region, the

numerical integration method and the UTD have excellent agreement, but the results of
the 3D PE model are slightly lower, but still have good agreement with the UTD and the
numerical integration method.
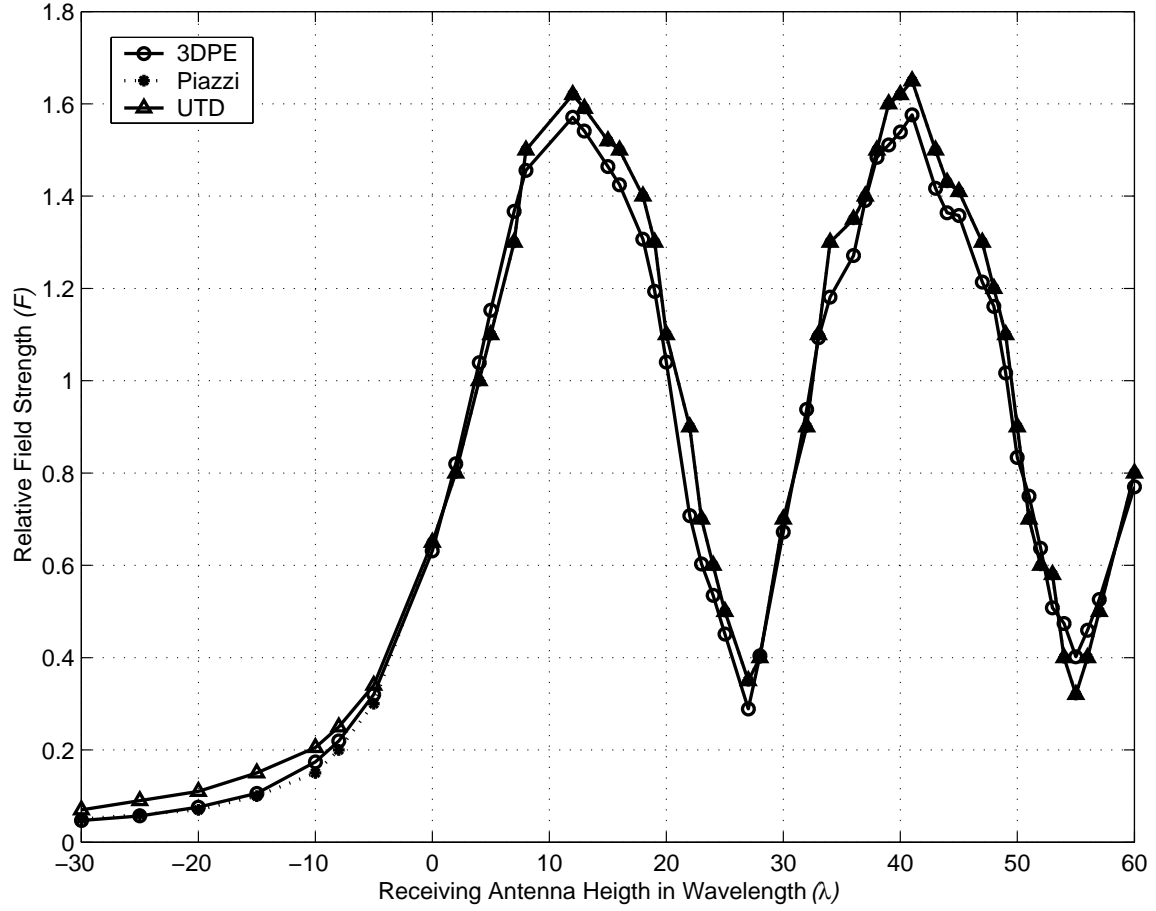
Figure 22.   3D PE, Bertoni, And UTD Results.

THIS PAGE INTENTIONALLY LEFT BLANK

IV. HILLY TERRAINS RESULTS

In this chapter, the propagation takes place over hilly terrains, and we study the field strengths. A single round is considered in Section A. The two hills of sinusoidal shape are considered in Section B. In both cases, we place multiple absorbing screens of uniform heights, equal spacing, and variable widths between the transmitter and the receiver. We measure the field strengths, instead of propagation factors, at the rooftops. The results of the 3D PE model are compared with the results presented by Piazzi and Bertoni [Refs. 8 - 10].

A. A ROUND HILL AND 3D PE MODEL

In the previous test cases, we have examined the propagation factors over flat earth with multiple screens of uniform heights, equal spacing, and variable widths. Now, we consider a rounded hill with multiple absorbing screens of uniform heights, equal spacing, and variable widths. We examine the diffracted field strengths at the rooftops, instead of the propagation factors as in the previous cases. We also consider the effects of finite screen widths on the field strengths. We compare simulation results of the 3D PE model with results presented by Piazzi [Ref. 8]. Figure 23 illustrates setup geometry for this test case. These screens represent a row of buildings or houses in residential areas of a well built-up city. The buildings are 7 m high and the row separation D_s is 50 m, and the screen widths are W_k = 100 m, 50 m, and 25 m. The cylindrical hill has a radius R_h of 10 km [Ref. 8]. The maximum height of the hill is 50 m. The base of the hill is at a distance of X_h =1000 m from the peak. For the simulation, the transmitting antenna is assumed to be located at the point x = -1000 m from the hilltop and has a height of H_t = 57 m, which places it at the same height as the highest rooftops [Ref. 10]. The current source is excited at an operating frequency of 900 MHz. The rounded hill is defined by equation (4.1).

$$Z = \sqrt{R_h^2 - x^2 - \left(R_h - H_h\right)},$$ (4.1)

where R_h is the radius of the hill, H_k is the height of the buildings, and x is the range in meter. The total simulation range is 6000 m.
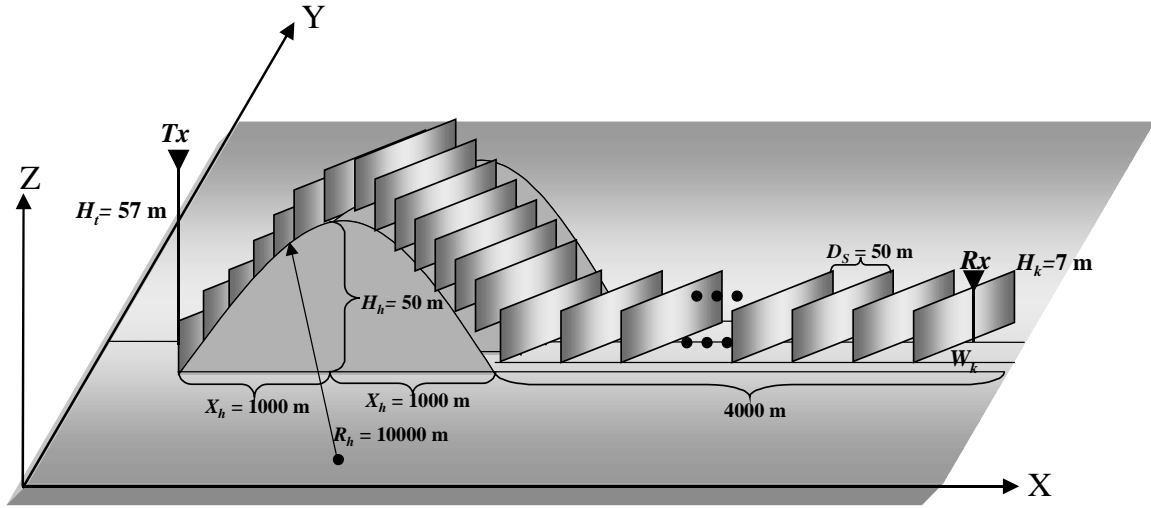
Figure 23.   A Round Hill with Multiple Screens of Uniform Heights and Equal
Distances.

Figure 24 shows the profile of multiple absorbing screens representing Figure 23 used to carry out the simulation in the 3D PE model. Furthermore, if we can model an urban area with multiple absorbing screens of variable heights, widths, and spacing, the 3D PE model can evaluate the propagation factors as well as field strengths at any point in the simulation.

Figure 25 shows the results of 3D PE model, the free-space result, and Piazzi's result. There are three 3D PE model results. The solid line is the result of the 3D PE model with 100 m screen width. The dashed line is the result of the 50 m screen width. The dashed and dot line is the result of the 25 m screen width. The triangle with solid line is the free-space result, and the circles are Piazzi's results. Up to 1000 m away from the base station, the field strength behaves like free-space. Then at the hilltop the field behaves like a single knife-edge case, where the magnitude of the field strength is 6 dB below the free-space. Between the base station and the peak of the hill, the field strength does not behave like a free-space field. Perhaps this is one of the limitations for the 3D PE model, but this is minor issue. After the hilltop and behind the hill up to $x = 1000$ m, the field strength decays rapidly and linearly with distance at a rate of approximately

42

0.055 dB per meter. This may be understood in terms of the creeping wave representation of the fields traveling over the houses. At the point of $x = 1000$ m from the hilltop, the field strength reaches its lowest point, but begins to increase rapidly to maximum and then decreases slowly with distance. We expect the field to continue decaying as it propagates away from the base of the hill, but that is not the case because the diffracted waves from the rooftops on the hillside. We also expect the field to eventually level off and begin to decay and behave like multiple knife-edges propagation case. As shown in Figure 25, the field levels off around $x = 3000$ m away from the base of the hill. If we continue to measure the field strength for both the 3D PE model and the free-space, the field strength of the 3D PE model will eventually be 6 dB below the free-space value as in the a single knife-edge case.
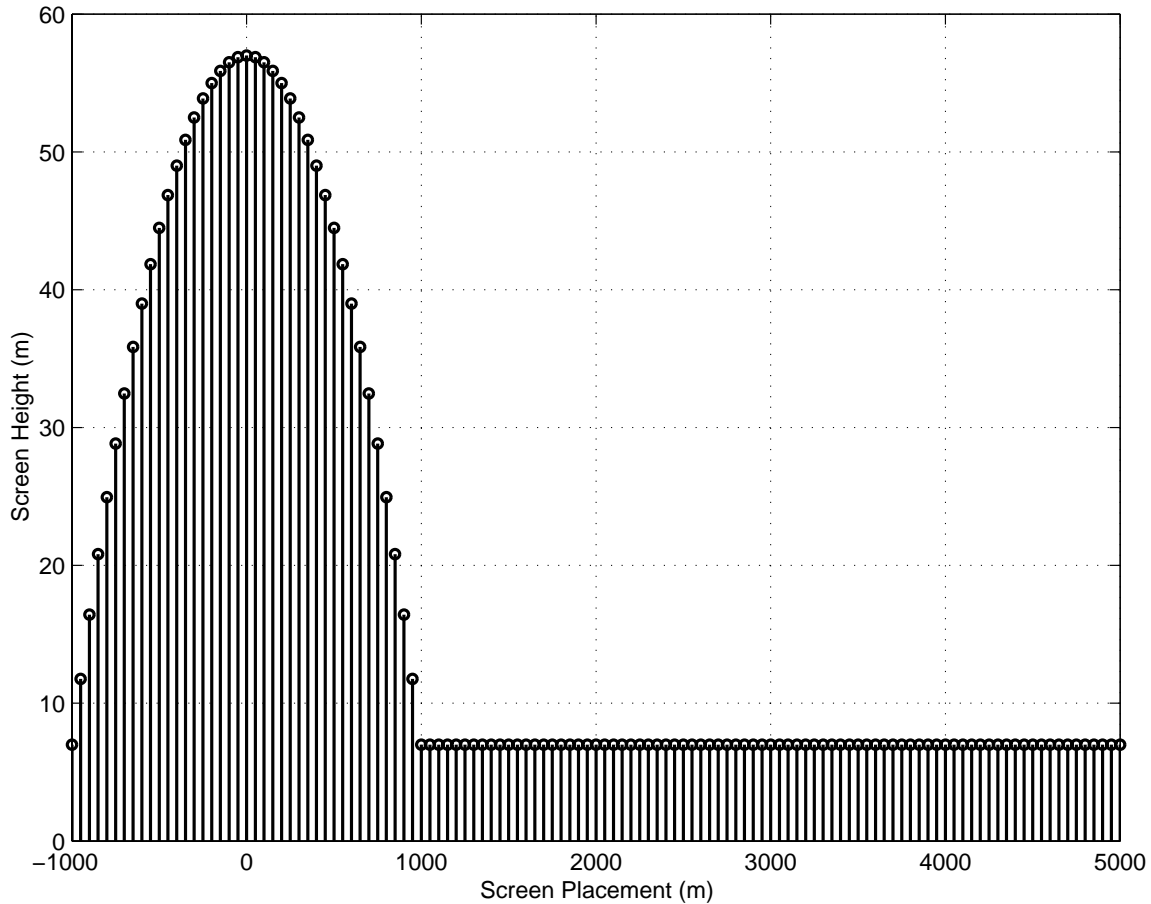
Figure 24.   Side View of a Single Hill with Rows of Uniform Heights and Spacing Buildings.

43

Figure 25 also shows that we have excellent agreement between Piazzi's result and the result of the 3D PE model especially with screen width $W_k =100$ m. However, it is not the case for the 50 m and 25 m screen widths. Furthermore, for both the 50 m and 25 m screen widths, there are oscillations as the fields move away from the base of the hill. There appears to be more oscillation in the 25 m screen width case than for the 50 m case. Its magnitude is also higher than the other cases, but it begins to approach other cases as it moves away from the base of the hill on backside. The oscillations and higher magnitudes are caused by lateral waves because of the finite screen widths. Therefore, if we increase the screen width, then we expect the result 3D PE model to agree with Piazzi's result because Piazzi assumed the screen width is infinitely long. This is equivalent to the 2D PE model which did not take into account the lateral waves. This is demonstrated the 100 m screen width case, which prevented the lateral waves from significantly contributing to the overall result.   We have shown that the 3D PE model is capable of supporting the variable screen widths. The last test problem we will present in this thesis is the two sinusoidal hills.
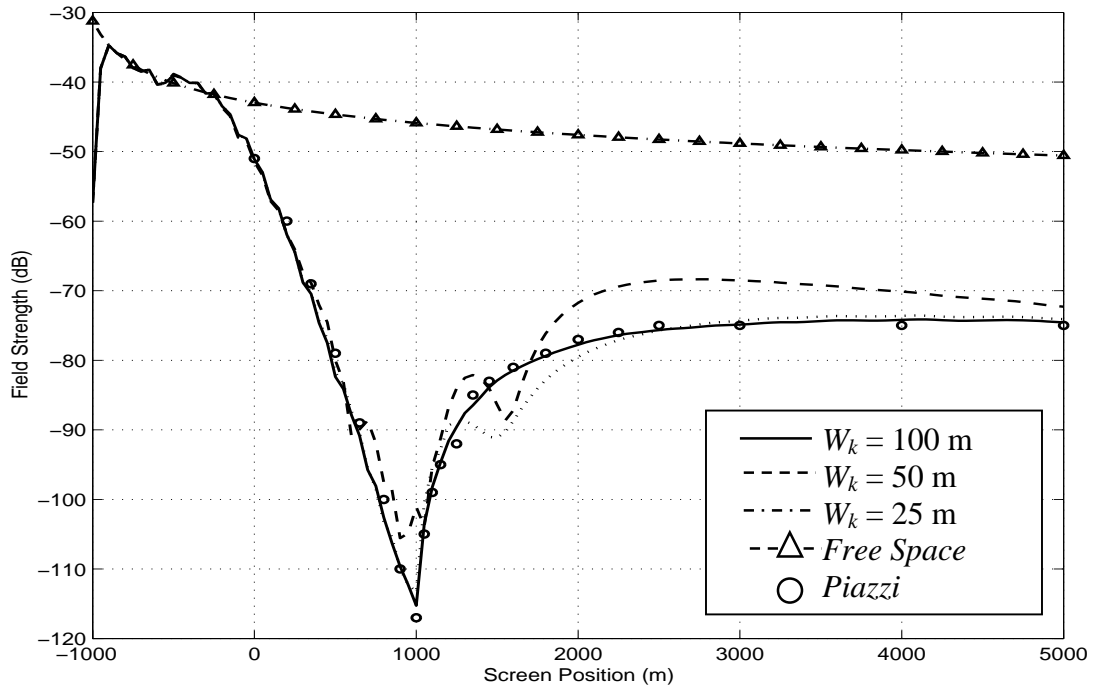
Figure 25.   A Single Hill with Rows of Buildings of Uniform Heights and Spacing Field Strength.

44

B.   3D PE MODEL AND TWO HILLS OF SINUSOIDAL SHAPE

In the previous section, we have considered a single rounded hill and demonstrated that the result of the 3D PE model agreed with Piazzi's result. We have also shown that the 3D PE model can support variable screen widths. Now we consider two sinusoidal hills, and this is the last test problem we will consider for this thesis. It has similar setup geometry as shown in Figure 23, except it has two hills of sinusoidal shape. Figure 26 illustrates setup geometry for this test case.
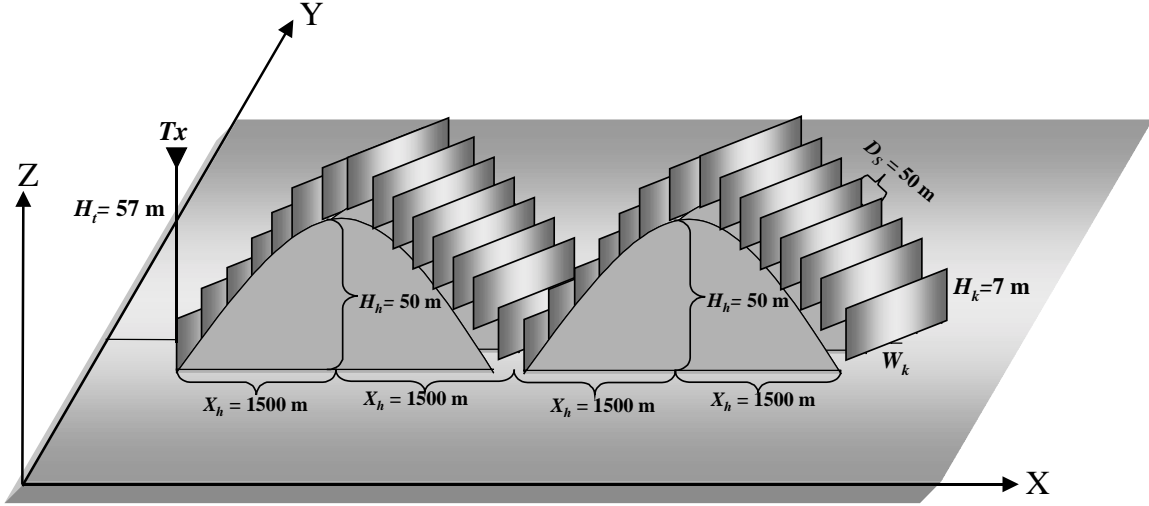
Figure 26.   Two Hills of Sinusoidal Shape.

Again, these screens represent a row of buildings or houses in residential areas of a well built-up city. The buildings are 7 m high and the row separation D_s is 50 m with building widths W_k = 100 m, 50 m, and 25 m. The maximum heights of the two hills are 50 m. The two sinusoidal shape hills have period of 3000 m [Ref. 9], which means the distance from peak to peak is 3000 m. The distance X_h from the first peak to its base, measured toward the second peak, is 1500 m. For the simulation, the transmitting antenna is assumed to be located at the point $x = $ -1500 m from the first hilltop and has a height of $H_t = $ 57 m, which again places it at the same height as the highest rooftops [Ref. 10]. The two hills of sinusoidal shape are defined by

$$Z(x) = H_k + 25 + 25\cos\left(\frac{2\pi x}{3000}\right)$$ (4.2)

where H_k is the height of the buildings and x is the range in meters.

Figure 27 shows the profile of multiple absorbing screens representing Figure 24 used to carry out the simulation in the 3D PE model. The operating frequency is 900 MHz and same as the previous case.
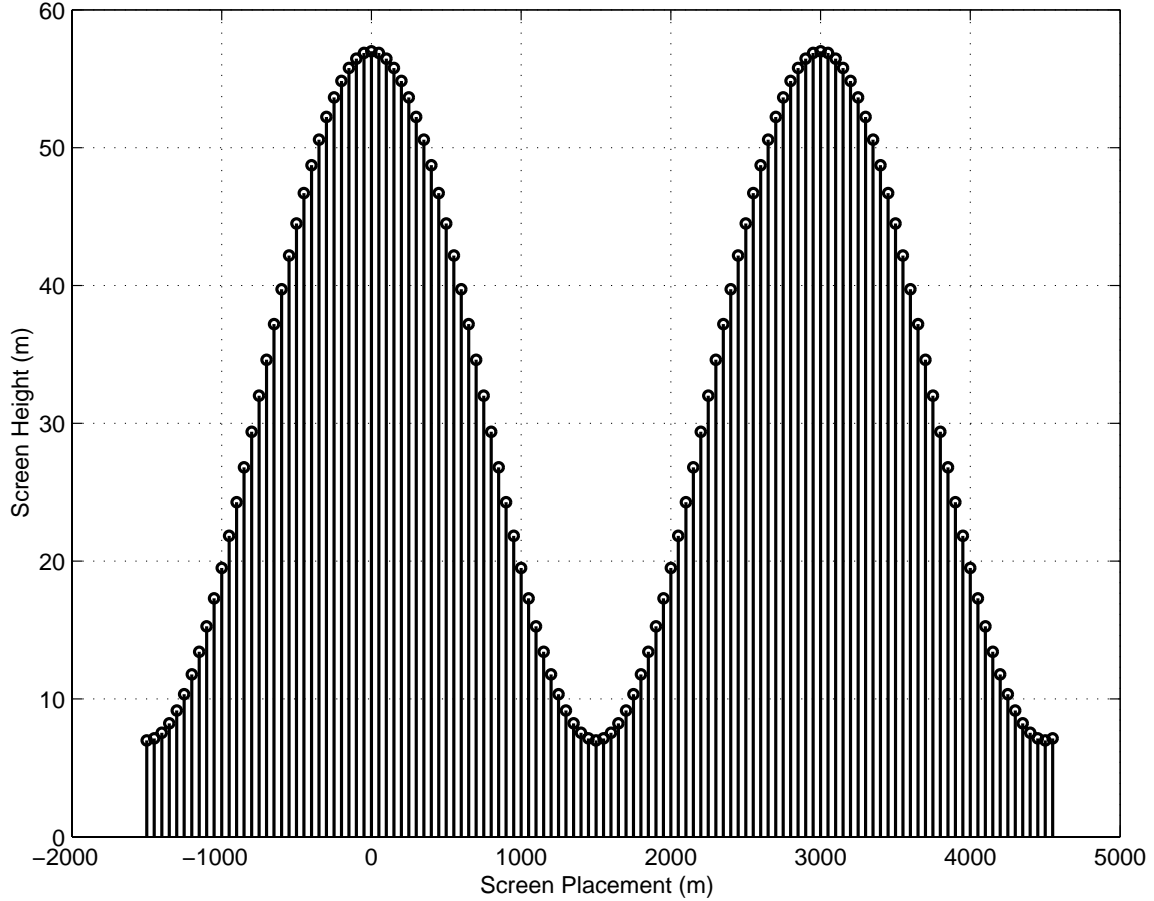
Figure 27.   Side View of two Sinusoidal Hills plus Buildings Profile.

Figure 28 shows the composite results of the 3D PE model, free-space and Piazzi. The solid line is the result of the 3D PE model with 100 m screen width. The dashed line is the result of the 50 m screen width. The dashed and dot line is the result of the 25 m screen width. The triangle with solid line is the free-space result. And the circles are Piazzi's results. Up to 1500 m away from the base station, the field strength behaves like free-space, which corresponds to the peak of the first hill. Then at the first hilltop the field behaves like a single knife-edge problem, same as the previous case, where the

magnitude of the field strength is 6 dB below the free-space. As in the one hill problem, the field does not behave like free-space field when it is close to the base station. The field strength minima occur at $x = 1000$ and 4000 m which do not correspond to the bases of the hills as it did in a single round hill case. When we decrease the widths of the screen, we see more oscillations as demonstrated in the one hill case. The oscillation appears to be more severe in the 25 m screen width case. These oscillations are caused by the lateral waves.
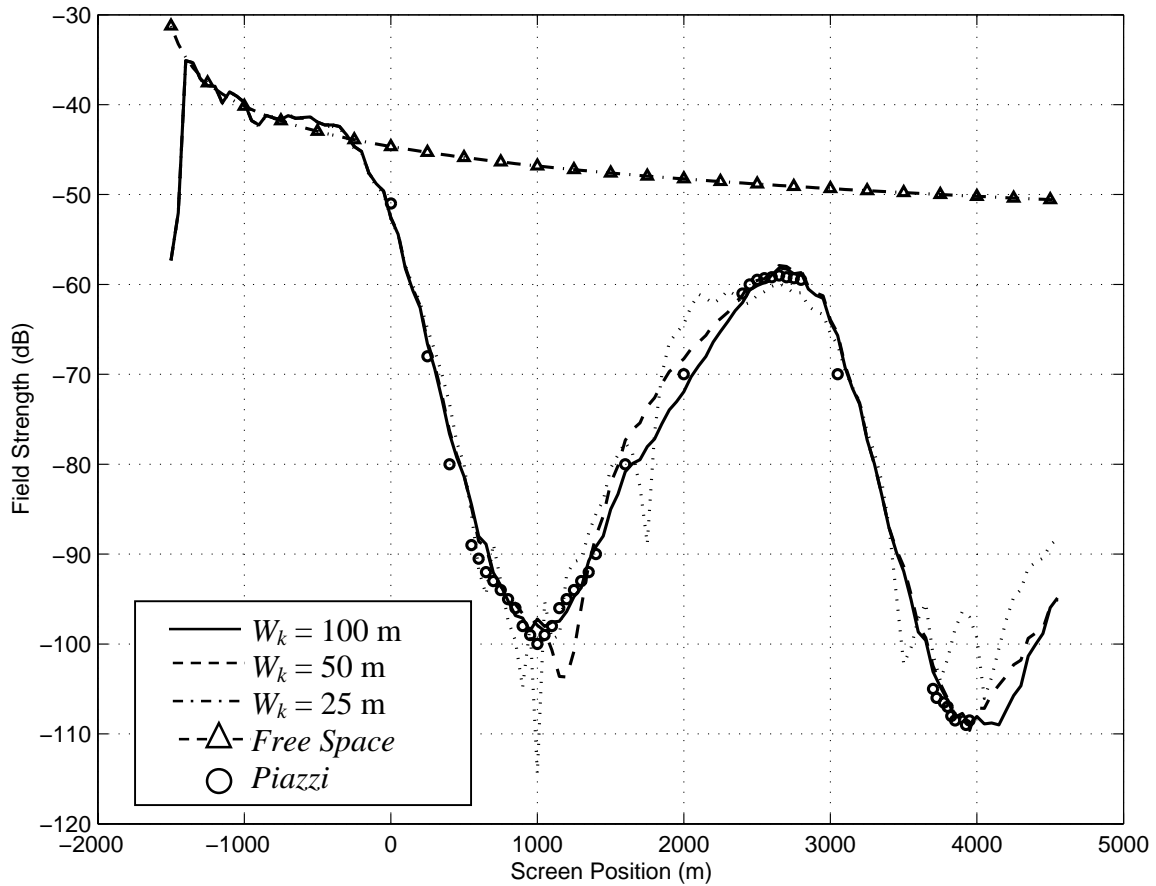
Figure 28.   Two Sinusoidal Hills with Rows of Buildings of Uniform Heights and Spacing Field Strength.

We have thus demonstrated that the 3D PE model can support both flat and hilly terrains with multiple absorbing screens of uniform heights, equal spacing, and variable screen widths.

THIS PAGE INTENTIONALLY LEFT BLANK

V.   CONCLUSIONS AND RECOMMENDATIONS

A.   CONCLUSIONS

A 3D model based on the parabolic equation (PE) for predicting propagation path loss has been developed in this thesis. Two types of terrains were considered: the flat earth and the hilly terrain. For the flat earth case, four test problems were examined. The results from these cases were compared with results available from the two-ray model, the four-ray model, the uniform theory of diffraction (UTD), Lee's formulation, and the numerical integration technique as proposed by Bertoni. For the hilly terrain case, two test problems were considered. The results from this case were compared with the results presented by Piazzi and Bertoni. For all these test problems, ground was assumed to be non-perfectly reflecting, and buildings as perfectly absorbing because all available results that were used in the comparisons made these assumptions.

For the flat earth case, the first test problem was to simulate and determine the propagation factor F at the final range over flat earth without any obstacles between the transmitter and the receiver. The transmitting antenna had a height $H_t = 30$ m, and the operating frequency was 1 GHz. The receiver located 1000 m from the transmitter. The results of the 3D PE model compared excellently with those of the two-ray model.

The second test problem was to simulate and determine F with a single absorbing screen placed between the transmitter and the receiver that had a height $H_k = 50$ m, and a width $W_k = 49.5$ m. The screen representing a building was located 125 m from the transmitter and 375 m to the receiver. The transmitting antenna height $H_t = 60$ m, and the operating frequency was 1 GHz. The results of the 3D PE model in this case were compared with the results of the four-ray model. Once again, the results had excellent agreement. F approached 0 dB as the receiving antenna height increased. In this case, both the 3D PE model and the four-ray results approached 0 dB at the receiving antenna height of 80 m.

In the third test problem, nine absorbing screens of uniform heights and equal spacing were placed between the transmitter and the receiver. This test case was

equivalent to a radiowave propagating over a row of houses in an urban area. The screens had a height $H_k = 10$ m and the widths, W_k. The three different screen widths W_k were 12.5 m, 25 m, 50 m. Each screen had a height of 10 m and a spacing distance of 50 m. Their effects on the propagation factor F were studied. The propagation factor in this case was determined at the rooftops. The results of the 3D PE model were compared with the UTD results presented by Andersen and the theoretical model results proposed by Lee. The 3D PE model results with the screen widths of 25 m and 50 m had excellent agreement with the UTD, and both the UTD and the 3D PE model results followed the theoretical results only up to the seventh screen. Then up to the ninth screen they were 0.5 dB higher than the theoretical predictions. For the 12.5 m case, the results were slightly higher than all cases up to the seventh screen; then they were lower than all cases up to the ninth screen. These differences were caused by the lateral waves due to the finite screen width.

The last test problem for the flat earth case involved 120 absorbing screens of uniform heights and equal spacing between the transmitter and the receiver. These screens represented row of buildings or houses. The transmitting antenna had a height of $H_t = 125$ m, and the operating frequency was 900 MHz. The screens had the height, $H_k = 20$ m, and the width, $W_k = 50$ m. They were spaced 50 m apart. The propagation factor was determined at the final range. The results were compared with the results of the numerical integration technique presented by Bertoni and the UTD. In the shadow region, the results of the 3D PE and the numerical integration method agreed, but the result of the UTD was slightly higher, which implied that the UTD overestimated the field amplitude. Above the shadow region, the numerical integration method and the UTD had excellent agreement, and although the results of the 3D PE model were 0.25 dB lower than those two models, nonetheless there was reasonably good agreement with them.

For the hilly terrain case, the first test problem was a single rounded hill with multiple absorbing screens of uniform heights and equal spacing. The screens had the heights $H_k = 7$ m. The field strengths were determined on rooftops, and were compared with the numerical integration technique results presented by Piazzi and Bertoni. The second test problem, the propagation took placed over two hills of sinusoidal shape with

multiple absorbing screens of uniform heights and equal spacing. Again, the results were compared with the results presented by Piazzi and Bertoni. The screens in this case also had the heights $H_k = 7$ m. In both cases, three variable screen widths W_k were considered: 25 m, 50 m and 100 m. Their effects on the field strengths were studied. For both cases, the transmitting antenna height was $H_t = 57$ m, and the operating frequency was 900 MHz.

For a single round hill, the result of the 3D PE model with screen width of 100 m compared excellently with the Piazzi's result. Before the hilltop, the field strength behaved like free-space. Then at the hilltop the field behaved as in a single knife-edge case, where the magnitude of the field strength was 6 dB below the free-space. On the backside of the hill, the field strength decayed rapidly and linearly with distance, but began to increase rapidly to maximum and then decreased slowly with distance. For the cases of 25 m and 50 m screen width, the field strengths agreed with the100 m case and Piazzi's result until after the base of the hill on the backside after which it began to increase rapidly with oscillations. These oscillations were caused by the laterally diffracted waves. The oscillations were more prominent in the 25 m case than the 50 m case.

For two sinusoidal hills, the field strengths behaved like free-space up to the first hilltop similar to the previous case. Then at the first hilltop the fields behaved like a single knife-edge problem, where the magnitude of the field strength is 6 dB below the free-space. The field strength minima occurred at $x = 1000$ m and 4000 m which did not correspond to the bases of the hills. When the widths of the screen were decreased, the oscillations showed up similarly to the single rounded hill case. The oscillations appeared to be more severe in the screen width of 25 m.

Finally, the 3D PE model for predicting propagation path loss in urban areas on flat and hilly terrains was developed. Six different test problems were considered. The results were compared with the results available in open literature and showed excellent agreement. We have also demonstrated that the 3D PE model can support both flat and hilly terrains with multiple absorbing screens of uniform heights, equal spacing and variable screen widths.

B.   RECOMMENDATIONS

Since realistic environments will have non-perfectly reflecting obstacles, a more complete 3D PE formulation for non-perfectly reflecting obstacles should be studied as well as the effects of the antenna depolarization. In addition, it is recommended that the algorithm be implemented in C or Fortran for faster computation, along with the automating terrain and building inputs for the model. It may be desirable to add the capability to utilize the Digital Terrain Elevation Data (DTED) and Digital Feature Attribute Data (DFAD) available at the National Imagery and Mapping Agency (NIMA).

APPENDIX A: 3D PE ALGORITHM AND 2RAY MODEL

Below is the MatLab program listing of the 3D parabolic equation model and the 2Ray model. This program will compute the propagation factors for the 3D PE with the 2Ray model over perfectly flat earth and constant admittance plane. The operating frequency is 1 GHz.

```matlab
%************************************************************************
%                      Declaring Contants
%************************************************************************

hold off;
tic
c=3e8;                      % Speed of light
f=1e9;                      % Operating frequency
Lamda=c/f;                  % Wavelength
ko=(2*pi)/Lamda;            % Wavenumber
S=25;                       % Ground conductivity in mS/m
Er=5;                       % Relative dielectric constant

Dz=Lamda;                   % Delta Z in meter
Dy=Lamda;                   % Delta Y in meter
sigmaz=Lamda;               % Current source standard deviation

%************************************************************************
%                      Input Parameters
%************************************************************************

Ht=30;              % Transmitting antenna height

D=1000;             % Range from the transmitter
Dx=100;             % Incremental range (Dx) in meter

Ny=1024;            % Sample size in the y-direction
Nz=1024;            % Sample size in the z-direction

%************************************************************************
%           Define range in y-direction and z-direction
%************************************************************************

ymax=Ny*Dy/2;           % maximum range in y-direction
y1=0:Dy:ymax;           % First half of y range incrementally increase
y=[y1 zeros(1,Ny/2-1)]; % y array

zmax = Nz*Dz/2;         % Find maximum z range (Zmax)
z1=0:Dz:zmax;           % First half of the range of Zmax+1
z=[z1 zeros(1,Nz/2-1)]; % Construct a full z array
```

```matlab
%***********************************************************************
%                  Define  Wavenumbers in Spatial Domain
%***********************************************************************

kymax=pi/Dy;                    % Maximum wavenumber in y-direction
Dky=2*kymax/Ny;                 % detla ky
ky1=-kymax:Dky:kymax;           % Range of ky
ky=[ky1(:,(Ny/2)+1:Ny+1) ky1(:,2:Ny/2)];

kzmax=pi/Dz;                    % Maximum wavenumber in z-direction
Dkz=2*kzmax/Nz;                 % detla kz
kz1=-kzmax:Dkz:kzmax;           % Range of kz
kz=[kz1(:,(Nz/2)+1:Nz+1) kz1(:,2:Nz/2)];

%***********************************************************************
%               Compute Wavenumbers in Frequency Domain, kx
%***********************************************************************

Ky=meshgrid(ky,1:Nz);           % Create a NyxNz matrix of ky row-repeat
Kz=meshgrid(kz,1:Ny).';         % Create a NyxNz matrix of kz column-
repeat
kx=sqrt(ko^2-Ky.^2-Kz.^2);      % Compute theNy x Nz kx matrix

clear Ky;                       % Clear matrices Ky and Kz from memory
clear Kz;                       % To make the algorithm run faster

%***********************************************************************
%                       Compute reflection coefficient
%***********************************************************************

Erc=Er+i*18*S/(f/1e6);          % Complex dielectric
Zs=1/sqrt(Erc);                 % Impedance
Gamma=(kz-ko*Zs)./(kz+ko*Zs);   % Complex reflection coefficient
%gamma=-ones(Nz,Ny);            % Setting gamma = -1
gamma=meshgrid(Gamma,1:Ny).';   % Create reflection coefficient matrix
                                % by column repeating

%***********************************************************************
%                       Define the Hanning Window
%***********************************************************************

Hya=[];                         % An empty vector
for t=0:Ny/2;                   % Define Ny/2 + 1 points
    if (t>=0 & t<=3*Ny/8)       % Define first 3Ny/8 +1 points
       hy=1;
  elseif (t>=3*Ny/8 & t<=Ny/2)% Define next Ny/8 points
       hy=(sin(4*pi*t/Ny))^2;
    end
   Hya=[Hya hy];                % Construct the first half of Hanning
end                             % window of  1+Ny/2  elements

Yy=fliplr(Hya(:,2:Ny/2));       % Flip left to right of the Hanning
                                        % windows from the
second element to
                                % Ny/2 element for total of [1x(Ny/2-1)]
HY=[Hya Yy];                    % Hanning window in y-direction
```

54

```matlab
Hzb=[];                          % An empty vector
for t=0:Nz/2;                    % Define Nz/2 + 1 points
    if (t>=0 & t<=3*Nz/8)        % Define first 3Nz/8 +1 points
      hz=1;
  elseif (t>=3*Nz/8 & t<=Nz/2)% Define next Nz/8 points
      hz=(sin(4*pi*t/Nz))^2;
    end
    Hzb=[Hzb hz];               % Construct the first half of Hanning
end                             % window of 1+Nz/2  elements

Yz=fliplr(Hzb(:,2:Nz/2));       % Flip left to right of the Hanning
                                % windows from the second element to
                                % Nz/2 element for total of [1x(Nz/2-1)]
HZ=[Hzb Yz]';                   % Hanning window in z-direction

Hmy=meshgrid(HY,1:Nz);          % Row repeat
Hmz=meshgrid(HZ,1:Ny)';         % Column repeat

H3D=(Hmy.*Hmz);                 % 3D Hanning window

%************************************************************************
%                        Gaussian Current Source
%************************************************************************

f=(1/(sqrt(2*pi)*sigmaz))*exp(-(z-Ht).^2/(2*sigmaz^2));

f_tilda=Dz*fft(f);              % Fourier transform of f(z)

%************************************************************************
%                        Initial H-field at x=0
%************************************************************************

g_tilda=exp(-kz.^2*sigmaz^2/2);     % initial g tilda
hye0_tilda=g_tilda.*cos(kz*Ht);     % Initial hye_tilda(0+,ky,kz) field
hyo0_tilda=-i*g_tilda.*sin(kz*Ht);  % Initial hyo_tilda(0+,ky,kz) field
                        % Initial even H-field, column repeat
Hye0_tilda=meshgrid(hye0_tilda,1:Ny).';
                        % Initial odd H-field, column repeat
Hyo0_tilda=meshgrid(hyo0_tilda,1:Ny).';
                        % Include the reflection coefficient
Hy0_tilda=0.5*(1+gamma).*Hye0_tilda+0.5*(1-gamma).*Hyo0_tilda;

Hy_tilda=Hy0_tilda.*H3D;% Hy_tilda(0+,ky,kz) at x=0

Exp2=exp(i*kx*Dx);      % Marching range
```

```
%***********************************************************************
%              3D Parabolic Equation Basic Algorithm
%***********************************************************************

for x=0:Dx:D-Dx;

    Hy_tilda_Dx=Hy_tilda.*Exp2;      % Hy_tilda(Dx,ky,kz)

    Hy=Dkz*Dky*(Ny*Nz*ifft2(Hy_tilda_Dx))/(2*pi)^2;
                                     % ifft2 wrt to ky and kz

    Hy_H=Hy.*H3D;                    % Apply the Hamming window

    Hyz1=Hy_H(1:Nz/2+1,:);          % H-field for z > 0

    Hyz0=flipud(Hy_H(2:Nz/2,:));    % H-field for z < 0

    Hye=[Hyz1; Hyz0];               % Even H-field

    Hyo=[Hyz1; -Hyz0];              % Odd H-field

    Hye_tilda=(Dz*Dy)*fft2(Hye);    % Take the FFT of the even H~
    Hye_tilda_H=Hye_tilda.*H3D;     % Apply the Hanning window in freq

    Hyo_tilda=(Dz*Dy)*fft2(Hyo);    % Take the FFT of the odd H~
    Hyo_tilda_H=Hyo_tilda.*H3D;     % Apply the Hanning window in freq
                               % Multiply by the reflection coefficient
    Hye_tilda_g=0.5*(1+gamma).*Hye_tilda_H;
                               % Multiply by the reflection coefficient
    Hyo_tilda_g=0.5*(1-gamma).*Hyo_tilda_H;

    Hy_tilda1=Hye_tilda_g + Hyo_tilda_g;% Hy_tilda(x,ky,kz)

    Hy_tilda=Hy_tilda1.*H3D;             % Apply the Hanning window

end

%***********************************************************************
%              Compute Propagation Factor at Final Range
%***********************************************************************
J=2;                               % Pick a column of H-field at final range

rho=sqrt(D^2+(J)^2);        % Distance from transmitter to receiver
R=sqrt((z(:,1:Nz/2+1)-Ht).^2 + rho^2);
                            % Distance from transmitter to receiver
theta=asin(rho./R);         % Angle Theta in spherical coordinate
phi=asin(J/rho);            % Angle Phi in spherical coordinate

g_tilda_fs=exp(-((cos(theta)*ko).^2*sigmaz^2)/2);
                            % Free-space g_tilda
Hyfs=-i*ko*sin(theta)*cos(phi).*g_tilda_fs.*exp(i*ko*R)./(4*pi*R);
                            % Free-space H-field
A=Hy_H(1:Nz/2+1,2);         % z > 0 of a column of the H-field
F=20*log10(abs(A./Hyfs'));  % Propagation factor

save H:\THESIS_2001\MATLAB_CODES\PERF2Ray F -ASCII
```

56

```matlab
%********************************************************************
%                         2Ray-Model
%********************************************************************

J=2;                            % A column final H-field

rho=sqrt(D^2+(J)^2);            % Distance from transmitter to the
receiver
Hr=z(1,1:Nz/2+1);               % The receiving antenna height
DR=2*Ht*Hr/rho;                 % Path difference between direct and
                                % ground reflected waves
psi=atan((Ht+Hr)/rho);          % Grazing angle

Z2ray=sqrt(Erc-cos(psi).^2)/Erc;% Normalized surface impedance Z(psi)
gamma2ray=((sin(psi)-Z2ray)./(sin(psi)+Z2ray));% Reflection coefficient
Tworay=abs(1+gamma2ray.*exp(i*ko*DR));% 2ray model propagation factor
F2ray=20*log10(Tworay);         % 2ray model propagation factor in dB

save H:\THESIS_2001\Base_Line_Codes\RF2Ray F2ray -ASCII
save H:\THESIS_2001\Base_Line_Codes\3DHanning H3D -ASCII

%********************************************************************
*                         Plot results
%********************************************************************

figure(1)
mesh(H3D)
view(-37.5, 70)

figure(2)
y=0:Dz:(Nz)*Dz/2;
plot(F,y,F2ray,y,'o-r')
axis([-30 6 0 Nz*Dz/2])
legend('3D Parabolic','2Ray')
toc
```

THIS PAGE INTENTIONALLY LEFT BLANK

APPENDIX B: A 3D PE MODEL AND 4RAY MODEL

Below is the MatLab program listing of the 3D parabolic equation model and the 4Ray model. This program will compute the propagation factors for the 3D PE model and the 4Ray model over perfectly flat earth and constant admittance plane. A single absorbing knife-edge is placed between he transmitter and receiver. The operating frequency is 1 GHz.

```matlab
%*********************************************************************
%                       Declaring Contants
%*********************************************************************
hold off;
tic
c=3e8;                          % Speed of light
f=1e9;                          % Operating frequency
Lamda=c/f;                      % Wavelength
ko=(2*pi)/Lamda;                % Wavenumber
S=400;                          % Ground conductivity in mS/m
Er=10;                          % Relative dielectric constant

Dz=Lamda;                       % Delta Z in meter
Dy=Lamda;                       % Delta Y in meter
sigmaz=Lamda;                   % Standard deviation of Z


%*********************************************************************
%                       Input Parameters
%*********************************************************************

Ht=60;                          % Transmitting antenna height
Hk=50;                          % Knife edge height
Wk=49.8;                        % Knife edge width

d1=125;                         % Distance from transmitter to knife
d2=375;                         % Distance from knife edge to receiver
D=500;                          % Range from the transmitter
Dx=125;                         % Incremental range (Dx) in meter

Ny=1024;                        % Sample size in the y-direction
Nz=1024;                        % Sample size in the z-direction


%*********************************************************************
%           Define range in y-direction and z-direction
%*********************************************************************

ymax=Ny*Dy/2;           % maximum range in y-direction
y1=0:Dy:ymax;           % First half of y range
y=[y1 zeros(1,Ny/2-1)]; % y array

zmax = Nz*Dz/2;         % Find maximum z range (Zmax)
z1=0:Dz:zmax;           % First half of the range of Zmax+1
z=[z1 zeros(1,Nz/2-1)]; % Construct a full z array
```

```matlab
%***********************************************************************
%                   Define  Wavenumbers in Spatial Domain
%***********************************************************************

kymax=pi/Dy;                    % Maximum wavenumber in y-direction
Dky=2*kymax/Ny;                 % detla ky
ky1=-kymax:Dky:kymax;           % Range of ky
ky=[ky1(:,(Ny/2)+1:Ny+1) ky1(:,2:Ny/2)];

kzmax=pi/Dz;                    % Maximum wavenumber in z-direction
Dkz=2*kzmax/Nz;                 % detla kz
kz1=-kzmax:Dkz:kzmax;           % Range of kz
kz=[kz1(:,(Nz/2)+1:Nz+1) kz1(:,2:Nz/2)];

%***********************************************************************
%            Compute Wavenumbers in Frequency Domain, kx
%***********************************************************************

Ky=meshgrid(ky,1:Nz);           % Create a NyxNz matrix of ky row-repeat
Kz=meshgrid(kz,1:Ny).';         % Create a NyxNz matrix of kz column-
repeat
kx=sqrt(ko^2-Ky.^2-Kz.^2);      % Compute theNy x Nz kx matrix

clear Ky;                       % Clear matrices Ky and Kz from memory
clear Kz;                       % To make the algorithm run faster

%***********************************************************************
%                        Compute reflection coefficient
%***********************************************************************

Erc=Er+i*18*S/(f/1e6);          % Complex dielectric
Zs=1/sqrt(Erc);                 % Impedance
Gamma=(kz-ko*Zs)./(kz+ko*Zs);   % Complex reflection coefficient
%gamma=-ones(Nz,Ny);            % Setting gamma = -1
gamma=meshgrid(Gamma,1:Ny).';   % Create reflection coefficient matrix
                                % by column repeating

%***********************************************************************
%                        Define the Hanning Window
%***********************************************************************

Hya=[];                         % An empty vector
for t=0:Ny/2;                   % Define Ny/2 + 1 points
    if (t>=0 & t<=3*Ny/8)       % Define first 3Ny/8 +1 points
      hy=1;
  elseif (t>=3*Ny/8 & t<=Ny/2)% Define next Ny/8 points
      hy=(sin(4*pi*t/Ny))^2;
    end
   Hya=[Hya hy];                % Construct the first half of Hanning
end                             % window of  1+Ny/2  elements

Yy=fliplr(Hya(:,2:Ny/2));       % Flip left to right of the Hanning
                                                % windows from the
second element to
```

```matlab
                                    % Ny/2 element for total of [1x(Ny/2-1)]
HY=[Hya Yy];                        % Hanning window in y-direction

Hzb=[];                             % An empty vector
for t=0:Nz/2;                       % Define Nz/2 + 1 points
    if (t>=0 & t<=3*Nz/8)           % Define first 3Nz/8 +1 points
       hz=1;
  elseif (t>=3*Nz/8 & t<=Nz/2)% Define next Nz/8 points
       hz=(sin(4*pi*t/Nz))^2;
   end
   Hzb=[Hzb hz];                    % Construct the first half of Hanning
end                                 % window of 1+Nz/2  elements

Yz=fliplr(Hzb(:,2:Nz/2));           % Flip left to right of the Hanning
                                    % windows from the second element to
                                    % Nz/2 element for total of [1x(Nz/2-1)]
HZ=[Hzb Yz]';                       % Hanning window in z-direction

Hmy=meshgrid(HY,1:Nz);              % Row repeat
Hmz=meshgrid(HZ,1:Ny)';             % Column repeat

H3D=(Hmy.*Hmz);                     % 3D Hanning window

%*********************************************************************
%                     Gaussian Current Source
%*********************************************************************

f=(1/(sqrt(2*pi)*sigmaz))*exp(-(z-Ht).^2/(2*sigmaz^2));

f_tilda=Dz*fft(f);              % Fourier transform of f(z)

%*********************************************************************
%                     Initial H-field at x=0
%*********************************************************************

g_tilda=exp(-kz.^2*sigmaz^2/2);     % initial g tilda
hye0_tilda=g_tilda.*cos(kz*Ht);     % Initial hye_tilda(0+,ky,kz) field
hyo0_tilda=-i*g_tilda.*sin(kz*Ht);  % Initial hyo_tilda(0+,ky,kz) field
                         % Initial even H-field, column repeat
Hye0_tilda=meshgrid(hye0_tilda,1:Ny).';
                         % Initial odd H-field, column repeat
Hyo0_tilda=meshgrid(hyo0_tilda,1:Ny).';
                         % Include the reflection coefficient
Hy0_tilda=0.5*(1+gamma).*Hye0_tilda+0.5*(1-gamma).*Hyo0_tilda;

Hy_tilda=Hy0_tilda.*H3D;% Hy_tilda(0+,ky,kz) at x=0

Exp2=exp(i*kx*Dx);      % Marching range
```

```matlab
%************************************************************************
%       3D Parabolic Equation Basic Algorithm
%************************************************************************
C=0;                                    % Setting the counter

for x=0:Dx:D-Dx;
   Hy_tilda_Dx=Hy_tilda.*Exp2;        % Hy_tilda(Dx,ky,kz)

   Hy=Dkz*Dky*(Ny*Nz*ifft2(Hy_tilda_Dx))/(2*pi)^2;% ifft2 wrt to ky and
kz

   Hy_H=Hy.*H3D;            % Apply the Hamming window in spatial domain

   C=C+Dx;                                 % Counter

   if (C == d1)                            % When X= 125 M zero out the field
       Hy_H(1:round(Hk/Dz),1:round(Wk/Dy/2))=0;
       Hy_H(1:round(Hk/Dz),(Ny-round(Wk/Dy/2)):Ny)=0;
   end

   Hyz1=Hy_H(1:Nz/2+1,:);              % H-field for z > 0

   Hyz0=flipud(Hy_H(2:Nz/2,:));        % H-field for z < 0

   Hye=[Hyz1; Hyz0];                    % Even H-field

   Hyo=[Hyz1; -Hyz0];                   % Odd H-field

   Hye_tilda=(Dz*Dy)*fft2(Hye);        % Take the FFT of the even H~
   Hye_tilda_H=Hye_tilda.*H3D;         % Apply the Hanning window in freq

   Hyo_tilda=(Dz*Dy)*fft2(Hyo);        % Take the FFT of the odd H~
   Hyo_tilda_H=Hyo_tilda.*H3D;         % Apply the Hanning window in freq
                              % Multiply by the reflection coefficient
   Hye_tilda_g=0.5*(1+gamma).*Hye_tilda_H;
                              % Multiply by the reflection coefficient
   Hyo_tilda_g=0.5*(1-gamma).*Hyo_tilda_H;

   Hy_tilda1=Hye_tilda_g + Hyo_tilda_g;% Hy_tilda(x,ky,kz)

   Hy_tilda=Hy_tilda1.*H3D;            % Apply the Hanning window

end

%************************************************************************
%          Compute the propagation factor at the final range
%************************************************************************
J=2;                                       % First column final H-field

rho=sqrt(D^2+(J)^2);                       % Distance from Tx base of Rx
R=sqrt((z(:,1:Nz/2+1)-Ht).^2 + rho^2);    % Distance from Tx to Rx

theta=asin(rho./R);                        % Angle Theta
phi=asin(J/rho);                           % Angle Phi
g_tilda_fs=exp(-((cos(theta)*ko).^2*sigmaz^2)/2);  % Free-space g_tilda
Hyfs=-i*ko*sin(theta)*cos(phi).*g_tilda_fs.*exp(i*ko*R)./(4*pi*R); %
Free-space H-field
```

```matlab
A=Hy_H(1:Nz/2+1,2);                  % 1st column of the final H-field
F=20*log10(abs(A./Hyfs'));           % Propagation factor

save H:\THESIS_2001\MATLAB_CODES\PERF4Ray F -ASCII
%**********************************************************************
%                                  Four-Ray Model
%**********************************************************************

% The radius of any member n of the family of ellipsoids in a plane
perpendicular to the LOS path

H1=sqrt((Lamda*d1*d2)/(d1+d2));

h1=Hk-(Ht*d2+z(:,1:Nz/2+1)*d1)/D;   % 1st clearance height
Gamma1=1;                            % Reflection coefficient for case 1
x1=sqrt(2)*h1/H1;
C1=mfun('FresnelC',x1);              % Real part of the Fresnel Integral
S1=mfun('FresnelS',x1);              % Imag part of the Fresnel Integral
Fn1=C1-j*S1;                         % Solution for the Fresnel Integral
F1=0.5*(1-(1+j)*Fn1)*Gamma1;         % First knife-edge normalized field
r1=sqrt(D^2+(Ht-z(:,1:Nz/2+1)).^2);
E01=exp(-j*ko*r1)./r1;
Ed1=E01.*F1;

h2=Hk+(Ht*d2-z(:,1:Nz/2+1)*d1)/D;   % 2nd clearance height
psiA=atan((Hk+Ht)/d1);              % Grazing angle of case 2
%GammaA=(sin(psiA)-Zs)/(sin(psiA)+Zs);% Refl. coefficient for case 2
GammaA=-1;
x2=sqrt(2)*h2/H1;
C2=mfun('FresnelC',x2);              % Real part of the Fresnel Integral
S2=mfun('FresnelS',x2);              % Imag part of the Fresnel Integral
Fn2=C2-j*S2;                         % Solution for the Fresnel Integral
F2=0.5*(1-(1+j)*Fn2)*GammaA;         % 2nd knife-edge normalized field
r2=sqrt(D^2+(Ht+z(:,1:Nz/2+1)).^2);
E02=exp(-j*ko*r2)./r2;
Ed2=E02.*F2;

h3=Hk-(Ht*d2-z(:,1:Nz/2+1)*d1)/D;   % 3rd clearance height
psiB=atan((Hk+z(:,1:Nz/2+1))/d2);   % Grazing angle of case 3
% GammaB=(sin(psiB)-Zs)./(sin(psiB)+Zs); % Refl. coefficient for case 3
GammaB=-1;
x3=sqrt(2)*h3/H1;
C3=mfun('FresnelC',x3);              % Real part of the Fresnel Integral
S3=mfun('FresnelS',x3);              % Imag part of the Fresnel Integral
Fn3=C3-j*S3;                         % Solution for the Fresnel Integral
F3=0.5*(1-(1+j)*Fn3).*GammaB;        % 3rd knife-edge normalized field
r3=sqrt(D^2+(Ht+z(:,1:Nz/2+1)).^2);
E03=exp(-j*ko*r3)./r3;
Ed3=E03.*F3;

h4=Hk+(Ht*d2+z(:,1:Nz/2+1)*d1)/D;   % 4th clearance height
GammaC=GammaA*GammaB;                % Reflection coefficient for case 4
x4=sqrt(2)*h4/H1;
C4=mfun('FresnelC',x4);              % Real part of the Fresnel Integral
S4=mfun('FresnelS',x4);              % Imag part of the Fresnel Integral
Fn4=C4-j*S4;                         % Solution for the Fresnel Integral
```

```matlab
F4=0.5*(1-(1+j)*Fn4).*GammaC;         % 4th knife-edge normalized field
r4=sqrt(D^2+(Ht-z(:,1:Nz/2+1)).^2);
E04=exp(-j*ko*r4)./r4;
Ed4=E04.*F4;

Fknife=(Ed1+Ed2+Ed3+Ed4)./E01;        % Total normalized fields

FknifedB=20*log10(abs(Fknife));       % Total normalized fields in dB

save H:\THESIS_2001\MATLAB_CODES\RF4Ray FknifedB -ASCII
%***********************************************************************
%                           Plot results
%***********************************************************************


figure(1)
y=0:Dz:(Nz)*Dz/2;
plot(F,y,FknifedB,y,'o-r')
axis([-30 6 0 Nz*Dz/2])
%xlabel('Relative Propagation Factor F(dB)'),ylabel('Altitude(m)')
%title(['Ny = 'num2str(Ny) ' Nz = ' num2str(Nz) ' Dx = 'num2str(Dx) '
meters' ' Ht = ' num2str(Ht) ' meters'])
legend('Parabolic','KnifedB')
```

APPENDIX C: A 3D PE MODEL FOR THE MULTIPLE SCREENS OF UNIFORM HEIGHTS AND EQUAL SPACING

Below is the MatLab program listing of the 3D parabolic equation model use to compute the propagation factors with multiple absorbing screens of uniform heights and equal spacing over perfectly flat earth and constant admittance plane. The operating frequency is 1 GHz and 900 MHz.

```
%*********************************************************************
%                       Declaring Contants
%*********************************************************************

hold off;
tic
c=3e8;                       % Speed of light
f=0.9e9;                     % Operating frequency
Lamda=c/f;                   % Wavelength
ko=(2*pi)/Lamda;             % Wavenumber
S=400;                       % Ground conductivity in mS/m
Er=10;                       % Relative dielectric constant

Dz=Lamda;                    % Delta Z in meter
Dy=Lamda;                    % Delta Y in meter
sigmaz=Lamda;                % Current source standard deviation

%*********************************************************************
%                       Input Parameters
%*********************************************************************

Ht=125;              % Transmitting antenna height

Hk=20;               % Knife edge height
Wk=50;               % Knife edge width

NS=120;              % Number of screens
Dns=50;              % Screen separation
M=50:Dns:Dns*NS;     % Location of the screens

D=Dns*(NS+1);        % Range from the transmitter
Dx=25;               % Incremental range (Dx) in meter


Ny=1024;             % Sample size in the y-direction
Nz=1024;             % Sample size in the z-direction
%*********************************************************************
%            Define range in y-direction and z-direction
%*********************************************************************

ymax=Ny*Dy/2;        % maximum range in y-direction
y1=0:Dy:ymax;        % First half of y range
y=[y1 zeros(1,Ny/2-1)]; % y array
```

```matlab
zmax = Nz*Dz/2;            % Find maximum z range (Zmax)
z1=0:Dz:zmax;              % First half of the range of Zmax+1
z=[z1 zeros(1,Nz/2-1)];    % Construct a full z array



%***********************************************************************
%                   Define  Wavenumbers in Spatial Domain
%***********************************************************************

kymax=pi/Dy;                    % Maximum wavenumber in y-direction
Dky=2*kymax/Ny;                 % detla ky
ky1=-kymax:Dky:kymax;           % Range of ky
ky=[ky1(:,(Ny/2)+1:Ny+1) ky1(:,2:Ny/2)];

kzmax=pi/Dz;                    % Maximum wavenumber in z-direction
Dkz=2*kzmax/Nz;                 % detla kz
kz1=-kzmax:Dkz:kzmax;           % Range of kz
kz=[kz1(:,(Nz/2)+1:Nz+1) kz1(:,2:Nz/2)];

%***********************************************************************
%               Compute Wavenumbers in Frequency Domain, kx
%***********************************************************************

Ky=meshgrid(ky,1:Nz);           % Create a NyxNz matrix of ky row-repeat
Kz=meshgrid(kz,1:Ny).';         % Create a NyxNz matrix of kz column-
repeat
kx=sqrt(ko^2-Ky.^2-Kz.^2);      % Compute theNy x Nz kx matrix

clear Ky;                       % Clear matrices Ky and Kz from memory
clear Kz;                       % To make the algorithm run faster

%***********************************************************************
%                       Compute reflection coefficient
%***********************************************************************

Erc=Er+i*18*S/(f/1e6);          % Complex dielectric
Zs=1/sqrt(Erc);                 % Impedance
Gamma=(kz-ko*Zs)./(kz+ko*Zs);   % Complex reflection coefficient
%gamma=-ones(Nz,Ny);            % Setting gamma = -1
gamma=meshgrid(Gamma,1:Ny).';   % Create reflection coefficient matrix
                                % by column repeating

%***********************************************************************
%                       Define the Hanning Window
%***********************************************************************

Hya=[];                         % An empty vector
for t=0:Ny/2;                   % Define Ny/2 + 1 points
    if (t>=0 & t<=3*Ny/8)       % Define first 3Ny/8 +1 points
       hy=1;
   elseif (t>=3*Ny/8 & t<=Ny/2)% Define next Ny/8 points
       hy=(sin(4*pi*t/Ny))^2;
    end
   Hya=[Hya hy];                % Construct the first half of Hanning
end                             % window of  1+Ny/2  elements
```

66

```matlab
Yy=fliplr(Hya(:,2:Ny/2));       % Flip left to right of the Hanning
                                  % windows from the
second element to
                                % Ny/2 element for total of [1x(Ny/2-1)]
HY=[Hya Yy];                      % Hanning window in y-direction

Hzb=[];                           % An empty vector
for t=0:Nz/2;                     % Define Nz/2 + 1 points
    if (t>=0 & t<=3*Nz/8)         % Define first 3Nz/8 +1 points
       hz=1;
   elseif (t>=3*Nz/8 & t<=Nz/2)% Define next Nz/8 points
       hz=(sin(4*pi*t/Nz))^2;
    end
    Hzb=[Hzb hz];                 % Construct the first half of Hanning
end                               % window of 1+Nz/2  elements

Yz=fliplr(Hzb(:,2:Nz/2));       % Flip left to right of the Hanning
                                % windows from the second element to
                                % Nz/2 element for total of [1x(Nz/2-1)]
HZ=[Hzb Yz]';                     % Hanning window in z-direction

Hmy=meshgrid(HY,1:Nz);           % Row repeat
Hmz=meshgrid(HZ,1:Ny)';          % Column repeat

H3D=(Hmy.*Hmz);                   % 3D Hanning window

%*********************************************************************
%                   Gaussian Current Source
%*********************************************************************

f=(1/(sqrt(2*pi)*sigmaz))*exp(-(z-Ht).^2/(2*sigmaz^2));

f_tilda=Dz*fft(f);              % Fourier transform of f(z)

%*********************************************************************
%                   Initial H-field at x=0
%*********************************************************************

g_tilda=exp(-kz.^2*sigmaz^2/2);     % initial g tilda
hye0_tilda=g_tilda.*cos(kz*Ht);     % Initial hye_tilda(0+,ky,kz) field
hyo0_tilda=-i*g_tilda.*sin(kz*Ht);  % Initial hyo_tilda(0+,ky,kz) field
                        % Initial even H-field, column repeat
Hye0_tilda=meshgrid(hye0_tilda,1:Ny).';
                        % Initial odd H-field, column repeat
Hyo0_tilda=meshgrid(hyo0_tilda,1:Ny).';
                        % Include the reflection coefficient
Hy0_tilda=0.5*(1+gamma).*Hye0_tilda+0.5*(1-gamma).*Hyo0_tilda;

Hy_tilda=Hy0_tilda.*H3D;% Hy_tilda(0+,ky,kz) at x=0

Exp2=exp(i*kx*Dx);      % Marching range
```

```matlab
%************************************************************************
%               3D Parabolic Equation Basic Algorithm
%************************************************************************
C=0;                              % Setting the counter

for x=0:Dx:D-Dx;
    Hy_tilda_Dx=Hy_tilda.*Exp2;       % Hy_tilda(Dx,ky,kz)
                                      % ifft2 wrt to ky and kz
    Hy=Dkz*Dky*(Ny*Nz*ifft2(Hy_tilda_Dx))/(2*pi)^2;

    Hy_H=Hy.*H3D;         % Apply the Hamming window in spatial domain

    C=C+Dx;               % Counter

    while M(M==C)
            Hy_H(1:round(Hk/Dz),1:round(Wk/Dy/2))=0;
            Hy_H(1:round(Hk/Dz),(Ny-round(Wk/Dy/2)):Ny)=0;
            break
    end

    Hyz1=Hy_H(1:Nz/2+1,:);            % H-field for z > 0

    Hyz0=flipud(Hy_H(2:Nz/2,:));      % H-field for z < 0

    Hye=[Hyz1; Hyz0];                 % Even H-field

    Hyo=[Hyz1; -Hyz0];                % Odd H-field

    Hye_tilda=(Dz*Dy)*fft2(Hye);      % Take the FFT of the even H~
    Hye_tilda_H=Hye_tilda.*H3D;       % Apply the Hanning window in freq

    Hyo_tilda=(Dz*Dy)*fft2(Hyo);      % Take the FFT of the odd H~
    Hyo_tilda_H=Hyo_tilda.*H3D;       % Apply the Hanning window in freq
                             % Multiply by the reflection coefficient
    Hye_tilda_g=0.5*(1+gamma).*Hye_tilda_H;
                             % Multiply by the reflection coefficient
    Hyo_tilda_g=0.5*(1-gamma).*Hyo_tilda_H;

    Hy_tilda1=Hye_tilda_g + Hyo_tilda_g;% Hy_tilda(x,ky,kz)

    Hy_tilda=Hy_tilda1.*H3D;             % Apply the Hanning window

end
%************************************************************************
%              Compute The Propagation Factor
%************************************************************************
J=4;                                    % First column final H-field

rho=sqrt(D^2+(J)^2);                    % Distance from Tx to base Rx
R=sqrt((z(:,1:Nz/2+1)-Ht).^2 + rho^2);  % Distance from Tx to Rx

theta=asin(rho./R);                     % Angle Theta
phi=asin(J/rho);                        % Angle Phi
g_tilda_fs=exp(-((cos(theta)*ko).^2*sigmaz^2)/2); % Free-space g_tilda

% Free-space H-field
Hyfs=-i*ko*sin(theta)*cos(phi).*g_tilda_fs.*exp(i*ko*R)./(4*pi*R);
```

68

```matlab
A=Hy_H(1:Nz/2+1,2); % z > 0 of the first column of the final H-field
F=(abs(A./Hyfs.')); % Propagation factor relative to the free-space

save H:\THESIS_2001\MATLAB_CODES\propfact F -ASCII

%**********************************************************************
%                                          Plot results
%**********************************************************************

figure(1)
%Z=linspace(0,3*Nz/8*Dz,513);
Z=(0:Dz:Nz/2*Dz)';
Y=(Z-Hk)/Lamda;
save H:\THESIS_2001\MATLAB_CODES\recantenna Y -ASCII
plot(Y,F)
axis([-30 60 0 1.8 ])
ylabel('Relative Propagation Factor, F'),xlabel('Receiving Antenna in
Wavelegth')
title(['Ny = 'num2str(Ny) ' Nz = ' num2str(Nz) ' Dx = 'num2str(Dx) '
meters' ' Ht = ' num2str(Ht) ' meters'])
grid

toc                                       % Stop stopwatch
```

THIS PAGE INTENTIONALLY LEFT BLANK

APPENDIX D: A 3D PE MODEL FOR A SINGLE ROUND HILL

Below is the MatLab program listing of the 3D parabolic equation model use to compute the field strengths for a single round hill with multiple absorbing screens of uniform heights and equal spacing. These screens represent a row of buildings or houses in residential areas of a well built-up city. The operating frequency is 900 MHz.

```matlab
%***********************************************************************
%                       Declaring Contants
%***********************************************************************

hold off;
tic
c=3e8;                      % Speed of light
f=0.9e9;                    % Operating frequency
Lamda=c/f;                  % Wavelength
ko=(2*pi)/Lamda;            % Wavenumber
S=400;                      % Ground conductivity in mS/m
Er=10;                      % Relative dielectric constant

Dz=Lamda;                   % Delta Z in meter
Dy=Lamda;                   % Delta Y in meter
sigmaz=Lamda;               % Current source standard deviation


%***********************************************************************
%                   Input Parameters
%***********************************************************************
Ht=57;                      % Transmitting antenna height
Hbs=7;                      % Receiving antenna height above KE's

Wk=100;                     % Knife edge width of 25 meter
Dns=50;                     % Screen separation

Dist=10000;                 % Final range
xs=-1000:Dns:1000;          % Horizontal hill width
ys=sqrt(1e4^2-xs.^2)-(9.95e3);% Equation for circle
xs1=1000+Dns:Dns:Dist+Dns;  % Equal heigth and equal distance screen
ys1=zeros(1,(length(xs1))); % Equal heigth screen height
xs2=[xs xs1];
Hk=[ys ys1];                % Knife edge height of meter
Hk(1)=0;                    % When screen height less than zeros
Hk(length(xs))=0;

NS=length(xs2);             % Number of screens
M=Dns:Dns:Dns*(NS);         % Location of the screens


D=Dns*(NS);                 % Range from the transmitter
Dx=50;                      % Incremental range (Dx) in meter

Ny=1024;                    % Sample size in the y-direction
Nz=1024;                    % Sample size in the z-direction
```

```matlab
%***********************************************************************
%                  Define range in y-direction and z-direction
%***********************************************************************

ymax=Ny*Dy/2;               % maximum range in y-direction
y1=0:Dy:ymax;               % First half of y range
y=[y1 zeros(1,Ny/2-1)];     % y array

zmax = Nz*Dz/2;             % Find maximum z range (Zmax)
z1=0:Dz:zmax;               % First half of the range of Zmax+1
z=[z1 zeros(1,Nz/2-1)];     % Construct a full z array



%***********************************************************************
%                  Define   Wavenumbers in Spatial Domain
%***********************************************************************

kymax=pi/Dy;                     % Maximum wavenumber in y-direction
Dky=2*kymax/Ny;                  % detla ky
ky1=-kymax:Dky:kymax;            % Range of ky
ky=[ky1(:,(Ny/2)+1:Ny+1) ky1(:,2:Ny/2)];

kzmax=pi/Dz;                     % Maximum wavenumber in z-direction
Dkz=2*kzmax/Nz;                  % detla kz
kz1=-kzmax:Dkz:kzmax;            % Range of kz
kz=[kz1(:,(Nz/2)+1:Nz+1) kz1(:,2:Nz/2)];

%***********************************************************************
%                  Compute Wavenumbers in Frequency Domain, kx
%***********************************************************************

Ky=meshgrid(ky,1:Nz);            % Create a NyxNz matrix of ky row-repeat
Kz=meshgrid(kz,1:Ny).';          % Create a NyxNz matrix of kz column-
repeat
kx=sqrt(ko^2-Ky.^2-Kz.^2);       % Compute theNy x Nz kx matrix

clear Ky;                        % Clear matrices Ky and Kz from memory
clear Kz;                        % To make the algorithm run faster

%***********************************************************************
%                          Compute reflection coefficient
%***********************************************************************

Erc=Er+i*18*S/(f/1e6);           % Complex dielectric
Zs=1/sqrt(Erc);                  % Impedance
Gamma=(kz-ko*Zs)./(kz+ko*Zs);    % Complex reflection coefficient
%gamma=-ones(Nz,Ny);             % Setting gamma = -1
gamma=meshgrid(Gamma,1:Ny).';    % Create reflection coefficient matrix
                                 % by column repeating

%***********************************************************************
%                          Define the Hanning Window
%***********************************************************************

Hya=[];                          % An empty vector
for t=0:Ny/2;                    % Define Ny/2 + 1 points
```

```matlab
    if (t>=0 & t<=3*Ny/8)      % Define first 3Ny/8 +1 points
       hy=1;
    elseif (t>=3*Ny/8 & t<=Ny/2)% Define next Ny/8 points
       hy=(sin(4*pi*t/Ny))^2;
    end
    Hya=[Hya hy];              % Construct the first half of Hanning
end                            % window of  1+Ny/2  elements

Yy=fliplr(Hya(:,2:Ny/2));      % Flip left to right of the Hanning
                                           % windows from the
second element to
                               % Ny/2 element for total of [1x(Ny/2-1)]
HY=[Hya Yy];                   % Hanning window in y-direction

Hzb=[];                        % An empty vector
for t=0:Nz/2;                  % Define Nz/2 + 1 points
    if (t>=0 & t<=3*Nz/8)      % Define first 3Nz/8 +1 points
       hz=1;
    elseif (t>=3*Nz/8 & t<=Nz/2)% Define next Nz/8 points
       hz=(sin(4*pi*t/Nz))^2;
    end
    Hzb=[Hzb hz];              % Construct the first half of Hanning
end                            % window of 1+Nz/2  elements

Yz=fliplr(Hzb(:,2:Nz/2));      % Flip left to right of the Hanning
                               % windows from the second element to
                               % Nz/2 element for total of [1x(Nz/2-1)]
HZ=[Hzb Yz]';                  % Hanning window in z-direction

Hmy=meshgrid(HY,1:Nz);         % Row repeat
Hmz=meshgrid(HZ,1:Ny)';        % Column repeat

H3D=(Hmy.*Hmz);                % 3D Hanning window

%***********************************************************************
%                     Gaussian Current Source
%***********************************************************************

f=(1/(sqrt(2*pi)*sigmaz))*exp(-(z-Ht).^2/(2*sigmaz^2));

f_tilda=Dz*fft(f);             % Fourier transform of f(z)

%***********************************************************************
%                    Initial H-field at x=0
%***********************************************************************

g_tilda=exp(-kz.^2*sigmaz^2/2);    % initial g tilda
hye0_tilda=g_tilda.*cos(kz*Ht);    % Initial hye_tilda(0+,ky,kz) field
hyo0_tilda=-i*g_tilda.*sin(kz*Ht); % Initial hyo_tilda(0+,ky,kz) field
                       % Initial even H-field, column repeat
Hye0_tilda=meshgrid(hye0_tilda,1:Ny).';
                       % Initial odd H-field, column repeat
Hyo0_tilda=meshgrid(hyo0_tilda,1:Ny).';
                       % Include the reflection coefficient
Hy0_tilda=0.5*(1+gamma).*Hye0_tilda+0.5*(1-gamma).*Hyo0_tilda;

Hy_tilda=Hy0_tilda.*H3D;% Hy_tilda(0+,ky,kz) at x=0
```

73

```matlab
Exp2=exp(i*kx*Dx);        % Marching range

%************************************************************************
%                3D Parabolic Equation Algorithm
%************************************************************************
C=0;                      % Setting the range counter
c=0;                      % Setting the index counter

for x=0:Dx:D-Dx;          % Define the total steps based on Dx and D
   c=c+1;                 % Starting the index counter

   Hy_tilda_Dx=Hy_tilda.*Exp2;      % Hy_tilda(Dx,ky,kz)
                                     % ifft2 wrt to ky and kz
   Hy=Dkz*Dky*(Ny*Nz*ifft2(Hy_tilda_Dx))/(2*pi)^2;


   Hy_H=Hy.*H3D;          % Apply the Hamming window in spatial domain

   %********************************************************************
   %                      Insert Screens (Buildings)
   %********************************************************************
   C=C+Dx;                % Range Counter

   while M(M==C)          % If location of screen = marching distance
           Hy_H(1:round((Hk(c)+Hbs)/Dz),1:round(Wk/Dy/2))=0;
           Hy_H(1:round((Hk(c)+Hbs)/Dz),(Ny-round(Wk/Dy/2)):Ny)=0;
           break
       end

   %********************************************************************
   %          Field Strength Convert from 3D to 2D
   %********************************************************************
   % Measure the field strength at the top of each screen
   %********************************************************************
   J=4;                   % First column final H-field

   rho=sqrt(C^2+(J)^2); % Distance from transmitter to the receiver
   R=sqrt(((Hk(c)+Hbs)-Ht)^2 + rho^2);
                          % Distance from transmitter to receiver

   theta=asin(rho/R);   % Angle Theta measured relative to the z-axis
   phi=asin(J/rho);     % Angle Phi measured relative to the x-axis
                        % Free-space g_tilda
   g_tilda_fs=exp(-((cos(theta)*ko).^2*sigmaz^2)/2);
                        % Free-space H-field
   Hyfs=-i*ko*sin(theta)*cos(phi).*g_tilda_fs.*exp(i*ko*R)./(4*pi*R);


                 % z > 0 of the first column of the final H-field
   A=Hy_H(round((Hk(c)+Hbs)/Dz)+1,4);

   Frel(c)=20*log10(abs(A/Hyfs));  % Relative Prop Factor
   % Convert propagation factor (F) to E-field by multiplying it by
   % 1/sqrt(ko*R)
   Field(c)=20*log10(abs(A/Hyfs)/sqrt(ko*R));  % E-Field strength
   FFreeSpace(c)=20*log10(1/sqrt(ko*R));    % 2D free-space pathloss
```

```
%*******************************************************************

    Hyz1=Hy_H(1:Nz/2+1,:);          % H-field for z > 0

    Hyz0=flipud(Hy_H(2:Nz/2,:));    % H-field for z < 0

    Hye=[Hyz1; Hyz0];               % Even H-field

    Hyo=[Hyz1; -Hyz0];              % Odd H-field

    Hye_tilda=(Dz*Dy)*fft2(Hye);    % Take the FFT of the even H-tilda
    Hye_tilda_H=Hye_tilda.*H3D;     % the Hanning window in freq domain

    Hyo_tilda=(Dz*Dy)*fft2(Hyo);    % Take the FFT of the odd H-tilda
    Hyo_tilda_H=Hyo_tilda.*H3D;     % The Hanning window in freq domain
                % Apply reflection coefficient to the even field
    Hye_tilda_g=0.5*(1+gamma).*Hye_tilda_H;


                % Apply reflection coefficiet to the odd field
    Hyo_tilda_g=0.5*(1-gamma).*Hyo_tilda_H;

    Hy_tilda1=Hye_tilda_g + Hyo_tilda_g;   % Hy_tilda(x,ky,kz)

    Hy_tilda=Hy_tilda1.*H3D;        % The Hanning window in freq domain

end

save H:\THESIS_2001\MATLAB_CODES\FieldSt100 Field -ASCII
save H:\THESIS_2001\MATLAB_CODES\Free_Space FFreeSpace -ASCII

%**********************************************************************
%                           Plot Results
%**********************************************************************
figure(1)
stem(xs2,Hk+Hbs),grid
xlabel('Screen Placement (m)')
ylabel('Screen Height (m)')

figure(2)
Z=(-1000:Dns:Dist+Dns)';
plot(Z,Frel),grid
axis([-1000 5000 -80 10])
ylabel('Relative Field Strength (dB)')
xlabel('Screen Position (m)')
title([' Wk = ' num2str(Wk)  ' meters' ' Dx = 'num2str(Dx) ' meters' '
Ht = ' num2str(Ht) ' meters'])

figure(3)
Z=(-1000:Dns:Dist+Dns)';
save H:\THESIS_2001\MATLAB_CODES\RHPlacement Z -ASCII
plot(Z,Field,Z,FFreeSpace),grid
axis([-1000 5000 -120 -30])
ylabel('Field Strength (dB)')
xlabel('Screen Position (m)')
title([' Wk = ' num2str(Wk)  ' meters' ' Dx = 'num2str(Dx) ' meters'])

toc                             % Stop stopwatch
```

THIS PAGE INTENTIONALLY LEFT BLANK

APPENDIX E: A 3D PE MODEL FOR TWO HILLS OF SINUSOIDAL SHAPE

Below is the MatLab program listing of the 3D parabolic equation model use to compute the field strengths for two sinusoidal hills with multiple absorbing screens of uniform heights and equal spacing. These screens represent a row of buildings or houses in residential areas of a well built-up city. The operating frequency is 900 MHz.

```matlab
%************************************************************************
%                    Declaring Contants
%************************************************************************

hold off;
tic
c=3e8;                      % Speed of light
f=0.9e9;                    % Operating frequency
Lamda=c/f;                  % Wavelength
ko=(2*pi)/Lamda;            % Wavenumber
S=400;                      % Ground conductivity in mS/m
Er=10;                      % Relative dielectric constant

Dz=Lamda;                   % Delta Z in meter
Dy=Lamda;                   % Delta Y in meter
sigmaz=Lamda;               % Current source standard deviation

%************************************************************************
%                    Input Parameters
%************************************************************************
Ht=57;                      % Transmitting antenna height
Hbs=7;                      % Receiving antenna height above KE's

Wk=100;                     % Knife edge width of 25 meter
Dns=50;                     % Screen separation

xs=-1500:Dns:4500+Dns;      % Horizontal hill width
Hk=Hbs+25+25*cos(2*pi*xs/3000);    % Equal space screen height

NS=length(xs);              % Number of screens
M=Dns:Dns:Dns*(NS);         % Location of the screens

D=Dns*(NS);                 % Range from the transmitter
Dx=50;                      % Incremental range (Dx) in meter

Ny=1024;                    % Sample size in the y-direction
Nz=1024;                    % Sample size in the z-direction

%************************************************************************
%            Define range in y-direction and z-direction
%************************************************************************

ymax=Ny*Dy/2;               % maximum range in y-direction
```

```matlab
y1=0:Dy:ymax;            % First half of y range
y=[y1 zeros(1,Ny/2-1)];  % y array

zmax = Nz*Dz/2;          % Find maximum z range (Zmax)
z1=0:Dz:zmax;            % First half of the range of Zmax+1
z=[z1 zeros(1,Nz/2-1)];  % Construct a full z array



%**********************************************************************
%                  Define  Wavenumbers in Spatial Domain
%**********************************************************************

kymax=pi/Dy;                  % Maximum wavenumber in y-direction
Dky=2*kymax/Ny;               % detla ky
ky1=-kymax:Dky:kymax;         % Range of ky
ky=[ky1(:,(Ny/2)+1:Ny+1) ky1(:,2:Ny/2)];

kzmax=pi/Dz;                  % Maximum wavenumber in z-direction
Dkz=2*kzmax/Nz;               % detla kz
kz1=-kzmax:Dkz:kzmax;         % Range of kz
kz=[kz1(:,(Nz/2)+1:Nz+1) kz1(:,2:Nz/2)];

%**********************************************************************
%            Compute Wavenumbers in Frequency Domain, kx
%**********************************************************************

Ky=meshgrid(ky,1:Nz);         % Create a NyxNz matrix of ky row-repeat
Kz=meshgrid(kz,1:Ny).';       % Create a NyxNz matrix of kz column-
repeat
kx=sqrt(ko^2-Ky.^2-Kz.^2);    % Compute theNy x Nz kx matrix

clear Ky;                     % Clear matrices Ky and Kz from memory
clear Kz;                     % To make the algorithm run faster


%**********************************************************************
%                     Compute reflection coefficient
%**********************************************************************

Erc=Er+i*18*S/(f/1e6);        % Complex dielectric
Zs=1/sqrt(Erc);               % Impedance
Gamma=(kz-ko*Zs)./(kz+ko*Zs); % Complex reflection coefficient
%gamma=-ones(Nz,Ny);          % Setting gamma = -1
gamma=meshgrid(Gamma,1:Ny).'; % Create reflection coefficient matrix
                              % by column repeating


%**********************************************************************
%                     Define the Hanning Window
%**********************************************************************

Hya=[];                       % An empty vector
for t=0:Ny/2;                 % Define Ny/2 + 1 points
    if (t>=0 & t<=3*Ny/8)     % Define first 3Ny/8 +1 points
       hy=1;
  elseif (t>=3*Ny/8 & t<=Ny/2)% Define next Ny/8 points
      hy=(sin(4*pi*t/Ny))^2;
    end
```

```matlab
    Hya=[Hya hy];              % Construct the first half of Hanning
end                            % window of  1+Ny/2  elements

Yy=fliplr(Hya(:,2:Ny/2));      % Flip left to right of the Hanning
                                             % windows from the
second element to
                               % Ny/2 element for total of [1x(Ny/2-1)]
HY=[Hya Yy];                   % Hanning window in y-direction

Hzb=[];                        % An empty vector
for t=0:Nz/2;                  % Define Nz/2 + 1 points
    if (t>=0 & t<=3*Nz/8)      % Define first 3Nz/8 +1 points
       hz=1;
   elseif (t>=3*Nz/8 & t<=Nz/2)% Define next Nz/8 points
       hz=(sin(4*pi*t/Nz))^2;
    end
    Hzb=[Hzb hz];              % Construct the first half of Hanning
end                            % window of 1+Nz/2  elements

Yz=fliplr(Hzb(:,2:Nz/2));      % Flip left to right of the Hanning
                               % windows from the second element to
                               % Nz/2 element for total of [1x(Nz/2-1)]
HZ=[Hzb Yz]';                  % Hanning window in z-direction

Hmy=meshgrid(HY,1:Nz);         % Row repeat
Hmz=meshgrid(HZ,1:Ny)';        % Column repeat

H3D=(Hmy.*Hmz);                % 3D Hanning window

%**********************************************************************
%                    Gaussian Current Source
%**********************************************************************

f=(1/(sqrt(2*pi)*sigmaz))*exp(-(z-Ht).^2/(2*sigmaz^2));

f_tilda=Dz*fft(f);             % Fourier transform of f(z)

%**********************************************************************
%                    Initial H-field at x=0
%**********************************************************************

g_tilda=exp(-kz.^2*sigmaz^2/2);     % initial g tilda
hye0_tilda=g_tilda.*cos(kz*Ht);     % Initial hye_tilda(0+,ky,kz) field
hyo0_tilda=-i*g_tilda.*sin(kz*Ht);  % Initial hyo_tilda(0+,ky,kz) field
                        % Initial even H-field, column repeat
Hye0_tilda=meshgrid(hye0_tilda,1:Ny).';
                        % Initial odd H-field, column repeat
Hyo0_tilda=meshgrid(hyo0_tilda,1:Ny).';
                        % Include the reflection coefficient
Hy0_tilda=0.5*(1+gamma).*Hye0_tilda+0.5*(1-gamma).*Hyo0_tilda;

Hy_tilda=Hy0_tilda.*H3D;% Hy_tilda(0+,ky,kz) at x=0

Exp2=exp(i*kx*Dx);      % Marching range
```

```matlab
%*******************************************************************
%                          3D PE Basic Algorithm
%*******************************************************************
C=0;                            % Setting the range counter
c=0;                            % Setting the index counter

for x=0:Dx:D-Dx;                % Define the total steps based on Dx and
D
    c=c+1;                      % Starting the index counter

    Hy_tilda_Dx=Hy_tilda.*Exp2;% Hy_tilda(Dx,ky,kz)
                               % ifft2 wrt to ky and kz
    Hy=Dkz*Dky*(Ny*Nz*ifft2(Hy_tilda_Dx))/(2*pi)^2;

    Hy_H=Hy.*H3D;       % Apply the Hamming window in spatial domain


%*******************************************************************
%                          Insert Screens (Buildings)
%*******************************************************************
    C=C+Dx;             % Range Counter

    while M(M==C)       % If location of screen = marching distance
            % only work if Dx = Dns; otherwise rewrite
             Hy_H(1:round((Hk(c))/Dz),1:round(Wk/Dy/2))=0;
            Hy_H(1:round((Hk(c))/Dz),(Ny-round(Wk/Dy/2)):Ny)=0;
            break
        end

%*******************************************************************
%                       Field Strength Convert from 3D to 2D
%*******************************************************************

    J=4;                                % First column final H-field

    rho=sqrt(C^2+(J)^2);                % Distance from Tx to Base Rx
    R=sqrt(((Hk(c))-Ht)^2 + rho^2);     % Distance from Tx to Rx
    theta=asin(rho/R);                  % Angle Theta
    phi=asin(J/rho);                    % Angle Phi
                                        % Free-space g_tilda
    g_tilda_fs=exp(-((cos(theta)*ko).^2*sigmaz^2)/2);
                                        % Free-space H-field
    Hyfs=-i*ko*sin(theta)*cos(phi).*g_tilda_fs.*exp(i*ko*R)./(4*pi*R);
                   % z > 0 of the first column of the final H-field
    A=Hy_H(round((Hk(c))/Dz)+1,4);

    Frel(c)=20*log10(abs(A/Hyfs));                    % Field strength
    Field(c)=20*log10(abs(A/Hyfs)/sqrt(ko*R));        % Field strength

    FFreeSpace(c)=20*log10(abs(Hyfs)/sqrt(ko*R));

%*******************************************************************
    Hyz1=Hy_H(1:Nz/2+1,:);          % H-field for z > 0

    Hyz0=flipud(Hy_H(2:Nz/2,:));    % H-field for z < 0

    Hye=[Hyz1; Hyz0];               % Even H-field
```

```matlab
    Hyo=[Hyz1; -Hyz0];                  % Odd H-field

    Hye_tilda=(Dz*Dy)*fft2(Hye);     % Take the FFT of the even H-tilda
    Hye_tilda_H=Hye_tilda.*H3D;        % the Hanning window in freq domain

    Hyo_tilda=(Dz*Dy)*fft2(Hyo);     % Take the FFT of the odd H-tilda
    Hyo_tilda_H=Hyo_tilda.*H3D;        % The Hanning window in freq domain
                    % Apply reflection coefficient to the even field
    Hye_tilda_g=0.5*(1+gamma).*Hye_tilda_H;

                    % Apply reflection coefficiet to the odd field
    Hyo_tilda_g=0.5*(1-gamma).*Hyo_tilda_H;

    Hy_tilda1=Hye_tilda_g + Hyo_tilda_g;    % Hy_tilda(x,ky,kz)

    Hy_tilda=Hy_tilda1.*H3D;          % The Hanning window in freq domain

end

save H:\THESIS_2001\Base_Line_Codes\TwoHField100 Field -ASCII


%***********************************************************************
%                              Plot Results
%***********************************************************************

figure(1)
stem(xs,Hk),grid
axis([-2000 5000 0 60])
xlabel('Screen Placement (m)')
ylabel('Screen Height (m)')

figure(2)
Z=(-1500:Dns:4500+Dns)';
plot(Z,Frel),grid
axis([-2000 5000 -80 10])
ylabel('Relative Field Strength (dB)')
xlabel('Screen Position (m)')
title([' Wk = ' num2str(Wk)  ' meters' ' Dx = 'num2str(Dx) ' meters' '
Ht = ' num2str(Ht) ' meters'])

figure(3)
Z=(-1500:Dns:4500+Dns)';
plot(Z,Field),grid
axis([-2000 5000 -120 -30])
ylabel('Field Strength (dB)')
xlabel('Screen Position (m)')
title([' Wk = ' num2str(Wk)  ' meters' ' Dx = 'num2str(Dx) ' meters'])


%legend('Parabolic','KnifedB')
%saveas(gcf,'3D_PE_4RAY.fig');
%saveas(gcf,'3D_PE_4RAY.bmp');

toc                              % Stop stopwatch
```

THIS PAGE INTENTIONALLY LEFT BLANK

LIST OF REFERENCES

1.   Rappaport, T. S., *Wireless Communications Principles and Practice*, Prentice-Hall, New Jersey, 1996.

2.   Janaswamy, R., *Radiowave Propagation and Smart Antennas for Wireless Communications*, Kluwer Academic Publishers, Massachusetts, 2000.

3.   Janaswamy, R., "Radio Wave Propagation Over a Non-Constant Immittance Plane," *Radio Science*, vol. 36, no. 3, pp. 387-405, May-June 2001.

4.   Janaswamy, R., "2.5D Hybrid Parabolic Equation/Ray Tracing Approach for Modeling Path Loss In Urban Environments," *National Radio Science Meeting*, 2001, Reference # C3-2.

5.   Janaswamy, R., "Parabolic Equation Modeling of Wave Propagation in an Inhomogeneous Atmosphere," Technical Notes, Naval Postgraduate School, Monterey, California.

6.   Andersen, J. B., "UTD Multiple-Edge Transition Zone Diffraction," *IEEE Trans. Antenna Propagation*, vol. 45, no. 7, pp.1093-1097, July 1997.

7.   Lee, S.W., "Path Integrals for Solving Some Electromagnetic Edge Diffraction Problems," *J. Mathem. Phys.*, vol. 19, pp. 1414-1422, June 1978.

8.   Piazzi, L. and Bertoni, L. H., "Effects of Terrain on Path Loss in Urban Environments for Wireless Applications," *IEEE Trans. Antenna Propagation*, vol. 46, no. 8, pp.1138-1147, August 1998.

9.   Piazzi, L. and Bertoni, L. H., "A Path Loss Formulation for Wireless Applications Considering Terrain Effects for Urban Environments," *Proc. IEEE VTC'98 Conference*, pp. 159-163, 1998.

10.   Bertoni, H. L., *Radio Propagation for Modern Wireless Systems*, Prentice Hall PTR, Upper Saddle River, NJ, 2000.

11.   Janaswamy, R., "A 3D PE Approach for Propagation Prediction in Urban Areas," Briefing Slides, Naval Postgraduate School, Monterey, CA.

12.   Janaswamy, R. and Andersen, J. B., "Path Loss Predictions in Urban Areas with Irregular Terrain Topography," *Wireless Personal Communications 12*: 255-268, 2000.

13. Piazzi, L. and Bertoni, L. H.," On Screen Placement for Building Representation in Urban Environments Considering 2D multiple Diffraction Problems," *Proc. IEEE Vehicular Technology Conference*, pp. 1977-81, 1999.

14. McNamara, D. A., Pistorius, C. W. I., and Malherbe, A. G., *Introduction to the Uniform Geometrical Theory of Diffraction*, Artech House, Nordwood, MA, 1990.

15. Janaswamy, R., "A 3D Parabolic Equation Method for Imperfectly Reflecting Vertical Obstacles on Flat Ground," *Session 103: Propagation Modeling, Joint IEEE AP-S International/URSI Meeting*, Boston, July 2001.

16. Janaswamy, R., "Efficient Parabolic Equation Solution of Radiowave Propagation in an Inhomogeneous Atmosphere and Over Irregular Terrain: Formulation," Report # NPS-EC-94-004, Naval Postgraduate School, Monterey, California, Nov. 1994.

17. Holm, P. D., "UTD-Diffraction Coefficient for Higher Order Wedge Diffracted Fields," *IEEE Trans. Antenna Propagation*, vol. 44, no. 7, pp.879-888, June 1996.

18. Janaswamy, R., "A Curvillinear Coordinate Based Split-Step Parabolic Equation Method for Propagation Predictions over Terrain," *IEEE Trans. Antennas Propagation*, vol. 46, no. 7, pp. 1089-1097, 1998.

19. Parsons, D., *The Mobile Radio Propagation Channel*, Pentech Publishers, London, 1992.

20. Neve, M.J. and Rowe, G.B., "Mobile Radio Propagation Prediction in Irregular Cellular Topologies Using Ray Methods," *Proc. IEE Microw. Antennas Propag.*, vol. 142, no. 6 pp. 447-451, 1995.

21. Barrios, A.E., "A Terrain Parabolic Equation Model for Propagation in the Troposphere," *IEEE Trans. Antennas Propagation*, vol. 42, no. 1, pp. 90-98, 1994.

22. Levy, M.F., "Diffraction Studies in Urban Environment with Wide-Angle Parabolic Equation Method," *Electronic Letter*, vol. 28, pp. 1491-1492, 1992.

INITIAL DISTRIBUTION LIST

1. Defense Technical Information Center 2
    8725 John J. Kingman Road, Suite 0944
    Ft. Belvoir, VA 22060-6218

2. Dudley Knox Library 2
    Naval Postgraduate School
    411 Dyer Road
    Monterey, CA 93943-5101

3. Chairman, Code EC 1
    Department of Electrical and Computer Engineering
    Naval Postgraduate School
    Monterey, CA 93943-5000
    Jknorr@nps.navy.mil

4. Professor Ramakrishna Janaswamy 1
    Department of Electrical and Computer Engineering
    201 Marcus Hall
    University of Massachusetts
    Amherst, MA 01003
    Janaswamy@ecs.umass.edu

5. Professor David Jenn, Code EC/Jn 1
    Department of Electrical and Computer Engineering
    Naval Postgraduate School
    Monterey, CA 93943-5000
    jenn@nps.navy.mil

6. Professor Tri Ha, Code EC/Th 1
    Department of Electrical and Computer Engineering
    Naval Postgraduate School
    Monterey, CA 93943-5000
    ha@nps.navy.mil

7. Keem B. Thiem 3
    2649 W. Trojan Pl.
    Anaheim, CA 92804
    javarman@yahoo.com

8.   Dwana Broussard 2
        95 MSS/DPET
        125 Methusa Ave
        Edwards AFB, CA 93524-1550
        Dwana.Broussard@edwards.af.mil

9.   Dr. James Harvey 1
        US Army Research Office
        ATTN: AMSRL – RO – EL
        P.O. Box 12211
        Research Triangle Park, NC 27709-2211

10.   Mark Trinklein 1
        412 TW/EWWE
        30 Hoglan Rd. , Bldg 1030
        Edwards AFB, CA 93524
        Mark.Trinklein@edwards.af.mil

11.   Professor Henry Bertoni 1
        Department of Electrical and Computer Engineering
        Polytechnic University
        6 MetroTech Center
        Brooklyn, NY 11201
        hbertoni@duke.poly.edu

12.   Professor Jorgen Bach Andersen 1
        Center for Personkommunikation
        Niels Jernes Vej 12
        9220 Aalborg
        Aalborg University, Denmark
        jba@cpk.auc.dk